PLEASE NOTE:

In all cases this material has been filmed in the best possible way from the available copy. Problems encountered with this document have been identified here with a check mark ✓.

1. Glossy photographs _____
2. Colored illustrations _____
3. Photographs with dark background _____
4. Illustrations are poor copy _____
5. Print shows through as there is text on both sides of page _____
6. Indistinct, broken or small print on several pages _____ throughout _____
7. Tightly bound copy with print lost in spine _____
8. Computer printout pages with indistinct print ✓
9. Page(s) _____ lacking when material received, and not available from school or author _____
10. Page(s) 78 seem to be missing in numbering only as text follows _____
11. Poor carbon copy _____
12. Not original copy, several pages with blurred type _____
13. Appendix pages are poor copy _____
14. Original copy with light type _____
15. Curling and wrinkled pages _____
16. Other _____

University Microfilms International

300 N. ZEEB RD., ANN ARBOR, MI 48106 (313) 761-4700

THE UNIVERSITY OF OKLAHOMA

GRADUATE COLLEGE

FRACTURE PREDICTION IN PLANE ELASTO-PLASTIC PROBLEMS BY THE FINITE ELEMENT METHOD

A DISSERTATION

SUBMITTED TO THE GRADUATE FACULTY

in partial fulfillment of the requirements for the degree of

DOCTOR OF PHILOSOPHY

BY

ROBERT GARY BELIE

Norman, Oklahoma

1978

FRACTURE PREDICTION IN PLANE ELASTO-PLASTIC PROBLEMS BY THE FINITE ELEMENT METHOD

APPROVED BY

J. Nagsimha Reddy

Franklin L. Appl

Charles W. Bert

Davis M. Egle

James A. Payne

DISSERTATION COMMITTEE

ACKNOWLEDGMENTS

I wish to thank my wife, Nanette, and our boys, Scott and Michael, for their patience, understanding, and sacrifice which greatly contributed to the successful completion of this effort.

I am indebted to Dr. J. N. Reddy, my advisor, and Dr. C. Bert and Dr. D. Egle for their guidance and discussion, and Dr. F. J. Appl whose encouragement many years ago has culminated in this work. Most of all, I wish to thank these men for assisting me develop an appreciation for freedom of thought and logical problem solution.

I would also like to acknowledge the support of the School of Aerospace, Mechanical, and Nuclear Engineering at the University of Oklahoma during the test phase of this research, and thank the Merrick Computing Center at the University of Oklahoma for providing the computational time.

Finally, assignment by the United States Air Force to the University of Oklahoma for the completion of this study is gratefully acknowledged.

ABSTRACT

A finite element program based on the plane stress assumption is developed and applied to elasto-plastic fracture problems involving monotonically increasing loads. The program directly predicts the initiation and propagation of fracture in the structure. That is, the concept of stress intensity factor is not utilized in the present approach. The approach uses a piecewise linear approximation of the actual stress-strain curve for the material, and the maximum strain criteria to predict both the yield and fracture. An incremental loading technique is employed to load the structure, and a "zero modulus-unload reload" scheme is developed to handle the response of the structure at fracture. Comparisons with published data on a cracked panel, and the experimental data obtained during this study on tensile and cracked specimens show that the finite element program developed herein can accurately predict load and deflection at fracture, load-deflection curves, fracture initiation locations, and stable or unstable crack propagation. This approach is shown to be highly dependent on the mesh density in areas of high strain gradients.

TABLE OF CONTENTS

LIST OF TABLES

LIST OF ILLUSTRATIONS

NOMENCLATURE

A_o	Initial area
D_g	Gage deflection
D_{pp}	Pin-to-pin deflection
DEPR	Incremental element principal strain
D_r	Pin-to-gage boundary deflection per unit load
E	Elastic modulus
E_e	Elastic modulus
E_i	Incremental tangent modulus
E_s	Secant modulus
E_{si}	Incremental secant modulus
ECH	Array of strains for next element property changes
EPRI	Total element principal strains
I	Potential energy
L	Load
LI	Incremental load
S_{ij}	Compliance coefficient
T	Temperature change
u ,v	Displacement in the x and y directions, respectively
u_i, v_i	Nodal displacements in the x and y directions, respectively
v	Volume
W	Width of tensile specimen neck
α_i	Coefficients of thermal expansion

$\alpha_i, \beta_i, \gamma_i$	Interpolation coefficients
Δ	Element area
ε_i	Strain components
$\varepsilon_x, \varepsilon_y, \varepsilon_z$	Strains in the x, y and z directions
ε_{xy}	Tensor shear strain relative to x and y axes
ε_{yp}	Yield strain
$\varepsilon_1, \varepsilon_2$	Principal strains
μ	Poisson's ratio
μ_e	Elastic Poisson's ratio
μ_i	Incremental Poisson's ratio
σ_j	Stress components
$\sigma_x, \sigma_y, \sigma_z$	Normal stresses in the x, y and z directions
$\sigma_{xy}, \sigma_{yz}, \sigma_{zx}$	Shear stresses relative to xy, yz, and zx axes
σ_{yp}	Yield stress
σ_1, σ_2	Principal stresses
ψ_i	Interpolation functions
$\{F\}$	Force vector
$\{u\}$	Displacement vector
$[B]$	Strain displacement coefficient matrix
$[E]$	Stress-strain coefficient matrix
$[K]$	Stiffness matrix

IT WOULD BE HARD TO IMAGINE A TIME WHEN SOMEONE, SOMEWHERE, DID NOT LOOK DOWN ON SOME BROKEN SOMETHING AND WONDER WHY.

FRACTURE PREDICTION IN PLANE ELASTO-PLASTIC PROBLEMS BY THE FINITE ELEMENT METHOD

CHAPTER I

INTRODUCTION

I.1 Historical Background

On the 10th of January 1954, a B.O.A.C. Comet, the first pressurized commercial jet airliner, fell into the sea near Rome, killing 29 passengers and its crew of 6. The Comet fleet was immediately grounded and carefully inspected and modified. Comet service resumed on the 23rd of March, and 16 days later, a second Comet was lost. Subsequent investigations determined that the Comet had met airworthiness requirements effective at the time; however, these requirements, based on static analysis and testing, were insufficient to predict the type of cyclic failure experienced by the Comets.

As a result of these accidents, fatigue analysis and testing became an integral part of aircraft design. Fatigue

analysis frequently took the form of a damage accumulation theory such as Miner's rule. With Miner's rule, the number of cycles at each stress level is divided by the number of cycles to failure at that level. These fractions are then summed with failure indicated by a total accumulation of one. Fracture testing was accomplished by subjecting an airframe to "blocks" of loading which would simulate those anticipated in actual service. The inaccuracies in this type of fatigue approach required considerable conservatism (along with the associated high cost) to insure the integrity of the structure. Typically, airframes were required to withstand one and a half times the maximum static load and four times the number of cyclic loads expected to be encountered in service. Additionally, most fatigue philosophies dictated that any cracking was to be considered a failure.

The loss of a U.S. Air Force F-111 in 1969 initiated a rethinking of airframe design and analysis concepts.[1] Failure in this aircraft was traced to a small manufacturing flaw in a wing pivot fitting, not to a design induced fatigue. In a fashion reminiscent of the Comet incidents, it became apparent that static and fatigue concepts alone would not predict the type of failure incurred by this aircraft. It also became clear that a more efficient approach would be to design a structure to be crack tolerant, and that some analytic method would be necessary to accomplish

this goal.

I.2 Fracture Mechanics

Fracture mechanics theory which had been successfully applied to crack instability research was adapted to this new design role. A popular form of the fracture mechanics "law" is

$$da/dN = C\ f(K)$$

where da/dN is the crack growth rate (a being the crack length, N the number of cycles), C is a material constant, and K is the stress intensity factor which relates the stress conditions with the crack length.[2] When coupled with a damage tolerance approach to design, an initial flaw size (usually the minimum crack size which can be repeatedly detected by nondestructive inspection) is assumed. The crack is then grown according to the appropriate fracture mechanics "law" until it reaches a critical crack length. This information is then used to establish inspection intervals for the structure. During the course of the design, any area found to have unacceptably rapid crack growth (i.e., inspection intervals are too close) must be redesigned. The advantage of such a procedure is that accurate analysis and inspection can safely extend the structure to its full useful life. However, due to the randomness of possible initiation sites, each area of the structure must be analyzed.

Unfortunately, the application of a fracture mechanics "law" to all areas of a large structure is a difficult, if not impossible, bookkeeping task. The stress intensity factors must be determined for each area of the structure for each type of loading, a time consuming effort even for simple geometries and loadings. Then these factors must be combined in the proper manner to establish the crack growth rates. Additionally, Boyd[3] pointed out that the assumptions associated with fracture mechanics "laws" are more restrictive than is generally realized. The most significant defect in the application of these fracture mechanics approaches to practical aircraft structures lies in their elastic formulation. Structural metals, however, exhibit a large degree of plastic deformation ahead of the crack tip which significantly affects their response. Some attempts have been made to provide correction factors for this effect, but they only further the gap between the physical phenomenon and the analytical technique.

I.3 The Finite Element Method

If the finite element method, which has enjoyed enormous success in the application to structural mechanics problems over the last three decades, could be employed successfully to directly predict fracture in structures, the shortcomings of present methods could be overcome. The method has already been used in fracture mechanics to cal-

culate stress intensity factors. However, a direct procedure of predicting fracture would eliminate the laborious task of calculating stress intensity factors for all regions of a structure and using them to predict fracture. Additionally, the fracture mechanics approach based on the stress intensity factor does not take into account the plastic deformation associated with the fracture phenomena in non-brittle materials. Since the finite element method can also be used to analyze structural problems involving material nonlinearities, it seems obvious to employ the method to directly predict fracture in elasto-plastic materials using a realistic stress-strain law.

In the finite element method (FEM), a given structure is divided into substructures, called finite elements. These elements can be of different shapes and sizes (a physical continuum can be viewed as a collection of smaller elements). A typical element is isolated from the collection and its physical properties, such as the stiffness coefficients, are developed using piecewise approximation of the variables. Then the discrete set of equations governing the complete structure are obtained by putting the element equations together. Generally, the accuracy of the predicted structural response improves with the number of elements (i.e., with the decrease of element size), and the order of approximation which is used to represent the solution. With respect to fracture studies, the FEM offers a

unique opportunity to include the effects of the material nonlinearities. The inherent flexibility and ease of application of the FEM suggests that it is a valuable design tool for direct prediction of fracture as well as the response of structures in the presence of cracks.

I.4 Brief Review of Pertinent Literature

The finite element method has already been used in many studies[4-11] to investigate fracture processes. Most of these investigations have centered on examining the localized effects of fracture and the effects of cracks on structures, rather than on predicting actual catastrophic failure loads and deflections. Newman[10] studied the effects of various parameters such as the mesh size, strain hardening, and critical strain on finite element fracture prediction; however, no experimental results were used for comparison. On the other hand, Miller et al.[11] presented a finite element solution and experimental results for a cracked panel under monotonically increasing stress. Unfortunately, the finite element predictions did not show close agreement with experimental data. These predictions also varied significantly with the method of load redistribution at fracture. Furthermore, the nodal uncoupling method used by Newman, Miller and others is restricted to fracture prediction along lines of symmetry.

I.5 Objectives of the Present Study

The present investigation is concerned with the development of a finite element program to directly predict fracture in non-brittle materials under monotonically increasing loads. The procedure involves the use of a piecewise linearized stress-strain curve, with an incremental loading. This study also involved experimental investigation of fracture to determine the accuracy of the numerical predictions. Thus, the goal of this research was to determine if the finite element method could provide an accurate and useable design tool for the analysis of fracture and crack growth in practical structures. To accomplish this goal, simple, non-trivial two dimensional (plane stress) structures under uniaxial loading were considered. This study further defines the factors affecting accurate prediction of fracture by the finite element method, and determines if the results obtained by Miller represent typical errors to be expected by such a method. Accuracy of the method is demonstrated by comparison with experimental data.

CHAPTER II

THEORETICAL CONSIDERATIONS

II.1 Governing Equations

In a continuum, application of loads results in stresses. At any point in the structure, there are nine stress components; however, only six of them, three normal stresses (σ_x, σ_y, σ_z) and three shearing stresses (σ_{xy}, σ_{yz}, σ_{zx}), are independent. The stresses induce strains in the material. For a three dimensional linear elastic anisotropic material, the six strains (ε_i) are related to these stresses as follows:

$$\varepsilon_i = S_{ij}\,\sigma_j + \alpha_i T \qquad (2.1)$$

where S_{ij}'s are the compliance coefficients, α_i's are the coefficients of thermal expansion, and T is the temperature change. There are 36 compliance coefficients, but due to symmetry of S_{ij} only 21 are independent. For isotropic materials the number of independent coefficients is two.

Here it is assumed that the material is isotropic and the temperature changes are negligible. Since only thin sections are to be modeled, a state of plane stress (with

respect to the xy-plane) is assumed to exist in the body. That is, $\sigma_{zz} = \sigma_{zx} = \sigma_{zy} = 0$. In view of these assumptions, Eq. (2.1) becomes

$$\begin{aligned} \varepsilon_x &= \frac{1}{E}(\sigma_x - \mu\sigma_y) \\ \varepsilon_y &= \frac{1}{E}(\sigma_y - \mu\sigma_x) \\ \varepsilon_z &= \frac{-\mu}{E}(\sigma_x + \sigma_y) \\ \varepsilon_{xy} &= \left(\frac{1+\mu}{E}\right)\sigma_{xy} \end{aligned} \tag{2.2}$$

where E is the modulus of elasticity, and μ is Poisson's ratio. These equations can be inverted to express the stresses in terms of the strains:

$$\begin{aligned} \sigma_x &= \frac{E}{1-\mu^2}(\varepsilon_x + \mu\varepsilon_y) \\ \sigma_y &= \frac{E}{1-\mu^2}(\varepsilon_y + \mu\varepsilon_x) \\ \sigma_{xy} &= \frac{E}{1+\mu}\varepsilon_{xy} \end{aligned} \tag{2.3}$$

Note that equations (2.2) and (2.3) are valid only in the linear elastic portion of the stress-strain curve.

The kinematic analysis of the body, under the assumption of small displacements, gives the following strain-displacement equations:

$$\varepsilon_x = \frac{\partial u}{\partial x}, \quad \varepsilon_y = \frac{\partial v}{\partial y}, \quad \varepsilon_{xy} = \tfrac{1}{2}\left(\frac{\partial u}{\partial y} + \frac{\partial v}{\partial x}\right) \tag{2.4}$$

where u and v denote the displacements along x and y-directions, respectively.

Finally, to complete the description of the equations, the equations of equilibrium must be added,

$$\frac{\partial \sigma_x}{\partial x} + \frac{\partial \sigma_{xy}}{\partial y} = 0, \quad \frac{\partial \sigma_{xy}}{\partial x} + \frac{\partial \sigma_y}{\partial y} = 0 \qquad (2.5)$$

wherein the body forces are assumed to be zero. Equations (2.3) - (2.5) must be appended with appropriate boundary conditions of the problem.

Since this study involves loading of the body through the linear elastic, nonlinear elastic and plastic regions of the stress-strain curve, we must have a relationship between the stresses and strains in these regions. In the present study, where aluminum (2024-T3) was used, it is assumed that the nonlinear elastic portion is negligibly small.

These two remaining regions are shown in Figure 2.1 for a uniaxial stress state. In the initial linear region, the material response is elastic and structures whose loads result in stresses in this region will return to their original shape when the loads are removed. Structures loaded into the plastic zone, however, take on a permanent set on unloading (dashed line of Figure 2.1).

In order to analyze the nonlinearity introduced by the plastic response, the curve in Figure 2.1a is divided into a series of linear portions as shown in Figure 2.1b, with the tangent modulus and incremental Poisson's ratio replacing the elastic constants previously mentioned.

Next, the choice of failure criteria to determine yield and fracture should be considered. The commonly

used failure criterion is that of von Mises, which shows the best agreement with experimental yield data for metals. For the case of plane stress, von Mises criterion takes the form

$$\sigma_1^2 - \sigma_1\sigma_2 + \sigma_2^2 = \sigma_{yp}^2 \tag{2.6}$$

where σ_1 and σ_2 are the principal stresses, and σ_{yp} is the yield stress. If the left hand side is less than σ_{yp}^2, yield does not occur. The surface described by Eq. (2.6) is shown in Figure 2.2. Problems arise in extending von Mises' criterion into the plastic range with the incremental approach used in this study (this will be discussed in detail in Chapter III); therefore, the maximum strain criterion was used. In this theory, yield occurs when the maximum strain exceeds the strain at yield. That is

$$\begin{aligned} &\varepsilon_1 = \pm \varepsilon_{yp} \\ \text{or} \quad &\varepsilon_2 = \pm \varepsilon_{yp} \\ \text{or} \quad &\varepsilon_3 = \pm \varepsilon_{yp} \end{aligned} \tag{2.7}$$

where ε_1, ε_2, and ε_3 are the principal strains. Conversion of these equations to equivalent principal stresses is also shown in Figure 2.2. As can be seen, when $\sigma_1 \gg \sigma_2$ or $\sigma_2 \gg \sigma_1$, both theories give approximately the same results. Since the stress fields in the parts to be analyzed meet this requirement, the use of the maximum strain criterion is justified for this study.

The maximum strain criterion can also be extended along the stress-strain curve to predict subsequent changes

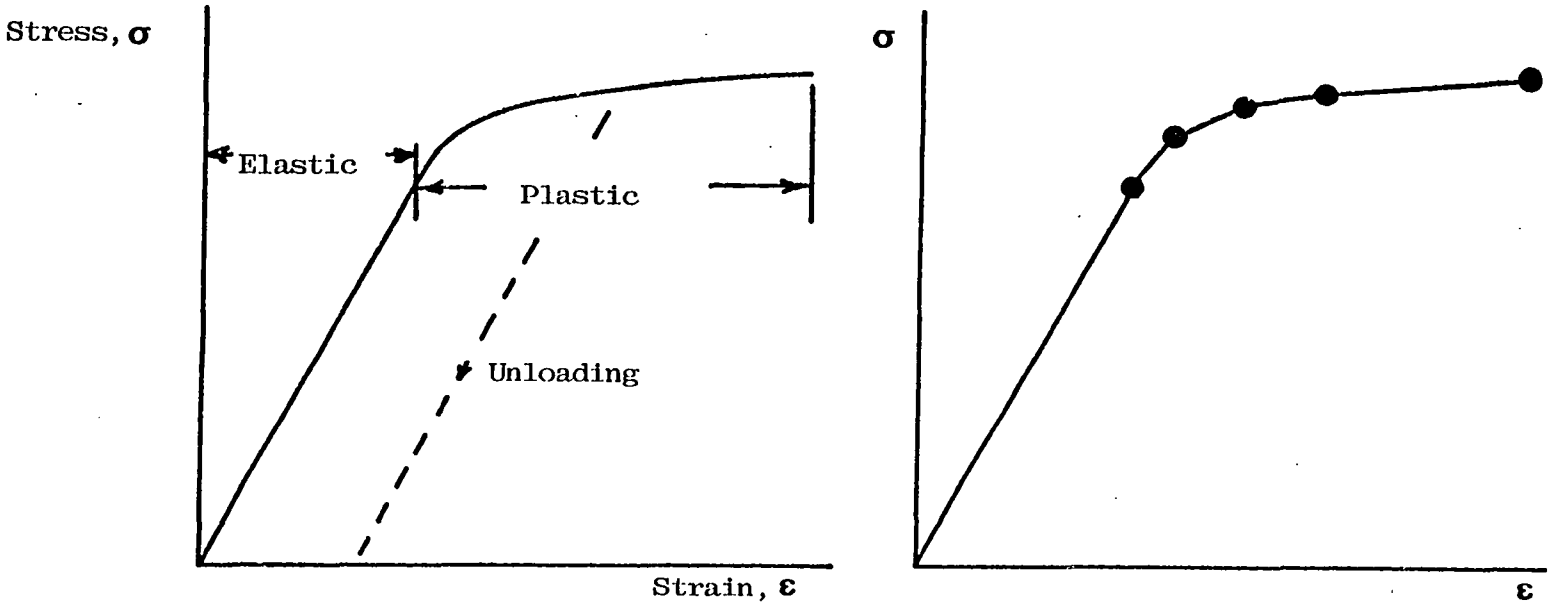

(a) Actual stress-strain curve (b) Linearized stress-strain curve

Figure 2.1. Elastoplastic Stress-Strain Curve

in modulus and finally the fracture.

The principal strains used in Eq. 2.7 can be obtained from the following equation:

$$\varepsilon_{1,2} = \frac{\varepsilon_x+\varepsilon_y}{2} \pm \sqrt{(\frac{\varepsilon_x-\varepsilon_y}{2})^2 + (\varepsilon_{xy})^2} \qquad (2.8)$$

A similar equation may be used to obtain principal stresses.

With the basic continuum equations developed here, a suitable procedure must be employed to obtain a solution.

II.2 The Finite Element Approach

The finite element method (FEM) is employed to solve the elasticity equations for each increment of load. Only a brief discussion of the method will be presented here; however, for a more thorough presentation, see Ref. 12.

The basic element used in this study is the standard constant strain triangle (CST) shown in Figure 2.3. The element has a total of six displacement degrees of freedom, one in each direction at each of three nodes. The displacement field is approximated by the linear relation of the form

$$u = \sum u_i \Psi_i \ (x,y), \quad v = \sum v_i \Psi_i (x,y) \qquad (2.9)$$

where u_i, v_i are the nodal values of the deflections (at node i), and the Ψ_i's are element interpolation functions, given by

$$\Psi_i = \frac{1}{2\Delta}(\alpha_i + \beta_i x + \gamma_i y) \qquad (2.10)$$

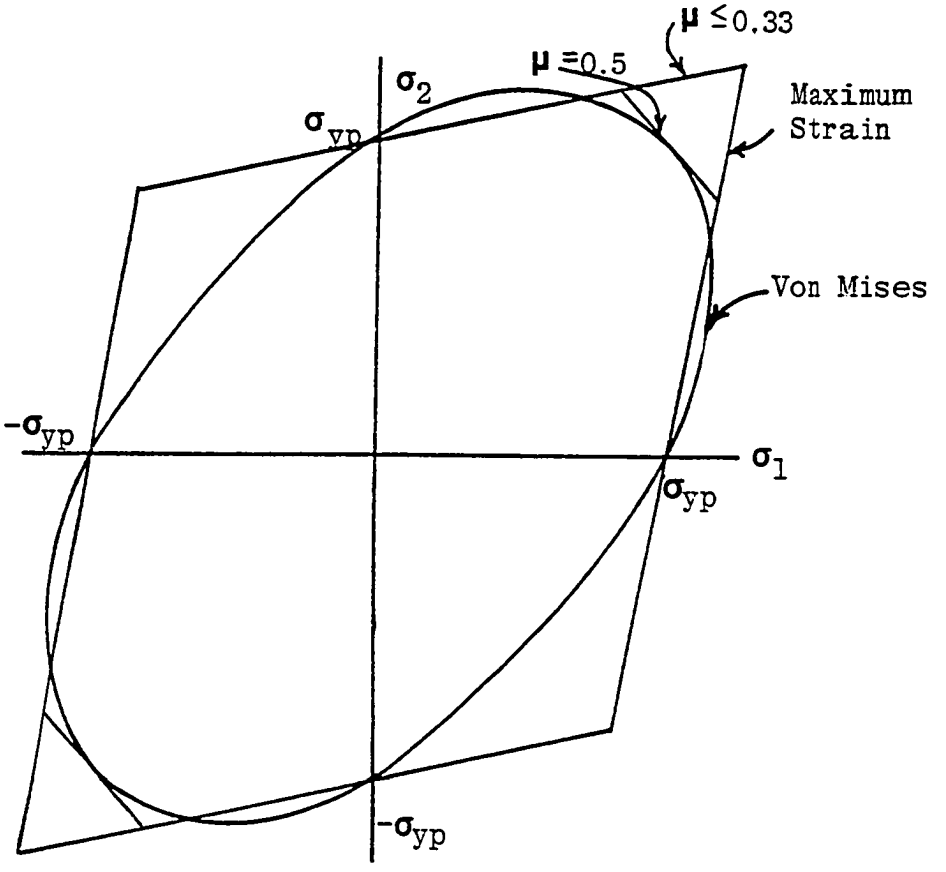

Figure 2.2. Yield Criteria

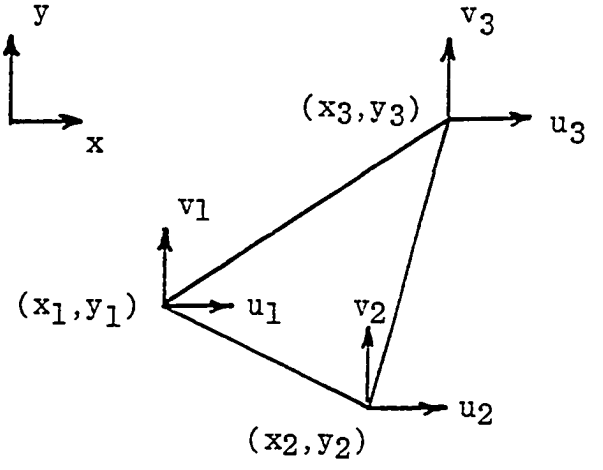

Figure 2.2. Maximum Strain and Von Mises Yield Criteria.

where Δ = area of the triangle,

$\alpha_i = x_j y_k - x_k y_j$, $\beta_i = y_j - y_k$, $\gamma_i = x_k - x_j$, and (x_i, y_i) are the coordinates of node i.

Combining Eqs. (2.4) and (2.9) gives:

$$\varepsilon_x = \frac{\partial u}{\partial x} = \sum_{i=1}^{3} u_i \frac{\partial \Psi_i}{\partial x}$$

$$\varepsilon_y = \frac{\partial v}{\partial y} = \sum_{i=1}^{3} v_i \frac{\partial \Psi_i}{\partial y} \qquad (2.12)$$

$$\varepsilon_{xy} = \tfrac{1}{2}\left(\frac{\partial u}{\partial y} + \frac{\partial v}{\partial x}\right) = \tfrac{1}{2}\left(\sum_{i=1}^{3} u_i \frac{\partial \Psi_i}{\partial y} + \sum_{i=1}^{3} v_i \frac{\partial \Psi_i}{\partial x}\right)$$

In matrix form

$$\begin{Bmatrix} \varepsilon_{xx} \\ \varepsilon_{yy} \\ 2\varepsilon_{xy} \end{Bmatrix} = \begin{bmatrix} \frac{\partial \Psi_1}{\partial x} & 0 & \frac{\partial \Psi_2}{\partial x} & 0 & \frac{\partial \Psi_3}{\partial x} & 0 \\ 0 & \frac{\partial \Psi_1}{\partial y} & 0 & \frac{\partial \Psi_2}{\partial y} & 0 & \frac{\partial \Psi_3}{\partial y} \\ \frac{\partial \Psi_1}{\partial y} & \frac{\partial \Psi_1}{\partial x} & \frac{\partial \Psi_2}{\partial y} & \frac{\partial \Psi_2}{\partial x} & \frac{\partial \Psi_3}{\partial y} & \frac{\partial \Psi_3}{\partial x} \end{bmatrix} \begin{Bmatrix} u_1 \\ v_1 \\ u_2 \\ v_2 \\ u_3 \\ v_3 \end{Bmatrix} \qquad (2.13)$$

$$= [B]\{u\}$$

The governing equations for this element are derived from a minimization of potential energy (I) for the system.

$$I = \tfrac{1}{2} \int_{vol} \{\varepsilon\}^T \{\sigma\}\, dv + \text{Force Terms} \qquad (2.14)$$

since from Eq. (2.3) (in matrix form)

$$\{\sigma\} = [E]\{\varepsilon\} \qquad (2.15)$$

$$I = \tfrac{1}{2}\int_{vol} \{\varepsilon\}^T[E]\{\varepsilon\}\ dv + \text{Force Terms} \qquad (2.16)$$

and substituting from Eq. 2.13,

$$I = \tfrac{1}{2}\int_{vol} \{u\}^T[B]^T[E][B]\{u\}\ dv + \text{Force Terms} \qquad (2.17)$$

Applying variational methods to this equation to minimize I ($\delta I=0$) results in the governing equation for this system.

$$\{F\} = [K]\{u\} \qquad (2.18)$$

where $\{F\}$ is the force vector, $[K]$ is the stiffness matrix, and $\{u\}$ is the displacement vector. The form of $[K]$ results from the variation of Eq. (2.17) and is given as

$$[K] = \int_{vol}[B]^T[E][B]\ dv \qquad (2.19)$$

which for the CST element becomes

$$[K] = [B]^T[E][B]\ At \qquad (2.20)$$

where A is the area and t is the thickness.

The procedure then becomes to assemble the stiffness matrix $[K]$, element by element. These are used to assemble the global stiffness matrix for the entire system. Boundary conditions must be applied to the assembled system of equations of the form of Eq. (2.18) before these equations are solved for $\{u\}$. If strain or stress values are desired Eq. (2.12) and Eq. (2.3) may then be applied..

This procedure is then automated, and the analyst only need describe the geometry in terms of elements and nodes and boundary conditions.

The programs that incorporate this development are described in the next chapter.

CHAPTER III

FINITE ELEMENT FRACTURE PROGRAMS

III.1 Introduction

Three two-dimensional plane stress finite element programs are developed herein to predict yield and fracture under monotonically increasing loads. These programs are:

1. FRACTURE: This finite element program is developed to analyze point loaded tensile and notched specimens. Engineering stress-strain relations are used; however, the model geometry is not updated during each load increment.

2. PANEL1: This program is a modification of FRACTURE and is used to analyze uniformly loaded panel specimens.

3. PANEL2: This is a modification of PANEL1 which uses incremental geometry changes and true stress-strain relationships.

Input was obtained from a mesh generation program, and all input data was plotted as a check for errors. All of the programs were run on the University of Oklahoma's Merrick Center IBM 370/158 computer.

The programs contained in this work are not optimized or even necessarily efficient from the programming point of view.

III.2 Formulation

The basis of the formulation of the programs developed herein is that each element of the finite element mesh has its own material properties (modulus and Poisson's ratio) based on its state of strain. These "local" properties should approximate those of the actual structure. Furthermore, these properties will be those of a uniaxial tensile test specimen of the same material under the same state of strain; that is, when an element has a principal strain equal to the uniaxial yield strain of the material, the element yields (changes tangent modulus and Poisson's ratio). In a similar manner, an element fractures (changes modulus to zero) when its maximum principal strain is equal to the strain at which the tensile specimen fractures.

To apply these concepts to an operational program, it is necessary to have the entire stress-strain curve from the elastic region all the way to fracture (while stress-strain curves are readily available, strain at fracture is not). The stress-strain curve is then divided into a series of linear segments as shown in Figure 3.1. From this linearized curve, values for modulus are obtained as

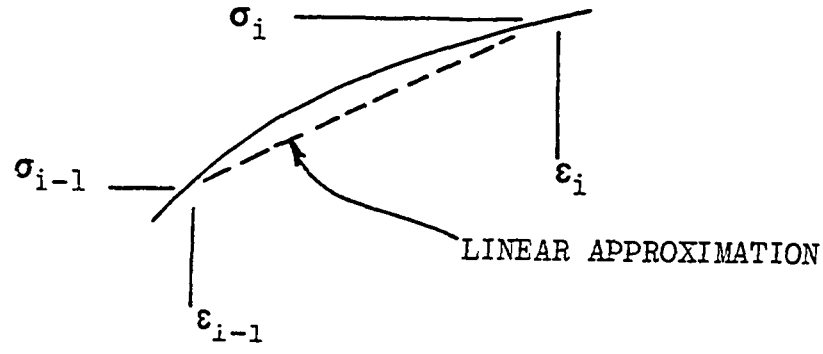

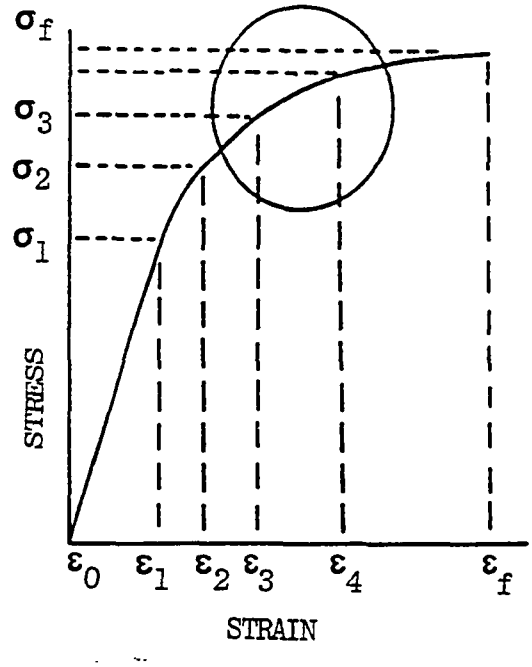

Figure 3.1. Linear Approximation of a Stress-Strain Curve.

$$E_i = \frac{\sigma_i - \sigma_{i-1}}{\varepsilon_i - \varepsilon_{i-1}} \tag{3.1}$$

where σ_i and ε_i are the engineering stress and strain, respectively.

The values of Poisson's ratio (μ) in the plastic range were calculated from the equation given by Bert, Mills, and Hyler[13] as proposed by Nadai:[14]

$$\mu = \tfrac{1}{2} - (\tfrac{1}{2} - \mu_e)(E_S/E_e) \tag{3.2}$$

where μ_e is the elastic Poisson's ratio, E_S is the secant modulus, and E_e is the elastic modulus. For any section, the secant modulus is taken as the average stress in the interval divided by the average strain in that interval; that is,

$$E_{S_i} = \frac{\sigma_i + \sigma_{i-1}}{\varepsilon_i + \varepsilon_{i-1}} \tag{3.3}$$

Therefore, the incremental Poisson's ratio (μ_i) becomes

$$\mu_i = \tfrac{1}{2} - \frac{(\tfrac{1}{2} - \mu_e)}{E_e} \frac{(\sigma_i + \sigma_{i-1})}{(\varepsilon_i + \varepsilon_{i-1})} \tag{3.4}$$

These material properties along with the terminal strains (ε_i) for each interval are stored in the program and referenced by an element material pointer. The properties for a fractured element are also stored, with the tangent modulus set to zero and Poisson's ratio equal to 0.5. As an example Table 3.1 gives the tabulated steel and aluminum properties used in the program FRACTURE.

With the material properties tabulated and referenced by strain level, the material nonlinearity of the problem

TABLE 3.1

EXAMPLE OF TABULATED MATERIAL PROPERTIES

Pointer	Region	E_i	μ_i	ε_i
1,1*	Elastic	29000000.	0.318	0.00200
1,2	Elastic	10500000.	0.313	0.00472
2,2	1st yield	1183000.	0.375	0.00753
3,2	2nd yield	462000.	0.443	0.01814
4,2	3rd yield	271000.	0.467	0.03286
5,2	4th yield	152000.	0.484	0.07817
6,2	5th yield	65000.	0.491	0.14291
7,2	Fracture	0.	0.500	999.

*First #=Region, Second #=Material (1=Steel, 2=Aluminum)

is approximated by considering the structure to be analyzed as a composite of a finite number (n) of elements with appropriate properties. At the start of the analysis, the entire composite is assumed to have the same properties (those of the elastic portion of the stress-strain curve). As the load increases, one element (say the k-th element) will reach a total principal strain value equal to the yield strain. This k^{th} element's properties (modulus and Poisson's ratio) are modified; therefore, the composition of the structure is n-1 elastic elements and one element with a reduced (plastic) modulus. Since the response of each element is again linear, the usual elastic finite element

analysis can be used until another element yields or the k^{th} element reaches the strain at which mext modulus change occurs. The process is repeated until at least one element fractures. The total load to this point is the sum of the incrementally applied loads, and the total deflections at any node are the sum of the incremental deflections.

At fracture, the procedure described above must be modified, since the loads carried by the fractured element to this point must now be carried by the remaining structure. In Ref. 10 and 11 the crack is advanced by removing the constraint at the fractured node and redistributing the force on that node to the remaining nodes along the appropriate line of symmetry; however, as Miller[11] points out, there is no obvious rationale which appears to govern the redistribution, while the effects of the redistribution method are significant. In the present program, a new and completely general procedure is applied. When an element reaches the strain for transition to fracture, the structure is unloaded following the elastic response of the unfractured specimen while retaining each element's progress along the stress-strain curve. It is then reloaded with the fracture surface extended. Any effects due to compression during this unloading are ignored since the actual structure never undergoes this unload reload cycle. If the main diagonal stiffness coefficient corresponding to a node is reduced to zero (the node is unconnected) as a result of a modulus change

at fracture, the node is constrained.

If another element fractures before the maximum load is reachieved, then the crack growth is unstable but may become stable again if the load subsequently increases over the previous maximum fracture load. Figure 3.2 illustrates this procedure for a stress-strain curve with 3 linear plastic regions. A sample mesh at a crack tip is shown in Figure 3.2 along with four sample elements numbered. The bottom four curves are plots of typical stress-strain responses of the four elements as load increases. Numbers along the curves indicate the load level at that point. At level 1, element 1 at the crack tip enters the first yield region. There is less stress (strain) concentration at the other three elements; therefore, they advance only partially along the elastic portion of the curve. At load level 2, element 1 changes modulus again, even before any of the other three elements have yielded for the first time. The load continues to increase to level 3, at which point the principal strain of element 2 indicates it has reached the transition strain for first yield. This continues through levels 4, 5, and 6. At level 7, element 1 has reached the fracture strain. The entire model is then unloaded (artificially). The modulus for element 1 is set to zero and reloading begins with all unfractured elements having an elastic modulus. Stress remains at the unloaded value for element 1, since all incremental stresses are zero. Strains

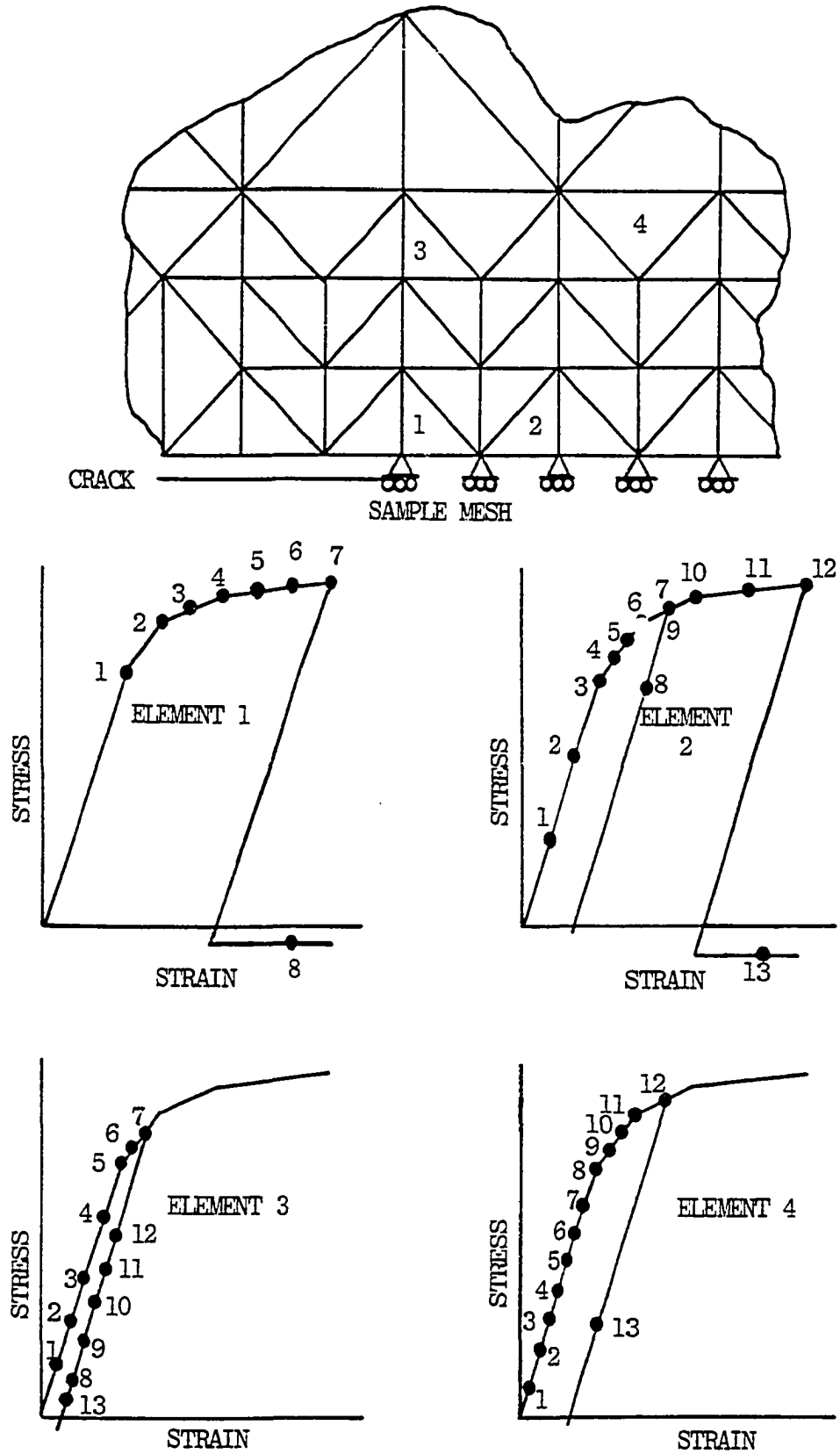

Figure 3.2. Typical Element Response, "Zero Modulus-Unload Reload" Method

for element 1, however, continue to increase. At level 8 element 4 changes modulus for the first time. At level 9, the stress and strain, but not the load, at element 2 equals the equivalent values at level 7. Here the element's properties, just at the elastic values, return to those of yield zone 2. Elements 3 and 4 retain the elastic modulus and Poisson's ratio. At level 10, element 2 enters the 3rd yield zone and at 11, element 4 enters the 2nd yield zone. At level 12, element 2 fractures and the structure is again artificially unloaded. Note that element 3 properties have remained elastic since element 1 fractured. At 13, reloading has begun but at a slower rate for element 3 due to the low strain behind the crack tip. If the load at level 12 is larger than the load at 7, then fracture at 7 is stable. On the other hand, if load 7 exceeds level 12, then fracture is unstable. This process continues until the stiffness matrix is no longer invertable.

The "zero modulus-unload reload" method just described has the following advantages over the nodal release-load redistribution approach of Ref. 10 and 11:

1. The method of redistribution is not arbitrary, but based on cracked specimen geometry.

2. Failures can occur anywhere in the model. With sufficiently small elements, the zero modulus elements act as the crack. Not only is the nodal release method incapable of predicting general crack growth, it is specifically

restricted to the study of fracture along axes of symmetry.

3. The "zero modulus-unload reload" method described herein is element oriented, whereas the load redistribution method is node oriented. Since only deflections are specified at the nodes and stresses and strains are specified over the elements, stress or strain data must be arbitrarily distributed to the nodes in the load redistribution method so that the failure criteria may be applied.

The current method does require the extra time used to unload and reload the structure.

This study uses maximum strain criteria both for yielding and fracture. Newman[10] and Miller et al.[11] both use maximum strain for fracture, but use von Mises criteria for yielding. A problem with the stress formulation of von Mises criteria is that not all practical materials (for example mild steel) have unique strains for a given stress. Thus if the material stress-strain curve is as shown in Figure 3.3, and one linearized section is taken from a to b, then the modulus for section ab is zero. The incremental stress for an element with properties in this portion of the curve will always be zero. Therefore, under the stress formulation of von Mises criteria, the stress will never advance past point b. This problem could be circumvented by reformulating von Mises criteria in terms of strain. Since the specimens for this study were uniaxially loaded and the minimum stress was low compared to the maximum stress, maximum strain

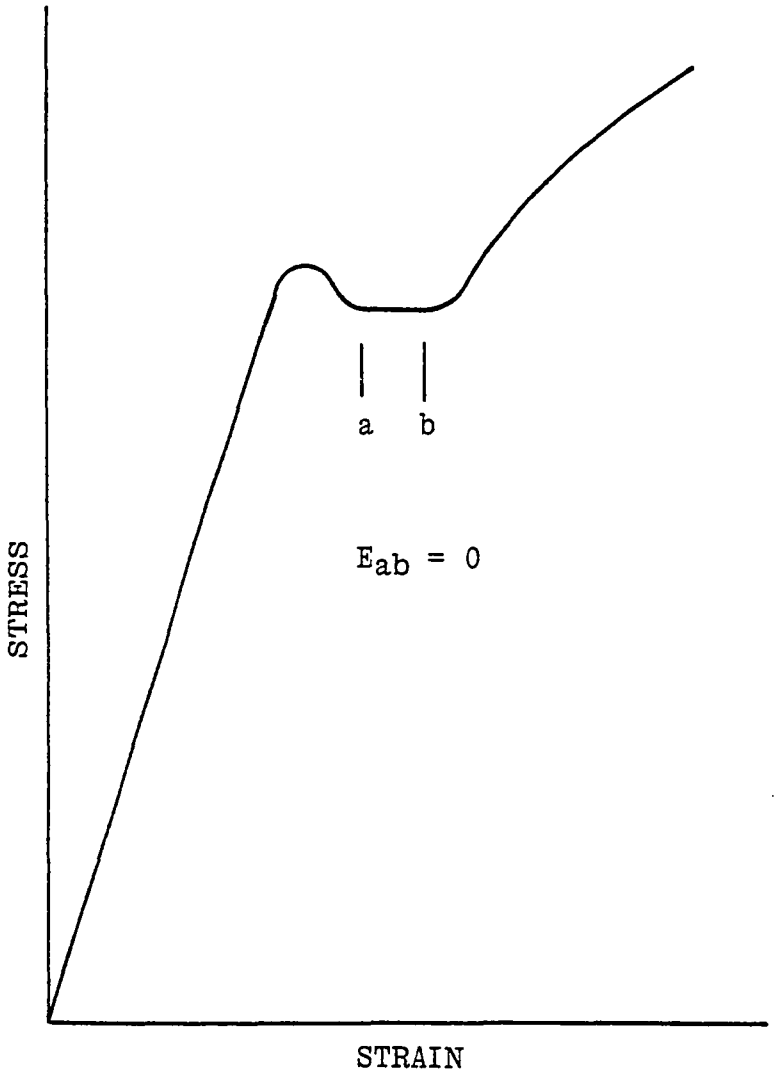

Figure 3.3. Stress-Strain Curve with Zero Modulus Section.

criteria and von Mises criteria are very similar, and therefore, this reformulation was not attempted. It should be remembered, however, that for geometries and/or loadings which result in approximately equal principal stresses, the principal strain criteria used in this program will introduce significant error.

As described in Chapter II, the programs developed here utilize a standard constant strain (linear deflection) triangular element, CST, under plane stress conditions. This element enables the use of a large number of elements in a given area with minimum storage requirements and mesh refinement is easier to accomplish. The predicted rate of crack growth must be independent of the element size (crack growth of 0.001 inches cannot be predicted using elements with sides 0.1 inches long); therefore, many small elements are needed along anticipated crack paths. If higher order elements (e.g., the linear strain triangle) are used in such a dense mesh, storage requirements become excessive. Therefore, the simplest two dimensional element (the CST) is used.

In the experimental procedure, the tensile specimens are loaded through a steel pin in the center of the head of the specimens. To realistically simulate this composite structure, the finite element analysis includes the pin as part of the system. One half of the pin is divided into six elements in the one quadrant models, and a full pin is divided into twelve elements in the half specimen models.

A unit load is applied to the center of the pin to distribute the load. In programs PANEL 1 and PANEL 2, the load is uniformly distributed to the nodes along the edge of the panel.

III.3 Description of the Computer Programs

Each of the three programs consists of a main program and six major subroutines as shown in Figure 3.4. Subroutines FAIL and CHANGE are the only routines not common to a standard elastic finite element analysis. Appendix I contains a listing of FRACTURE with significant differences between FRACTURE, PANEL1, and PANEL2 discussed in this section.

The main program first calls IREAD, which reads in the geometric description (nodal locations and element conductivity) from the mesh generator as well as the nodal constraints. IREAD also prints out the data as a check on proper input.

The subroutine PROP sets up the material property matrix. This matrix contains the modulus, Poisson's ratio, and strain for next transition indexed by a pointer and type of material. Recall that programs FRACTURE and PANEL use material properties that are based on the engineering stress-strain relation while program PANEL2 uses the true stress-strain relation. The subroutines IREAD and PROP are called

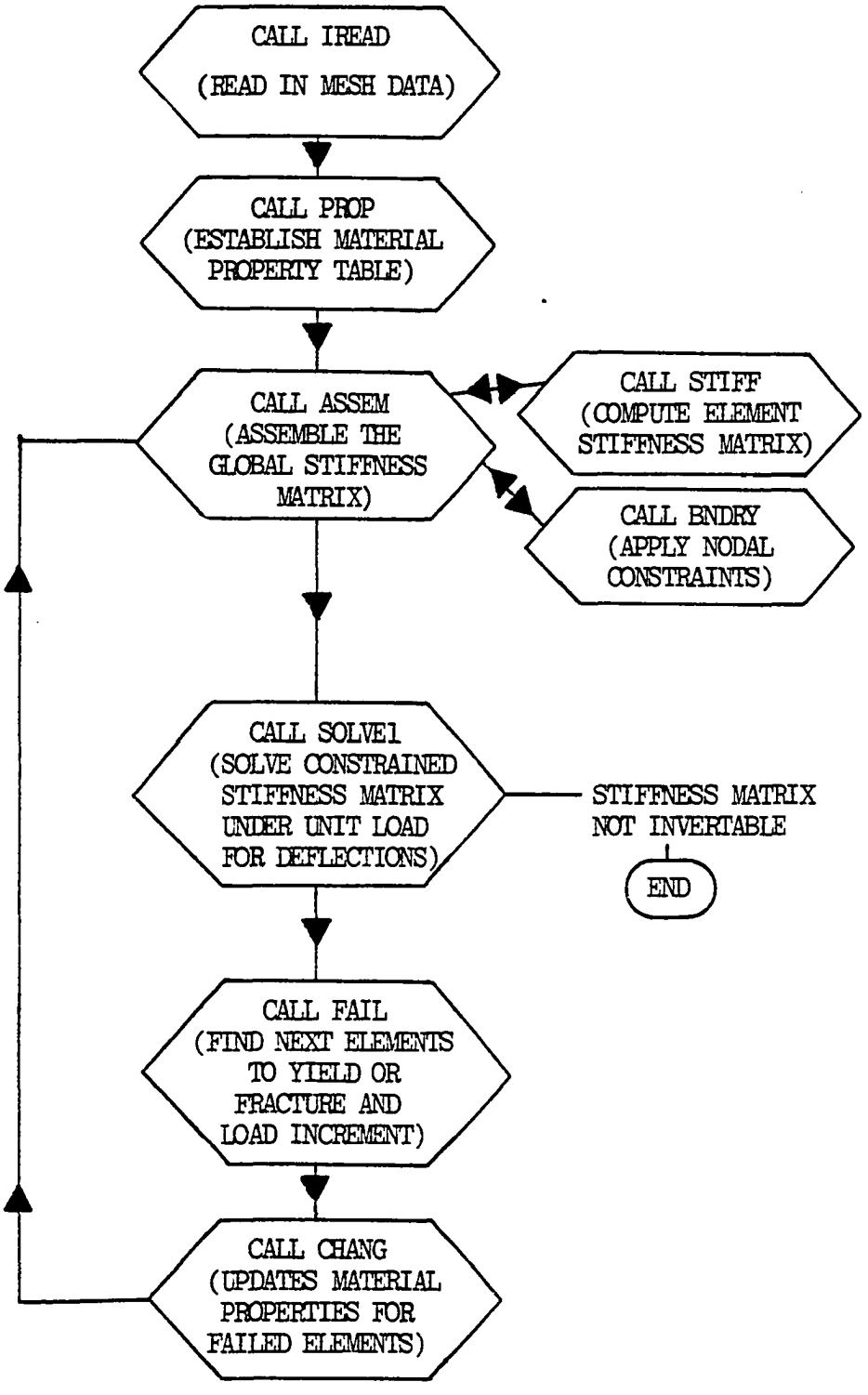

Figure 3.4. Flow Chart for the Program FRACTURE.

only once in the program and no further reference is made to them later in the program.

The subroutine ASSEM assembles the element stiffness properties to obtain the global stiffness matrix, GSTIF. For each element, ASSEM calls STIFF which calculates the element stiffness matrix. The global stiffness is stored in a banded form in the interest of storage and computational efficiency. The appropriate boundary conditions on the nodal deflections are then applied by calling the subroutine BNDRY. Finally, a check is made to insure that no main diagonal terms are zero. This occurs if the stiffness contribution of each element touching the node is zero; if any diagonal term is zero, the node is condensed out by BNDRY.

Subroutine SOLVE1 solves the banded system of equations,

$$\{F\} = [K] \{u\} \tag{3.4}$$

for the unknown displacements $\{u\}$. Here $\{F\}$ is the nodal force vector and $[K]$ is the global stiffness matrix. The program was originally developed using a Gauss-Seidel iterative solution technique since $[K]$ and $\{u\}$ change very little from load increment to increment. This eliminates the need to reassemble the stiffness matrix for each load increment. For a small mesh, the iterative method converged rapidly for the first few iterations, but the time required for accurate solutions greatly exceeded that required for the Gauss

elimination method. As a result, the Gauss elimination method was used exclusively in this study; however, for the very large meshes used in the following chapters, this iterative scheme may deserve more attention. When the specimen fails, the stiffness matrix is no longer invertable and the computation is terminated. The load matrix for FRACTURE consists of a unit load applied to the center node of the pin (used to distribute the load to the specimen) in the longitudinal direction. For the PANEL programs, where the specimen is uniformly loaded, the unit load is divided between the top five nodes of the specimen in ratios of 1/8, 1/4, 1/4, 1/4, and 1/8 starting from the edge node. Double precision is used in this subroutine and throughout the program to reduce roundoff errors.

Subroutine FAIL is the first non-standard subroutine of FRACTURE; i.e., it cannot be found with the usual finite element analysis programs. First, FAIL calculates the unit strains in the x and y directions along with the shear strains for each element. These are a function of the deflections calculated in SOLVE1. The first time through FAIL, all elements are in the elastic range and the initial strains are zero. Therefore, the principal strains for a unit load are calculated and the load at first yield is taken to be the tabulated strain at first yield divided by the maximum principal strain for a unit load. Next, the unit strains are multiplied by the calculated load to obtain

the total strains for each element at first yield.

For subsequent calls to FAIL, the total strains for each element are not zero and their directions are not the same as those of the incremental strains. This makes direct calculation of the next yield or fracture load impossible; therefore, an incremental scheme must be used to predict the next load increment. This is accomplished by storing the next strain for modulus change for each element in an array called ECH, and calculating the incremental principal strain (DEPR) and total principal strain (EPRI). If the incremental principal strains are in the same direction as the total principal strains, the incremental load (LI) for the next failure is given by

$$LI = (ECH - EPRI)/ DEPR \qquad (3.5)$$

Since EPRI and DEPR are not in general in the same direction, Eq. (3.5) is only an approximation. This calculation is made for each element and the smallest load increment is then used as the trial load increment which will cause the next element to change modulus. In order to reduce the computational time, this increment may be increased to cause more elements to fail for each solution of Eq. (3.4). With the incremental load now calculated, the total strains are set equal to the previous total strains plus the incremental strains times the incremental load. The total principal strains for each element are then calculated and compared

with the tabulated strains for next modulus change. If no elements exceed the next change strains, the incremental strains are again multiplied by the incremental load and added to the total strains. The principal strains are again calculated and are compared to the tabulated values. The cycle continues until at least one value of the tabulated maximum allowable strain for the interval is exceeded. All such elements are printed along with the new total load and the corresponding property intervals. If only yielding has occurred, control is returned to the main program. If fracture has occurred, the total strains are reduced by the elastic response due to a unit load times the total load at fracture, and then control is returned to the main program.

Subroutine CHANG was originally conceived to update the global stiffness matrix for failed elements in conjunction with the SOLVE (Gauss-Seidel) iterative routine. Since the entire stiffness matrix must now be regenerated (because it is changed during the Gauss elimination in SOLVE1) for each pass, the function of CHANG has been reduced to updating the material pointer for failed elements. Element thickness was also updated in CHANG for the PANEL2 program.

The program continues to cycle from ASSEM to SOLVE1 to FAIL to CHANG until the stiffness matrix can no longer be inverted or the program exceeds the estimated time limit.

CHAPTER IV

CRACKED PANEL ANALYSIS

IV.1 Introduction

After the present study was undertaken, and the FRACTURE program was completed, the article by Miller[11] on fracture prediction became available. Miller's work raised two questions pertinent to the present study. First, can the present program improve on Miller's prediction of fracture load, and second, can the program accurately predict the experimental results presented by Miller?

To answer these questions and to determine the parameters that effect FEM fracture prediction, a modification of FRACTURE, called PANEL1, was made. The essential differences between FRACTURE and PANEL1, the method of load application and the size of the incremental load steps, are minor. A third program, PANEL2, used true stress-strain relations and updated geometric coordinates and element thicknesses for each load increment.

IV.2 Finite Element Analysis

Due to the geometric and loading symmetry of the panel, only one quadrant of the panel is used in the finite element analysis. Figure 4.1a shows the dimensions of the 0.10", 2024-T3 aluminum test panel. A nonuniform finite element mesh of the panel is shown in Figure 4.1b. To predict the response at the crack tip more accurately, further refinement was made there, as shown in Figure 4.1c. The crack-tip portion is blown up in Figure 4.1d to show the mesh details. The stress-strain curve data for the material was obtained from published data[15]. Some error is introduced by this selection since the exact material properties are not known. The stress-strain curve was then divided into one elastic and three linearly plastic regions. The panel was first analyzed using a coarse mesh. Subsequent refinements of the mesh were made at the crack tip. The loads predicted by each of these meshes are shown in Figure 4.2 as a function of the minimum element area at the crack tip. Entry into each plasticity region of the stress-strain curve is shown by the lower three curves with initial fracture and final fracture shown in the top curves. The horizontal line represents Miller's[11] experimental results. The elements on the right side of the figure are too large to predict stable fracture; therefore, only initial fracture is shown in this area. As can be seen in the figure, as element size becomes smaller at the tip, the load at entry into each of the

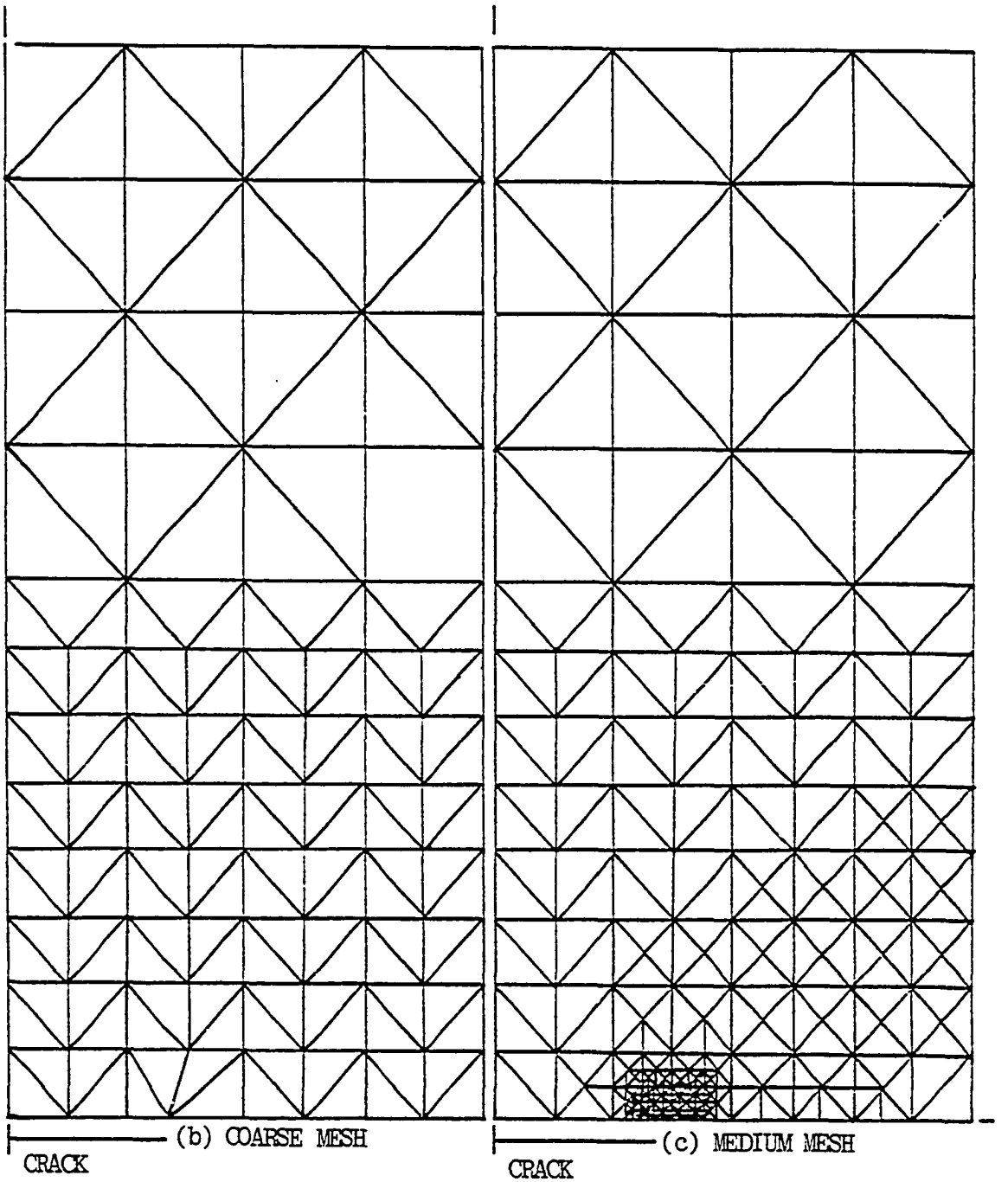

Figure 4.1. Cracked Panel Dimensions and FEM Models.

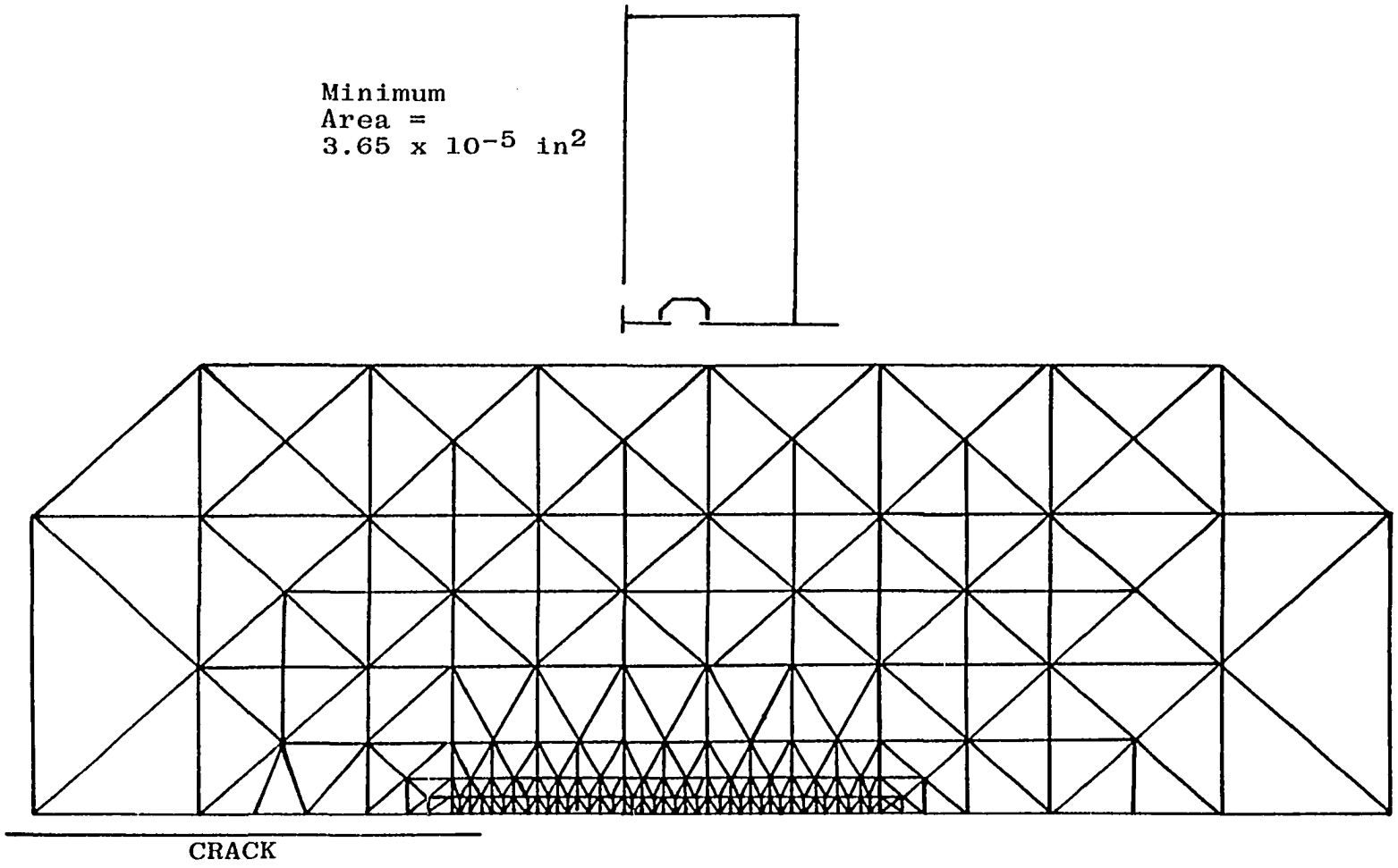

Figure 4.1d. Details of the Fine Mesh (c).

plasticity regions decreases, and the predicted final fracture curve converges to the experimental value. Note that there is no significant difference in the present solution and that of Miller's for equivalent mesh sizes. The large differences between Miller's experimental and numerical results appears to be due solely to the refinement of the mesh. While the methods do appear to have similar accuracies, it should be remembered from earlier discussions that Miller's method only applies to failure along lines of symmetry, and load redistribution procedures are arbitrary.

For stable fracture prediction, the mesh not only needs to be refined at the crack tip, but also along the projected crack path. The element meshes for the data shown in Figure 4.2 are basically the same except for refinements at the crack tip. The mesh shown in Figures 4.1c and 4.1d, however, is refined along the entire path of anticipated stable fracture. While the element size at the crack tip is larger for this fine mesh than those at the extreme left of Figure 4.2, the predictions are more accurate as can be seen in Figure 4.3. This refined mesh also predicted the crack growth as a function of load as shown in Figure 4.4. While no experimental data is available to confirm these predictions, it is interesting to note that each increment of crack growth advanced over several nodes.

Element orientation also plays a role in fracture load prediction. Figure 4.5 shows one example of this effect.

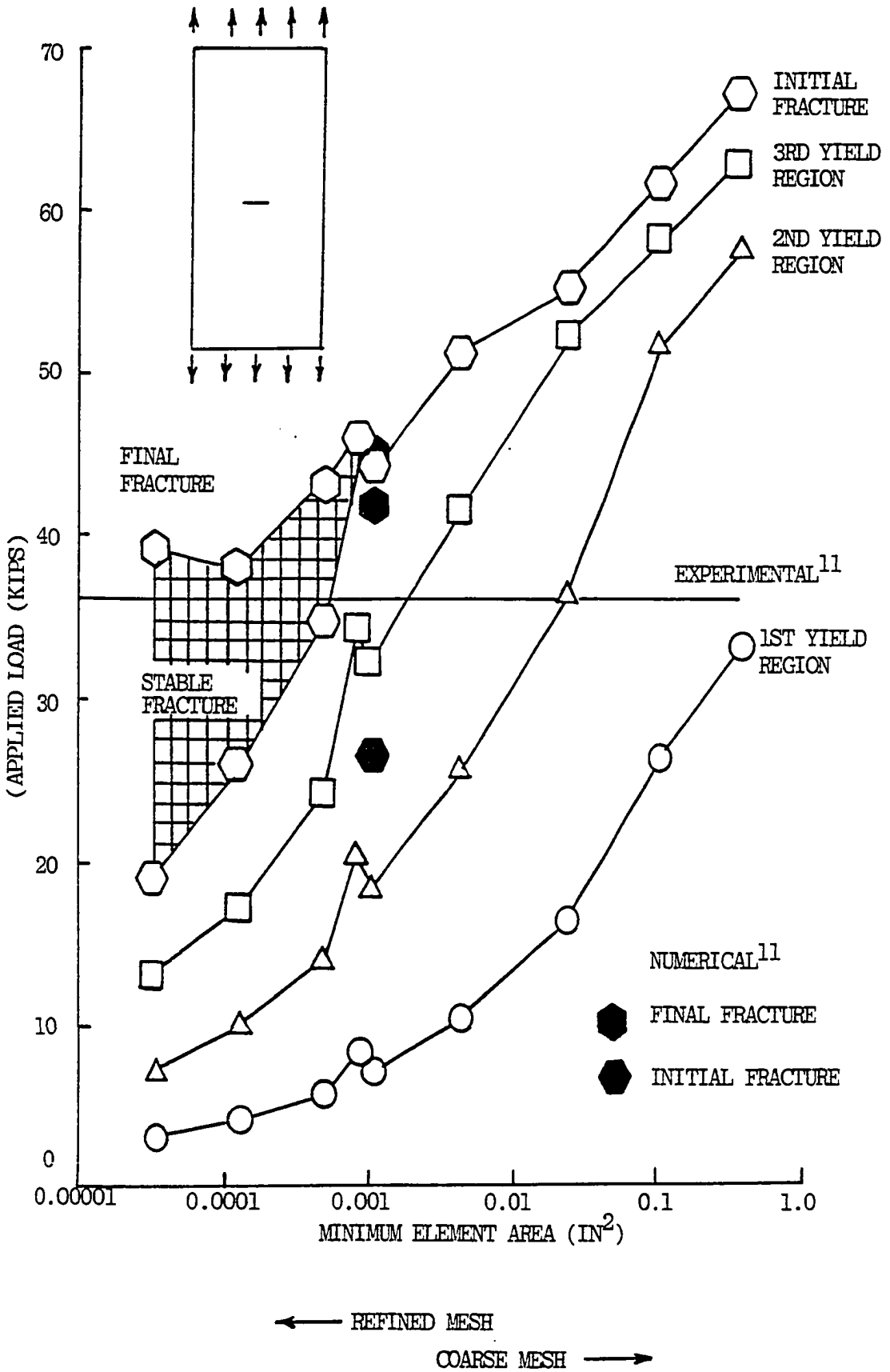

Figure 4.2. Numerical Convergence, Cracked Panel Study.

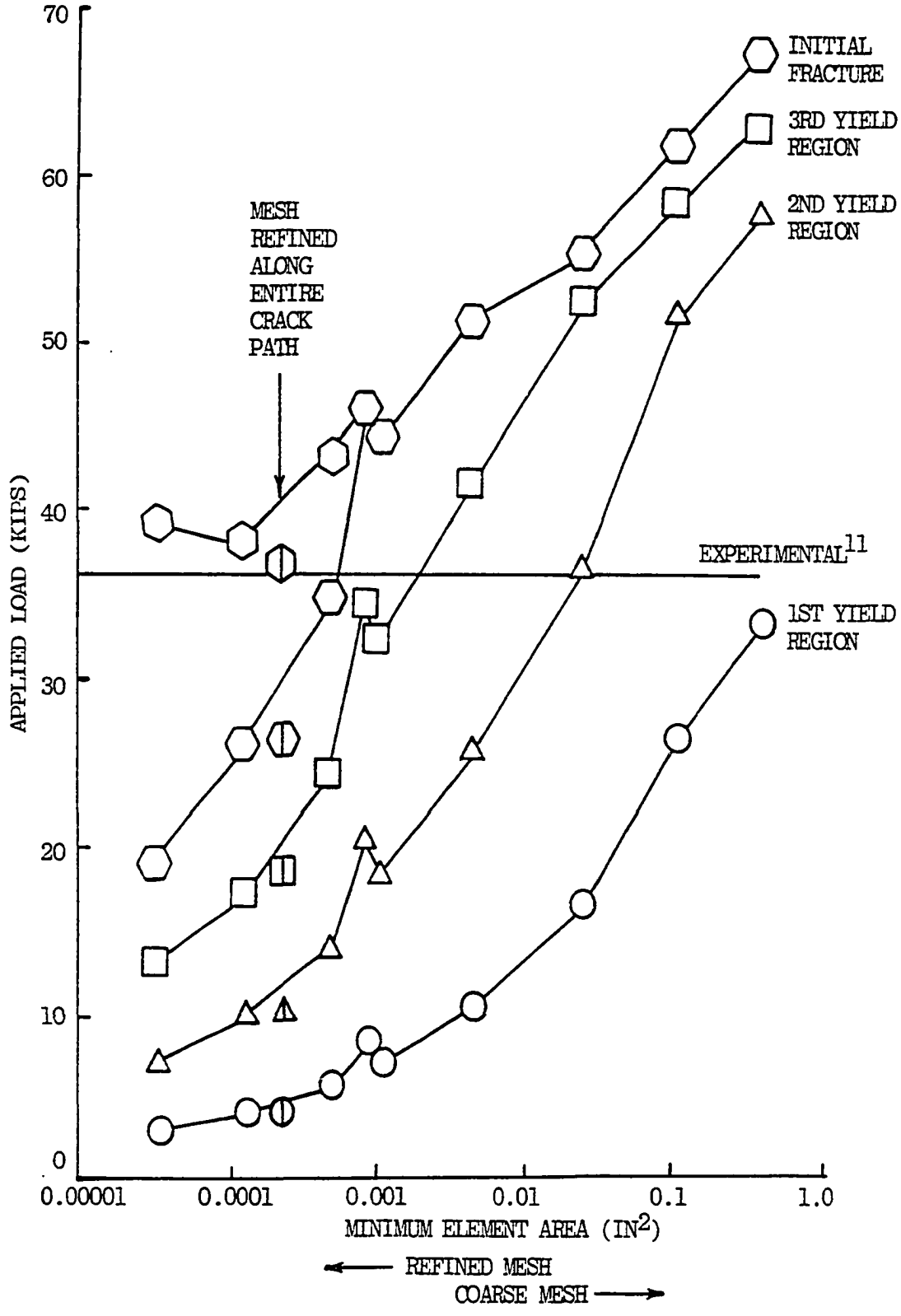

Figure 4.3. Effect of Mesh Refinement Along the Crack Path

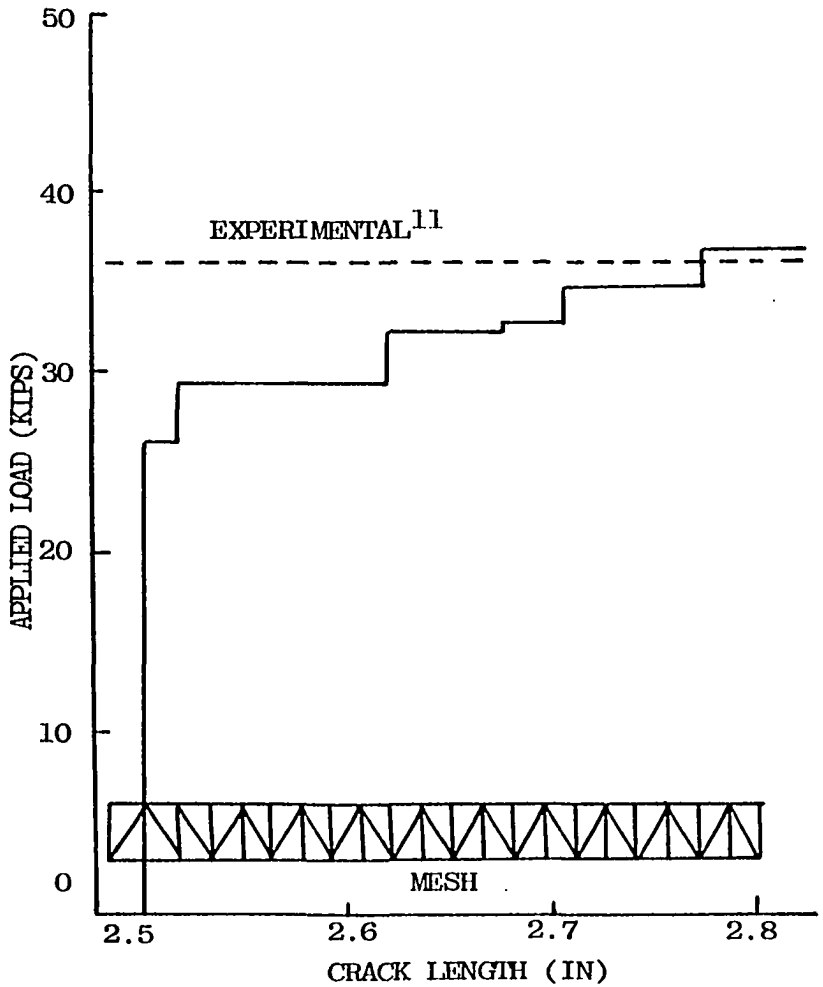

Figure 4.4. FEM Crack Growth Prediction.

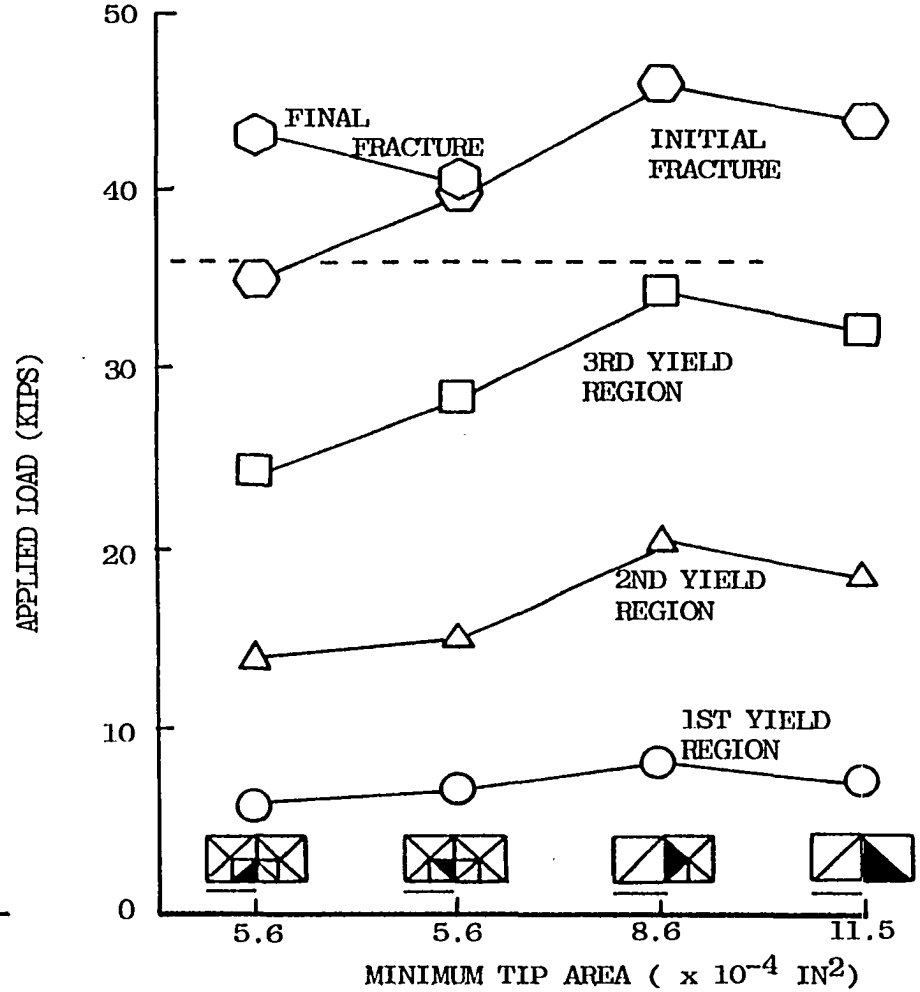

Figure 4.5. Effects of Element Orientation.

This difference in element orientation accounts for the slight upswing near the middle of Figure 4.2.

Finally, the program shows the material state of each element as the load increases. This data is plotted at selected load intervals in Figure 4.6. Part (a) shows the initial formation of the plastic zone at a load of 10,000 pounds. As the load increases to 20,000 pounds (Part (b)), the region of the specimen with properties in the first plasticity section increases and a small region in the second and third sections begin to form at the crack tip. Part (c) shows the expansion of all three regions just prior to initial fracture. One quadrant of the specimen is also shown in (c) to indicate the relative size of the plasticity zones. Figure 4.6d shows the plasticity zones after a significant amount of stable cracking. Note that after initial fracture and unloading, an element may go directly from an elastic response into any of the plasticity sections depending on its previous progress along the stress-strain curve (strain hardening). Note also that the plasticity zone is still increasing in size as the crack advances. In Figures 4.6e and 4.6f the plasticity zones move partially outside the magnified area of the crack tip with the region shown in Figure 4.6f being the plasticity zone at fracture.

PANEL2 was also used to analyze several panel meshes to determine the effects of using true stress-strain and updating specimen geometry during each load increment. No

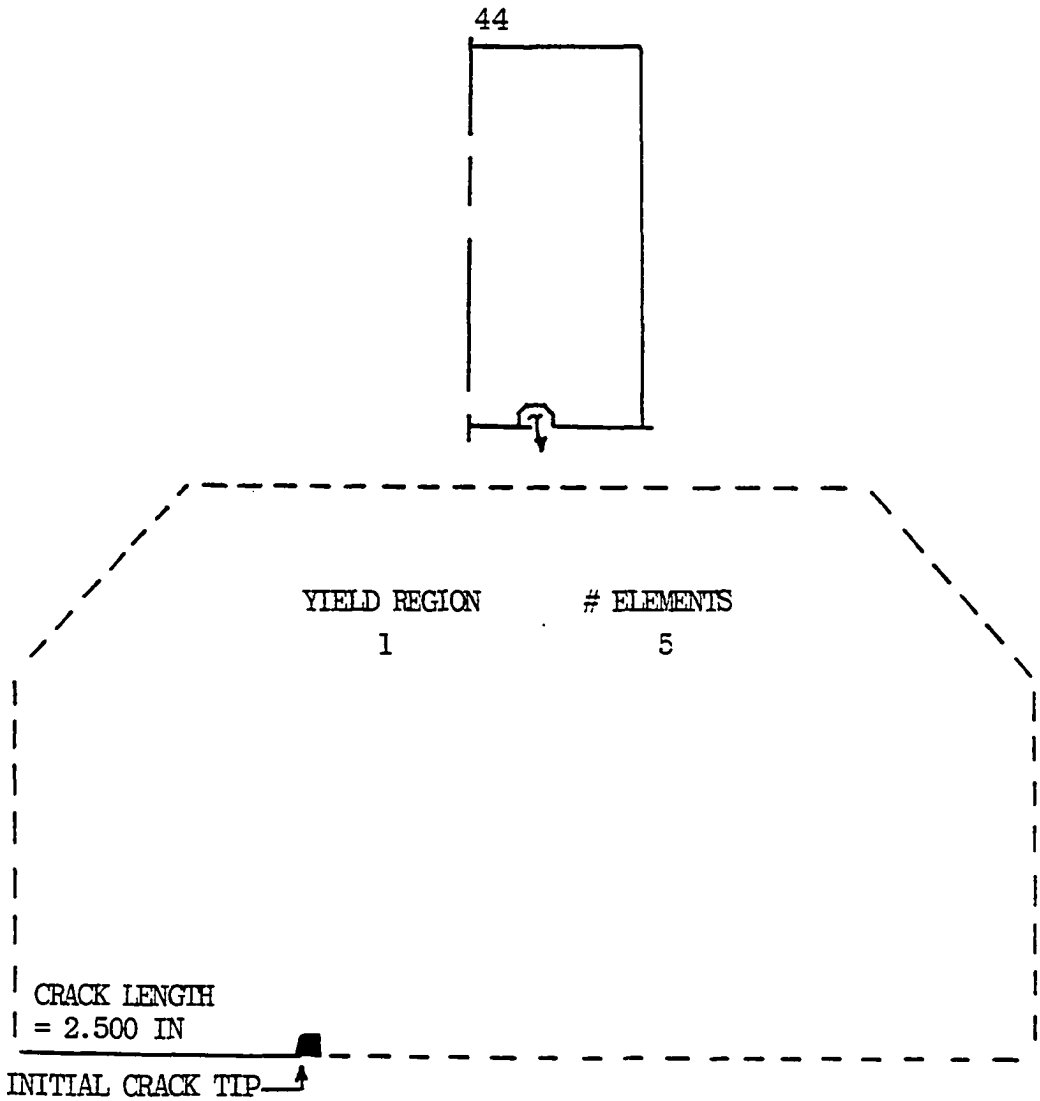

Figure 4.6a. Plastic Regions - Load = 10,000 LB.

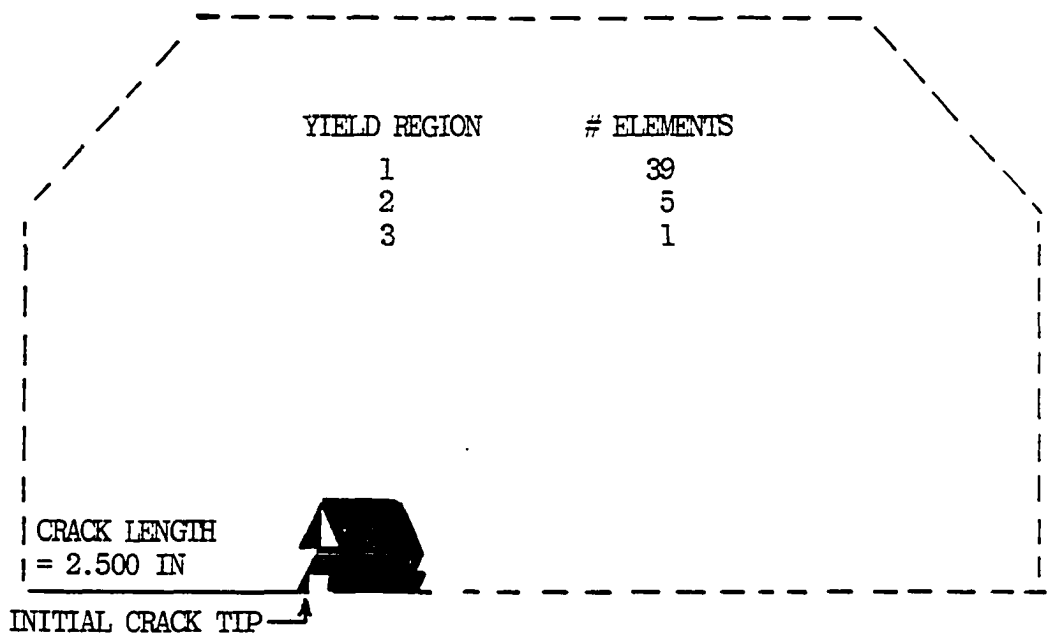

Figure 4.6b. Plastic Regions - Load = 20,000 LB.

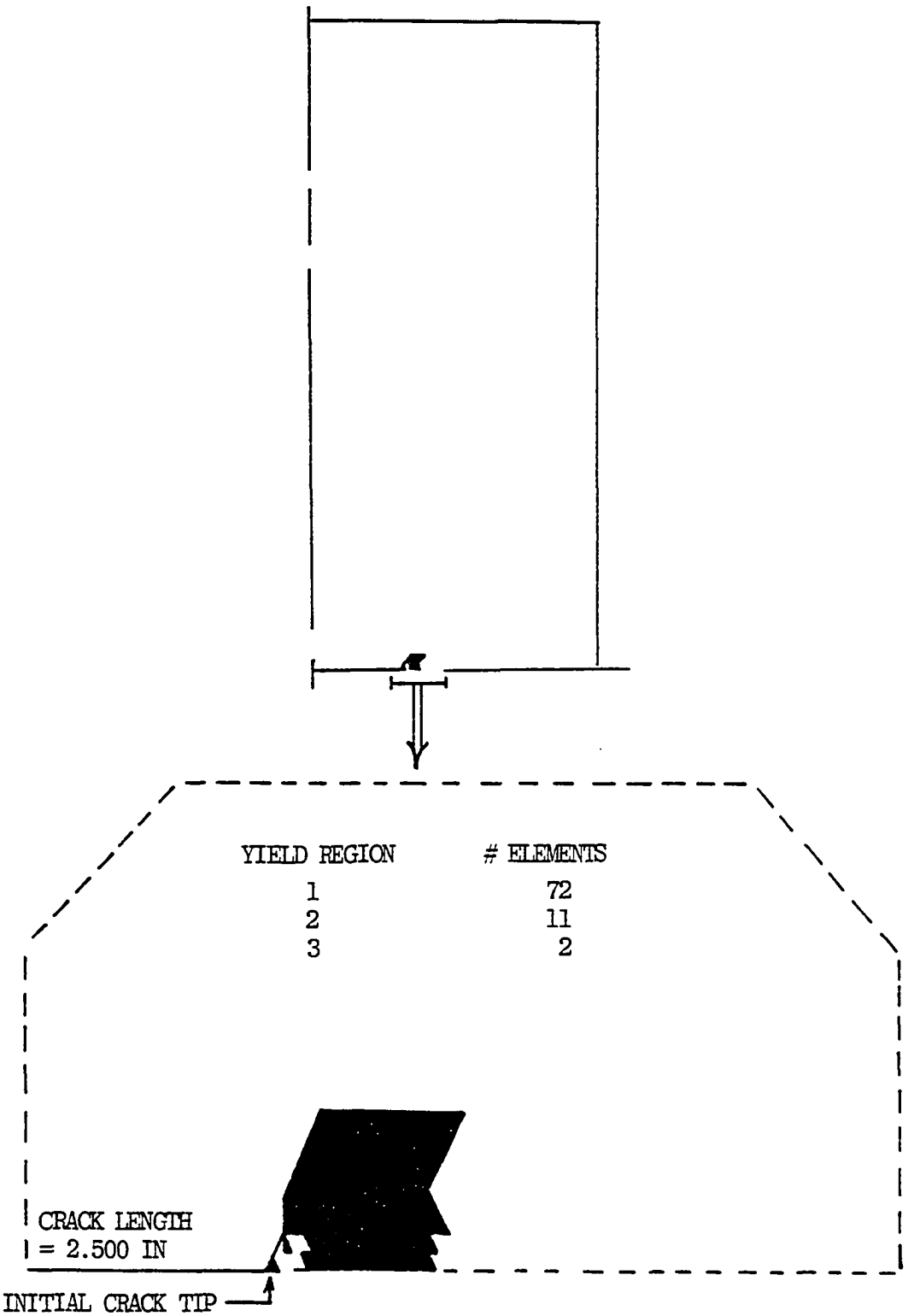

Figure 4.6c. Plastic Regions - Load = 25,000 LB.

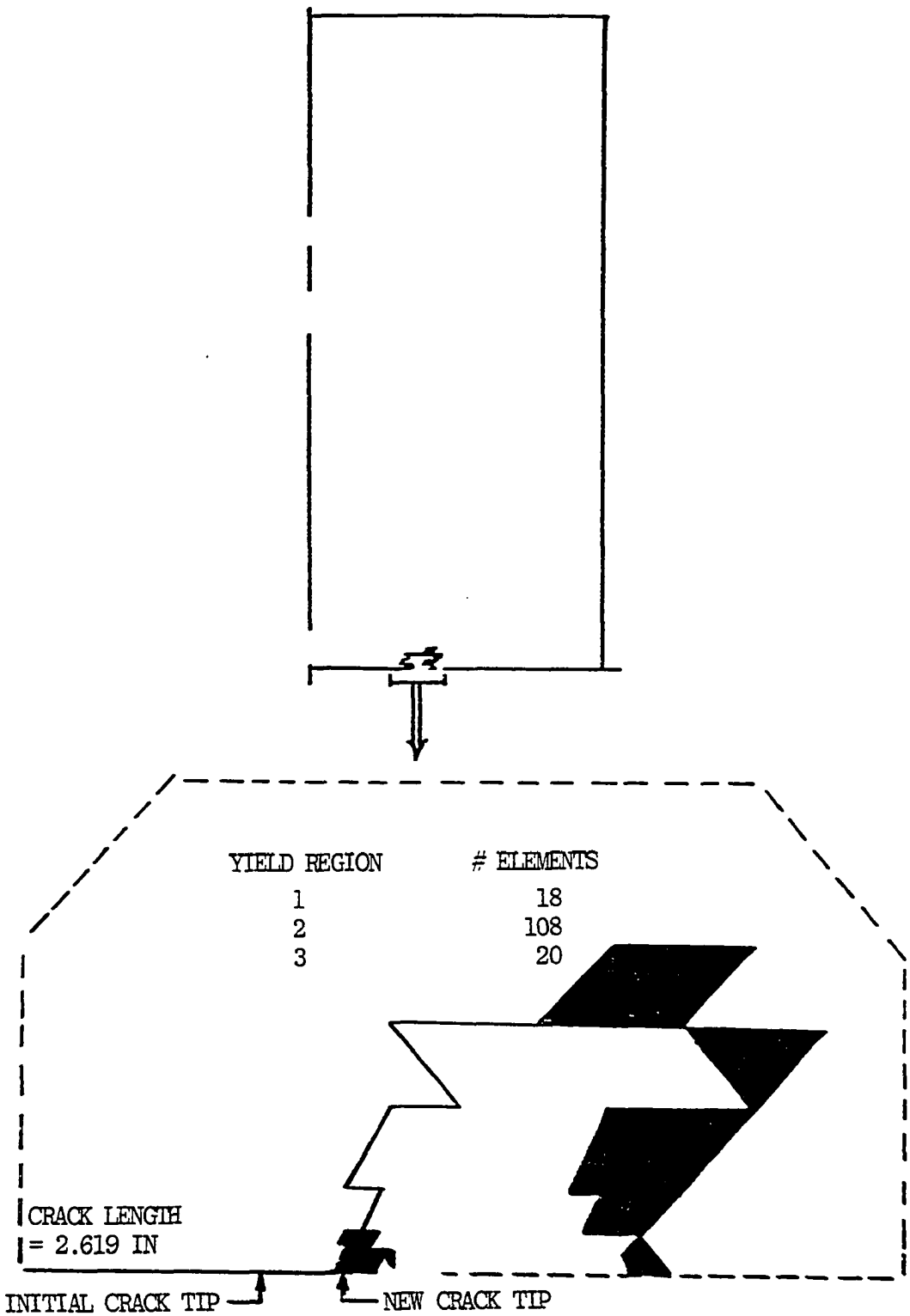

Figure 4.6d. Plastic Regions - Load = 30,000 LB.

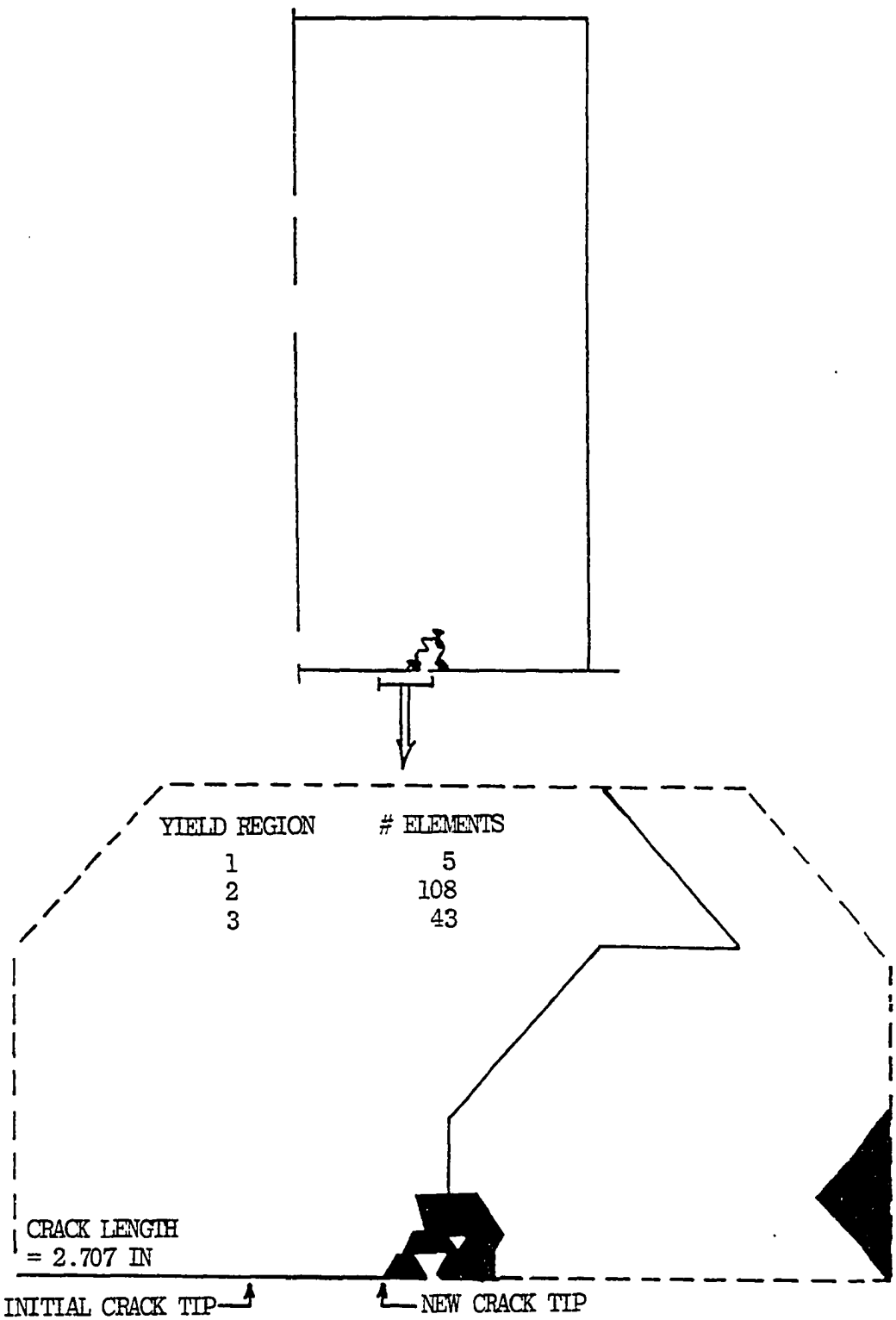

Figure 4.6e. Plastic Regions - Load = 34,000 LB

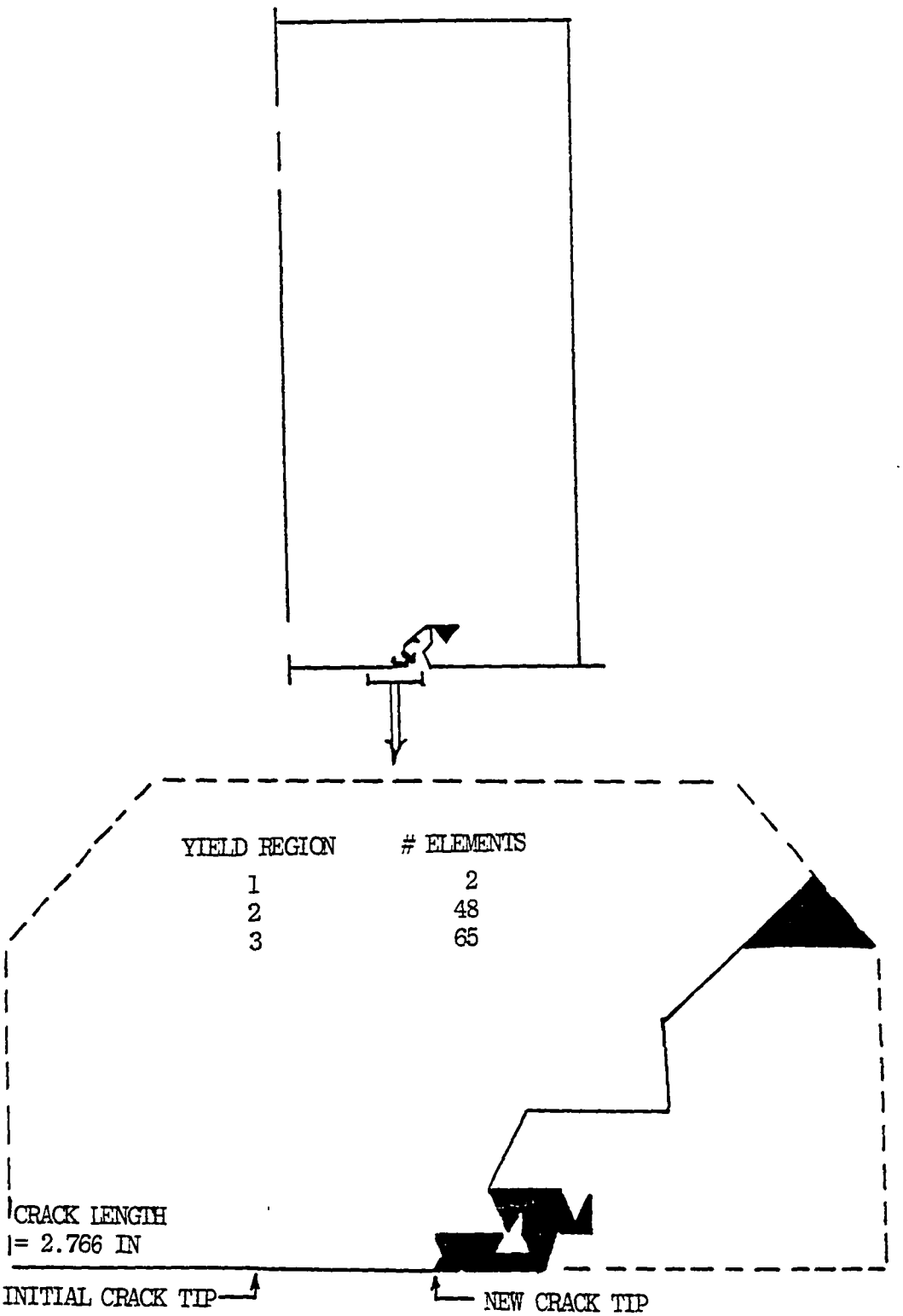

Figure 4.6f. Plastic Regions - Load = 36087 LB.

significant improvement was noted; therefore, only the engineering stress-strain programs, PANEL1 and FRACTURE, were used in the subsequent analyses.

IV.3 Cracked Panel Summary

The analysis of a centrally cracked panel under monotonically increasing load using the modified finite element program, PANEL, demonstrated that unstable fracture prediction using the FEM is highly dependent on the mesh size at the crack tip. Additionally, the prediction of stable fracture requires that a suitably refined mesh be extended along the entire length of the anticipated crack growth. For monotonically increasing load, accurate predictions can be made using the engineering stress-strain relation and initial specimen geometry.

CHAPTER V

TENSILE SPECIMEN ANALYSIS

V.1 Introduction

As mentioned in Chapter IV, the fracture prediction programs require stress-strain data all the way to ultimate load. This data is not generally published for the high strain range. Even if it were, the scatter in properties might introduce error into the analysis since published stress capabilities are normally statistical minimums. Therefore, the entire stress-strain curve was determined experimentally for the 2024-T3 sheet from which experimental specimens were fabricated. This data was converted to sectional modulus and Poisson's ratio which were then used in the program. Models of the tensile test specimens were also run in FRACTURE to evaluate the effectiveness of the program.

V.2 Experimental Study

The stress-strain relation for the 0.125 inch thick, 2024-T3 aluminum sheet used in the fractured specimen analysis (Chapter VI) was obtained from uniaxial tensile tests on specimens whose dimensions are shown in Figure 5.1. These specimens were loaded to fracture on a Riehle test machine which provides calibrated load data. Pin to pin deflections for the specimens were obtained from a spring loaded potentiometer attached to the pins. These deflections were recorded as a function of the applied load. The resultant load-deflection curves are plotted in Figure 5.2.

The loads (L) were converted to engineering stress (σ) by dividing by the original cross sectional area (A_0):

$$\sigma = L / A_0 \qquad (5.1)$$

Only pin to pin deflection data was obtained to avoid damage to instrumentation when specimens were loaded to catastrophic failure. It was therefore necessary to adjust the pin to pin deflection (D_{pp}) to a gage deflection (D_g). This was accomplished by selecting a two inch gage length on the neck section and assuming that outside this region the material remained elastic. An elastic finite element program, based on published Young's modulus and Poisson's ratio,[16] was then used to determine the relative elastic deflections between the pin and a point on the gage boundary

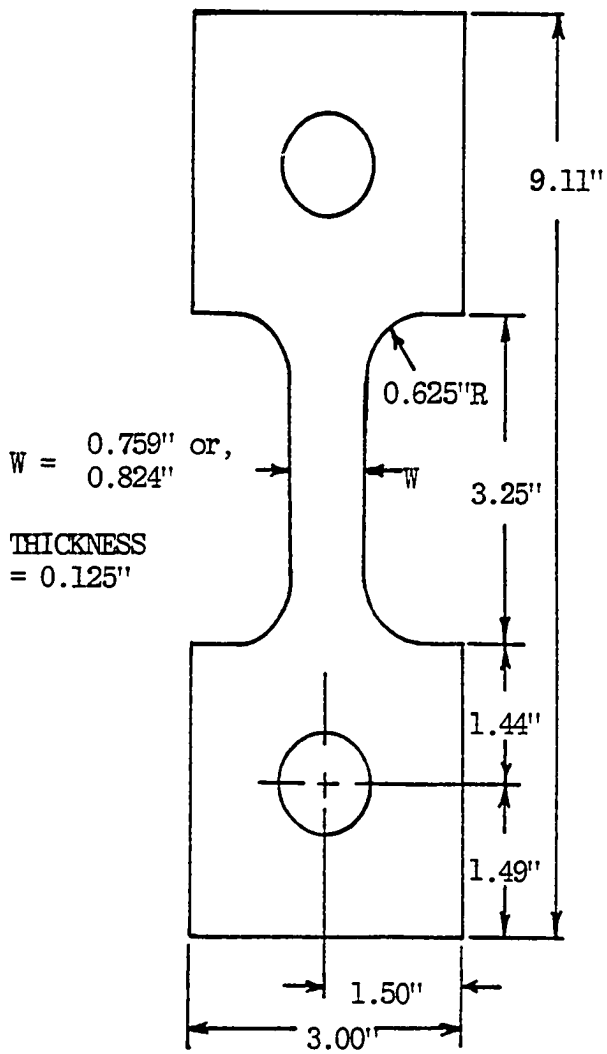

Figure 5.1. Tensile Test Specimen Dimensions.

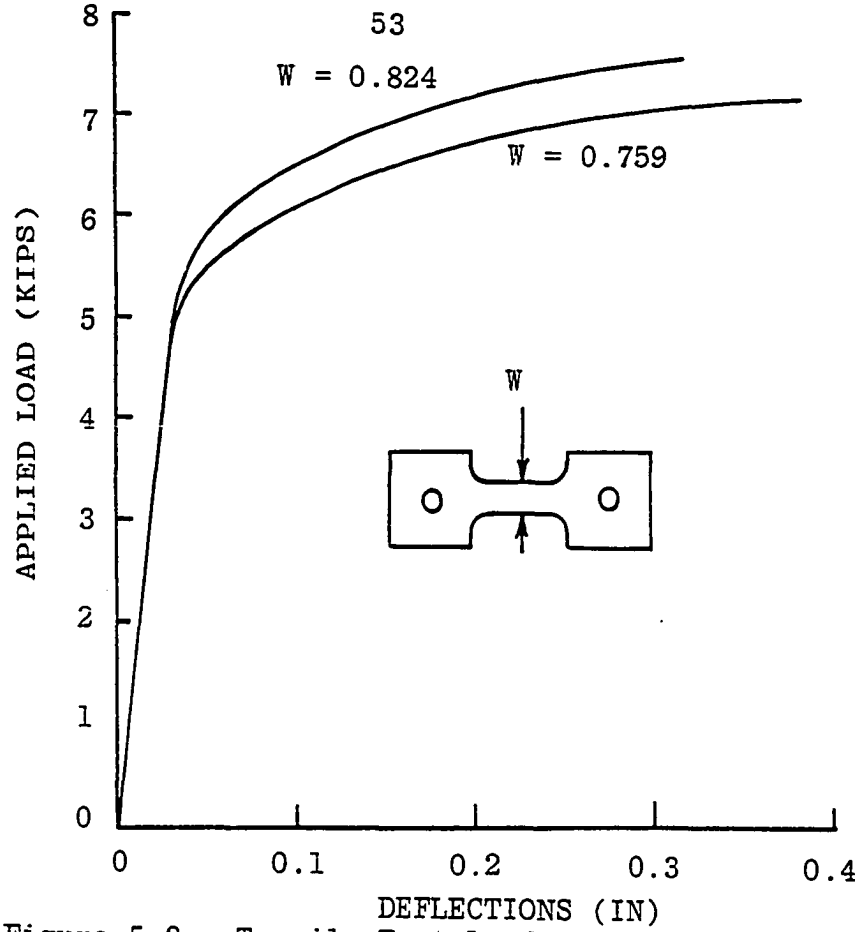

Figure 5.2. Tensile Test Load Deflection Curves.

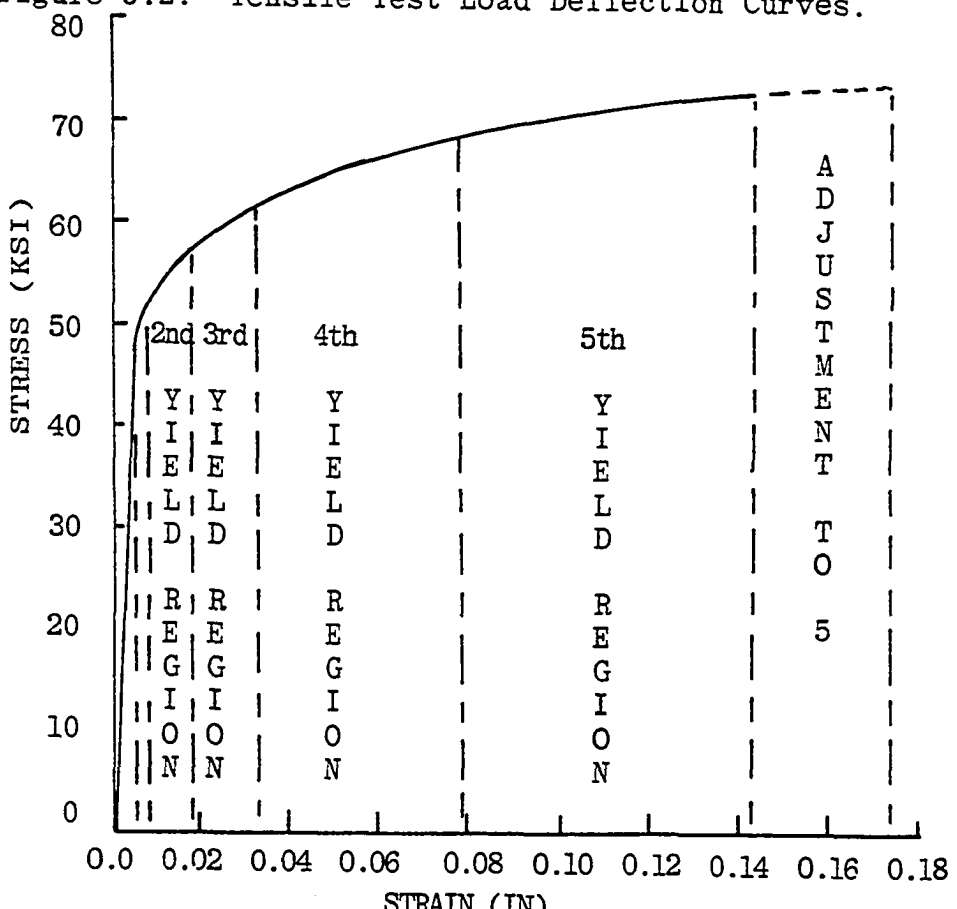

Figure 5.3. Linearized Stress-Strain Curve.

as a function of load. Calling this deflection D_r, the gage deflection is approximated by

$$D_g(L) \cong D_{pp}(L) - 2.0\ D_r(L)\ L \qquad (5.2)$$

The factor two in Eq. (5.2) results from there being two pin to gage boundary regions. While, as will be shown shortly, some plastic region exists outside of this gage region, the error is considered small. This results in a strain (ε) of the form

$$\varepsilon = D_g/2.0 \qquad (5.3)$$

or, in view of (5.2),

$$\varepsilon = (D_{pp}/2.0) - D_r\ L \qquad (5.4)$$

The resulting stress-strain curve is shown as the solid line in Figure 5.3. Note that the strain at fracture was initially determined from the 0.824 inch width specimen. The stress-strain curve was then approximated by the six linear sections as shown in Figure 5.3.

V.3 Finite Element Analysis

The finite element models from the mesh generator program were run in the FRACTURE program to test its ability to duplicate the load deflection curves which generated the stress-strain data used in the program. Figure 5.4a shows the original coarse mesh and Figure 5.4b shows a medium mesh. The medium mesh is refined in the area of the fillet and pin sections. The fine mesh is used at the midsection

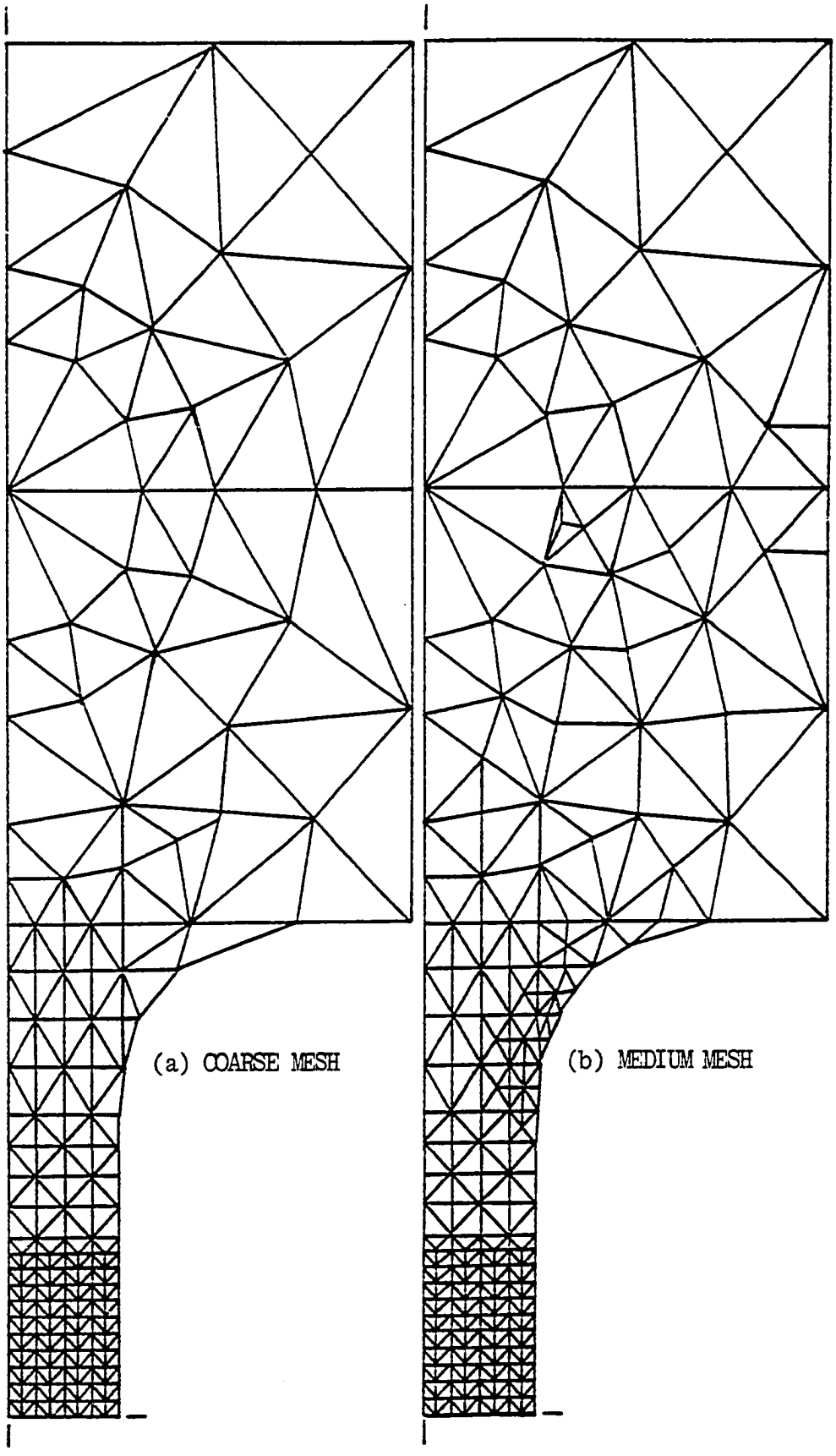

Figure 5.4. Tensile Test FEM Models.

in both models in anticipation of fracture in this area. Again, only one quadrant of the specimen was modeled due to symmetry.

Figure 5.5 shows a comparison of the results of the FEM analysis with the experimental loads and deflections. For the 0.824 inch wide specimen (used to obtain the stress-strain curve for the program), the results obtained from both meshes are very accurate; however, the medium mesh, with refinements in the pin and fillet areas, gives slightly more accurate results in the elastic and fracture regions. A further refinement of the mesh in the neck area was found to have negligible effect on the results. The results obtained for 0.759 inch wide coarse model shows good agreement with experimental results except at fracture, even though the material properties were obtained from the wider specimen. When a medium mesh (results not shown for clarity) was run for the 0.759" model, fracture occurred at approximately the same deflection as the 0.824" model, as opposed to the larger deflection of the test specimen. This suggests that, if the FEM analysis is assumed to be correct, the difference in deflections at fracture for the two experimental specimens is not accurate; indeed, the difference was traced to a slight anomaly in width of the 0.824" specimen. To compensate, the 0.824" load-deflection curve was extrapolated out to the 0.759" deflection at failure, and an adjustment, shown in Figure 5.3, was made to the program's

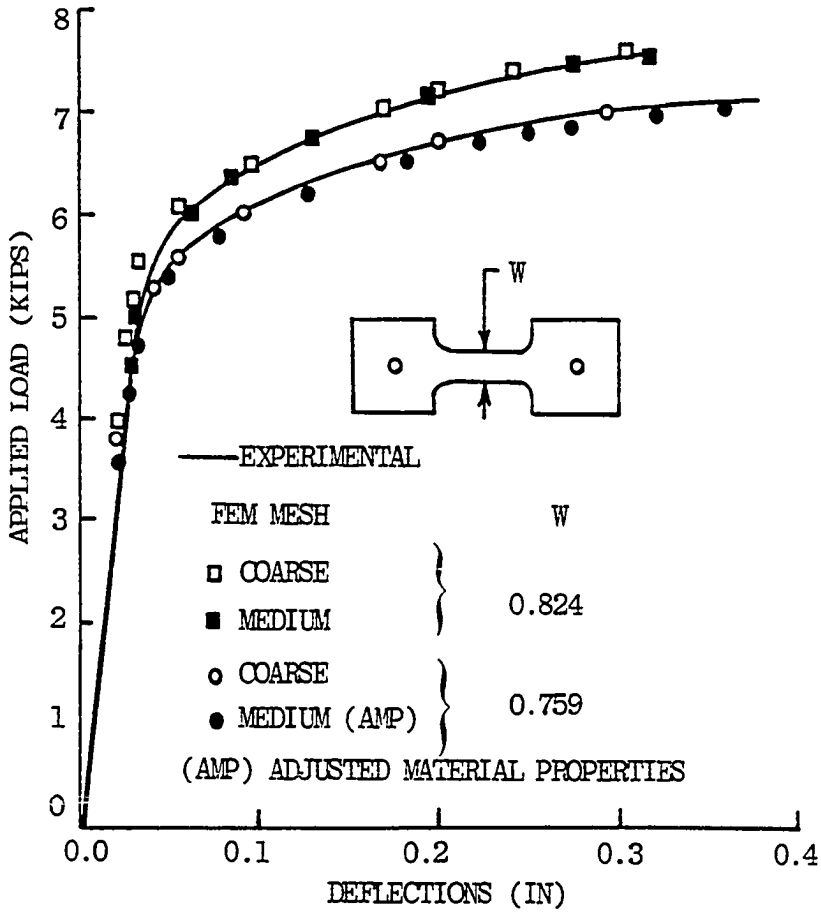

Figure 5.5. FEM Load Deflection Predictions for Tensile Test Specimens.

stress-strain data. The medium mesh was then used in the program with the new yield region 5 material properties. Correlation with the experimental results was much better. The remaining difference is most probably due to the fact that the deflection at fracture should be higher for the 0.824" specimen than for the 0.759" specimen since there is additional deflection in the elastic region for the 0.824" specimen due to its increased load carrying capability at fracture. The adjusted stress-strain curve was then used for the fracture studies of Chapter VI.

Not only did the program demonstrate the ability to accurately predict the load-deflection curves which generated its material properties, it also yielded the following important and useful data: First, note on Figure 5.5 that local yielding occurred well before yielding became apparent in the load deflection curve. Second, the program provided data on the progression of yield through the specimen. Figure 5.6 shows the smoothed yield response. Initial yielding occurs at the fillet as shown in Figure 5.6a. At a load of approximately 1000 pounds below the apparent yield, this region spreads through the fillet area and begins at the edge of the pin (while the yielding at the pin was confirmed by measuring the hole after fracture, the coarseness of the mesh in this region may not have given an accurate map of the yield zone). In Figure 5.6c, one element at the fillet has moved into the second yield region, the

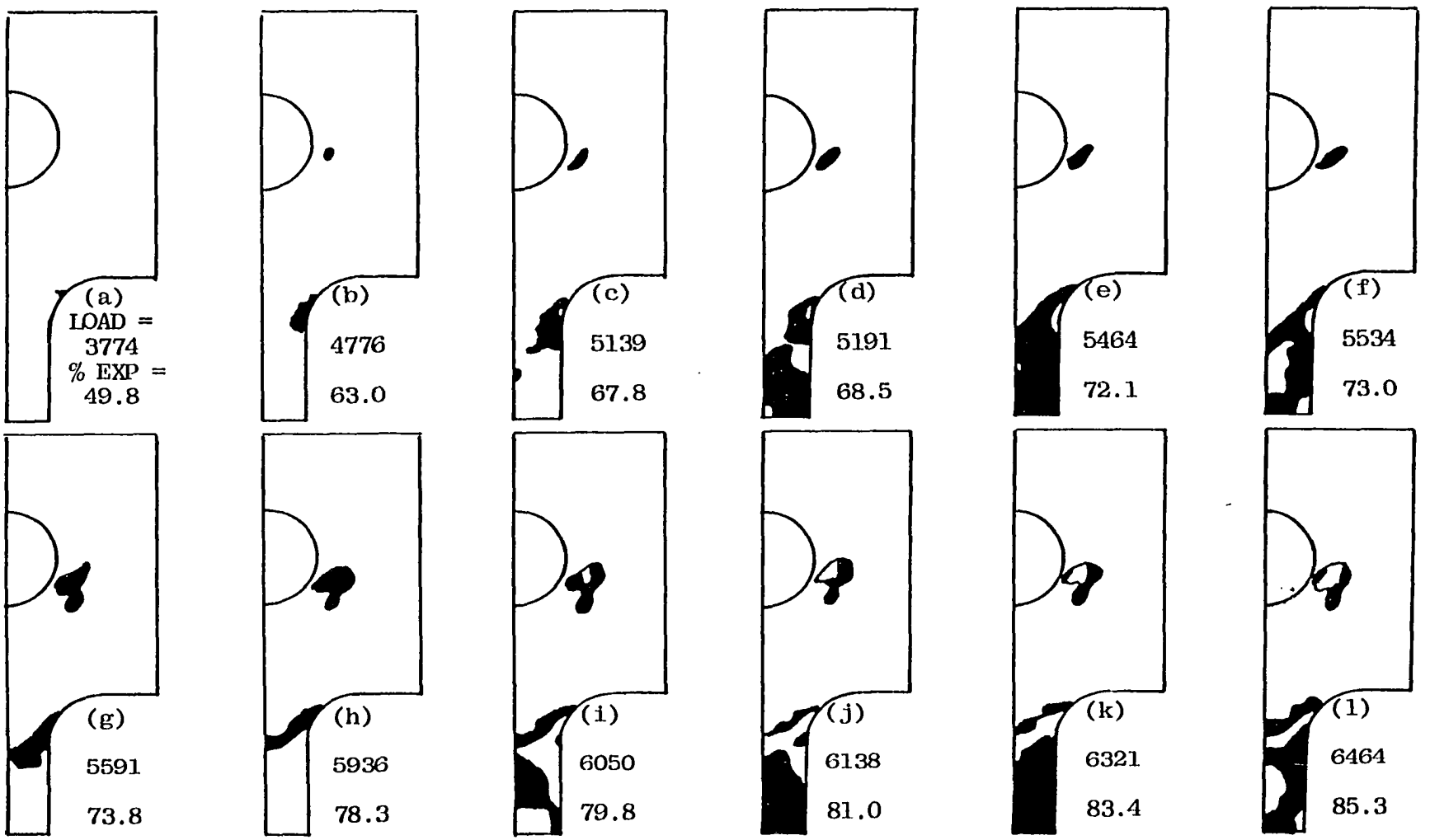

Figure 5.6. Yield Regions for Tensile Test Specimens.

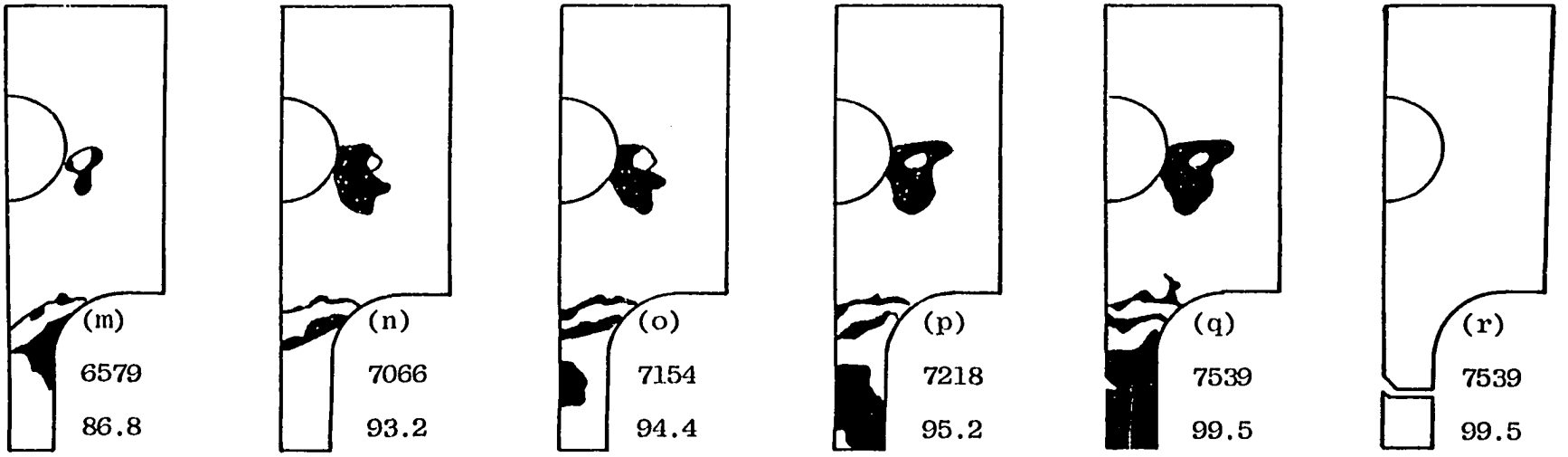

EXPERIMENTAL LOAD (EXP) = 7580 LB

FIGURE FIRST ENTRY INTO

(a) 1st YIELD REGION
(c) 2nd YIELD REGION
(i) 3rd YIELD REGION
(l) 4th YIELD REGION
(o) 5th YIELD REGION
(q) INITIAL FRACTURE
(r) FINAL FRACTURE

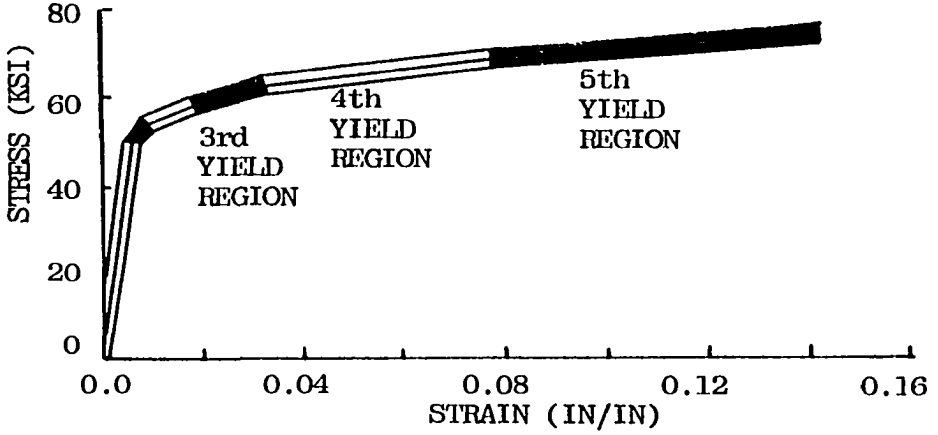

Figure 5.6 (cont). Yield Regions, Tensile Test Specimen.

fillet yield region has expanded, and yielding has begun on the center axis. In Figure 5.6d, the neck area is almost entirely involved in the first yield region. The two large white areas in the neck are still elastic. In Figure 5.6e, the entire neck is involved in the first yield region, the second yield region at the fillet is expanding, and second yield has occurred at the center axis. The second region at the fillet is expanding in Fig. 5.6f, g and h with the first yield region moving up to the base of the neck while the first yield zone spreads at the pin. In Figure 5.6i, third yield (dark area) is progressing in much the same way as the second did in Figure 5.6f. Also in Figure 5.6i, the second yield region is entered at the pin. Figure 5.6j and k show the further expansion of the third yield zone with Figure 5.6(l) showing the beginning of the fourth yield region. The first, second, and third yield zones are compressed toward the base of the neck as zone four expands in Figure 5.6m and n, with the pin zone continuing to expand. Fifth yield initiates from the center axis as shown in Figure 5.6(o). In Figure 5.6p the pin zone increases further along with the fifth yield region while zones one, two, three and four are pushed further toward the base of the neck. Initial fracture occurs in Figure 5.6q initiating from the center axis and propagating unstablely to the edge as shown in Figure 5.6r. Note that the FEM prediction for fracture load is 99.5% of the experimentally obtained load.

Third, as mentioned above, the FEM analysis predicted an initiation and unstable propagation of the crack from a point on the longitudinal centerline of the specimen. This phenomenon was confirmed on the test specimens by placing the fractured surfaces together and observing that the end sections fit together while the center sections did not. This is due to the increased plastic strain on the outer sections after the center section failed and unloaded. Failure of mildly notched tensile specimens from the center axis has also been reported by Drucker.[17] Since initial yield occurred at the fillet, and fracture initiated on the center axis, it can readily be seen that fracture initiation location can not be predicted by using the maximum elastic stress location. Fourth, while the mesh was refined on the mid-section in anticipation of failure along the centerline, the FEM prediction showed that fracture occurred off the mid-section centerline as shown in Figure 5.6r. Each of the tensile test specimens also broke along a line off the centerline. Figure 5.7 shows the location of fracture predicted by the FEM analysis and as occured in the tensile tests. The test specimens failed on a 45^{o} line through the thickness. This is the scatter band shown in the figure with the experimental location shown in both the deflected and undeflected geometries. Note that the FEM prediction indicates that a perfect specimen would break into three pieces. As can be seen, the FEM accurately predicts the failure location.

Finally, the load and deflection at fracture for both the experimental test and the FEM analysis are shown in Table 5.1. The load predictions for the medium mesh models are extremely accurate (less than three percent for the 0.759" specimen and less than one percent for the 0.824" specimen), and deflections are also a good approximation of measured values (about four percent and one percent for the two respective specimens). As previously discussed, accurate prediction of fracture deflection is highly dependent on accurate material maximum strain data.

V.4 Tensile Test Analysis Summary

The finite element program, FRACTURE, demonstrated the following capabilities for the analysis of two tensile test specimens:

1. Ability to predict load-deflection curves,
2. Ability to demonstrate the importance of local material properties,
3. Ability to provide data on the complete field response for the specimen, thus a better understanding of the failure process,
4. Ability to predict fracture initiation location, both with respect to the midsection and longitudinal axis, and
5. Ability to predict load and deflection at fracture.

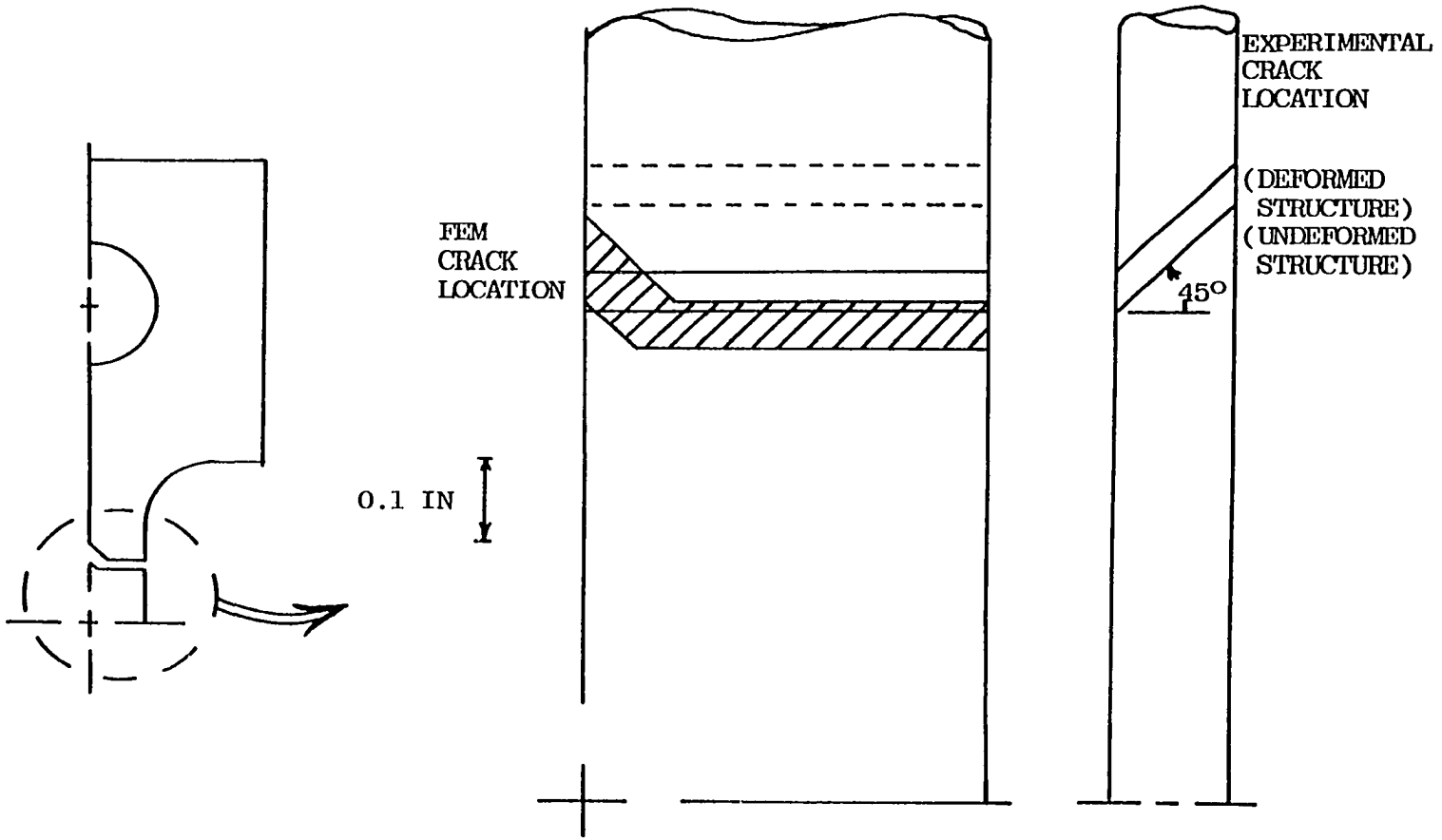

Figure 5.7. Crack Locations, FEM Predictions and Experimental Results for Tensile Test Specimen.

TABLE 5.1

COMPARISON OF EXPERIMENTAL AND FEM LOADS AND DEFLECTION AT FRACTURE

SPECIMEN	0.759"		0.824"	
	LOAD (lb)	DEFL. (in)	LOAD (lb)	DEFL. (in)
EXPERIMENTAL	7180	0.3750	7580	0.3125
COARSE MESH	6953	0.2928	7532	0.3035
PERCENT ERROR	3.16	21.92*	0.63	2.88
MEDIUM MESH	7015	0.3588	7539	0.3158
PERCENT ERROR	2.30	4.32	0.54	1.06

*Based on uncorrected stress-strain data.

CHAPTER VI

CRACKED SPECIMEN ANALYSIS

VI.1 Introduction

The tensile test specimen analysis demonstrated the effectiveness of the current method in predicting experimental behavior for mild stress concentrations and the panel study showed that for sufficiently fine meshes, this method can also predict load at fracture in specimens with severe stress concentrations (cracks). Unfortunately, no experimental deflection data was presented for the panel study; therefore, the ability of the program to predict load deflection curves for severely notched specimens could not be addressed without further testing. To obtain the needed data, three tensile test specimens were notched and loaded to fracture. Comparisons of this experimental data and the finite element predictions were made and are presented in this chapter.

VI.2 Experimental Tests

The testing procedure for notched specimens was the same as that presented in Chapter V, and the three specimens tested were made from blanks of the same dimensions as the 0.824" wide specimen of Chapter V. Sharp notches of lengths 0.008", 0.023", and 0.129" were then introduced in the blanks on one edge of the neck at the centerline. The 0.008" and 0.023" cracks were obtained using an X-Acto knife blade, and the 0.129" crack was machined on a band saw with the final tip also being formed by an X-Acto knife.

VI.3 Finite Element Analysis

Introduction of the single edge notch (SEN) in the specimen removed one plane of symmetry necessitating the use of a two quadrant finite element model. The overall mesh is shown in Figure 6.1a with details for the different crack lengths shown in Figure 6.1b, c, and d.

Figure 6.2 shows the same type of result that was demonstrated in Chapter IV, Figure 4.2; that is, the accuracy of the FEM predictions of fracture load is highly dependent on the element size at the tip of the crack.

The load deflection curves for two different size elements are shown in Figure 6.3. Note that the shape of the predicted curves are essentially the same. With large elements at the tip, the CST elements can not model the large

gradients at the tip, and therefore, the load and deflection exceed the experimental values. The slight upward trend in the load for the finer mesh is due to the size of the minimum load increments used to reduce the computational time. As the mesh is refined, the computational time increases due to increased band width of the stiffness matrix and the increased number of nodes and elements. The computational time can be reduced by increasing the minimum load increment; however, the predicted load and deflection at fracture are affected since elements tend to remain stiffer during the loading process.

The load deflection curves for the three different size notches are shown in Figure 6.4. The results improve as the crack size increases. This can be attributed to increasing the minimum load increment to allow enough time to advance the crack along the additional specimen width for smaller cracks. Also the deflections are slightly low for each given load. This same effect can be observed in Figure 5.5 for the tensile specimen coarse mesh. As discussed in Chapter V, the tensile predictions were improved by refining the mesh in the area of the fillet and pin.

Finally, the yield regions for a 0.023" initial crack size are plotted for selected loads in Fibure 6.5. The initial yield zone formation is shown in Figure 6.5a and b. Figure 6.5c and d show the first, second, third and fourth yield regions expanding outward from the crack tip. At the

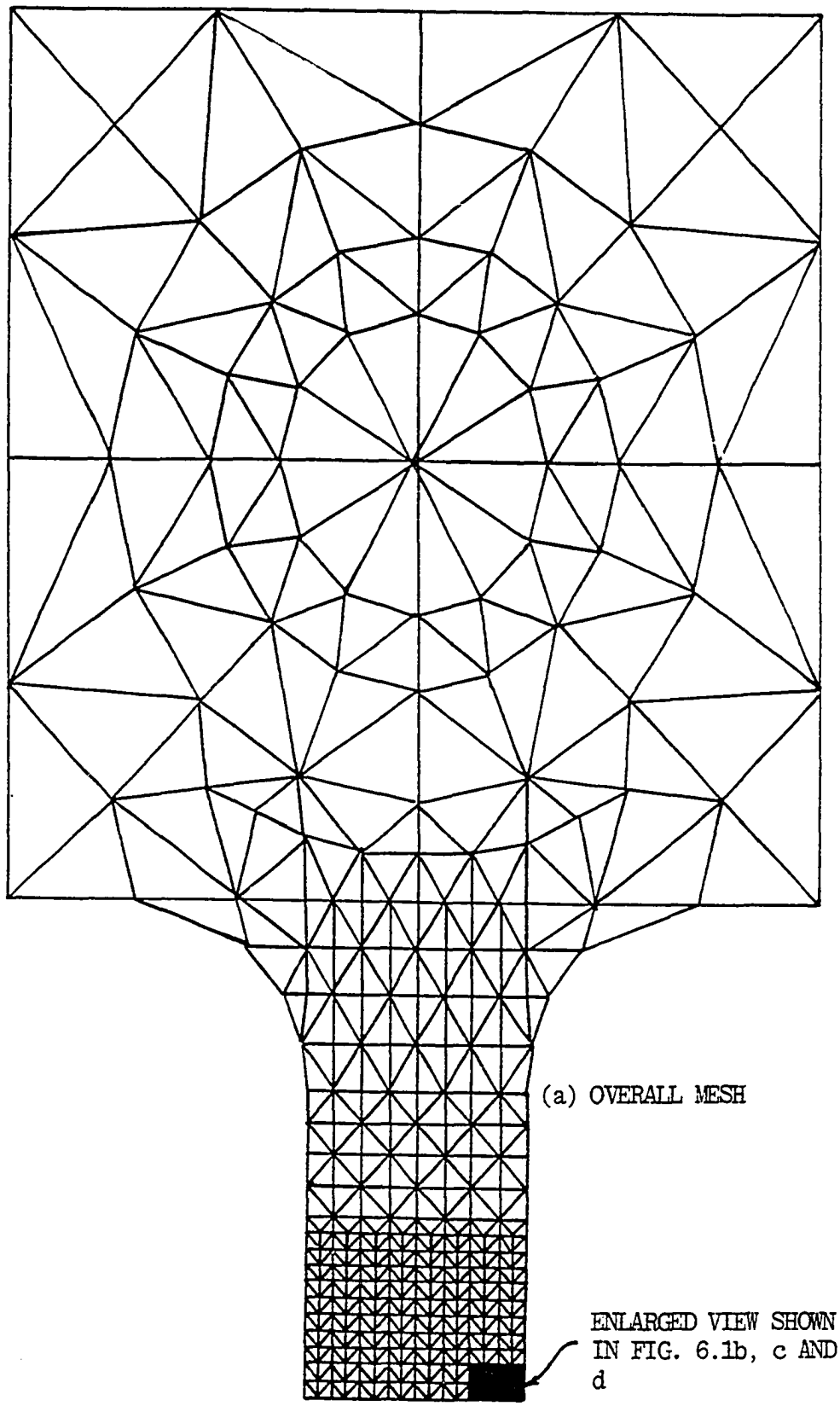

Figure 6.1. FEM Models of Cracked Specimens.

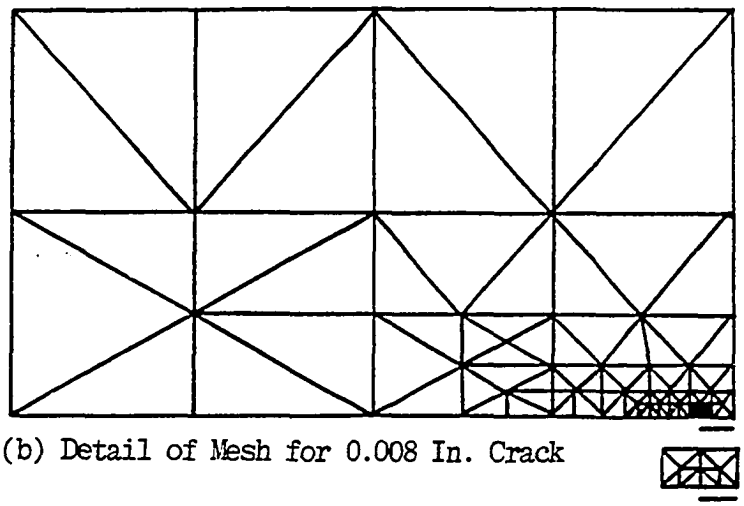

(b) Detail of Mesh for 0.008 In. Crack

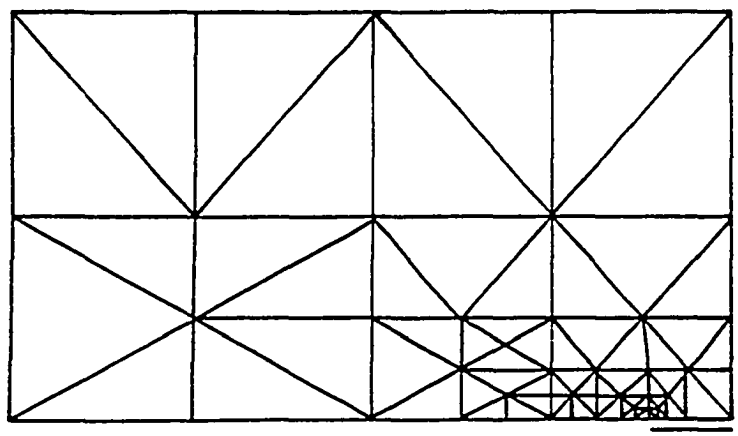

(c) Detail of Mesh for 0.023 In. Crack

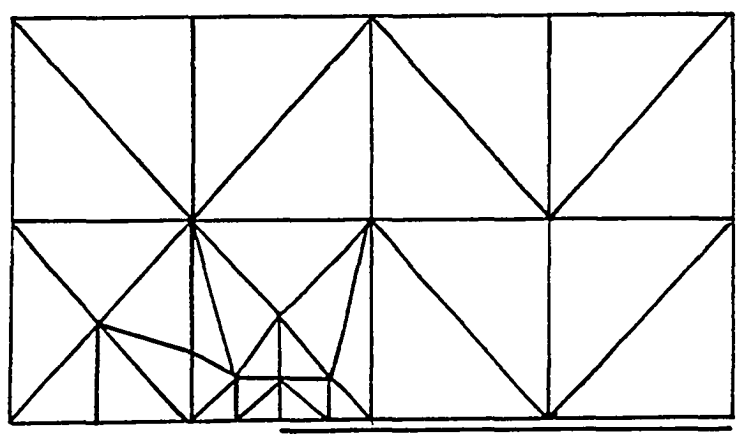

(d) Detail of Mesh for 0.129 In. Crack

Figure 6.1 (cont). FEM Models of Cracked Specimens.

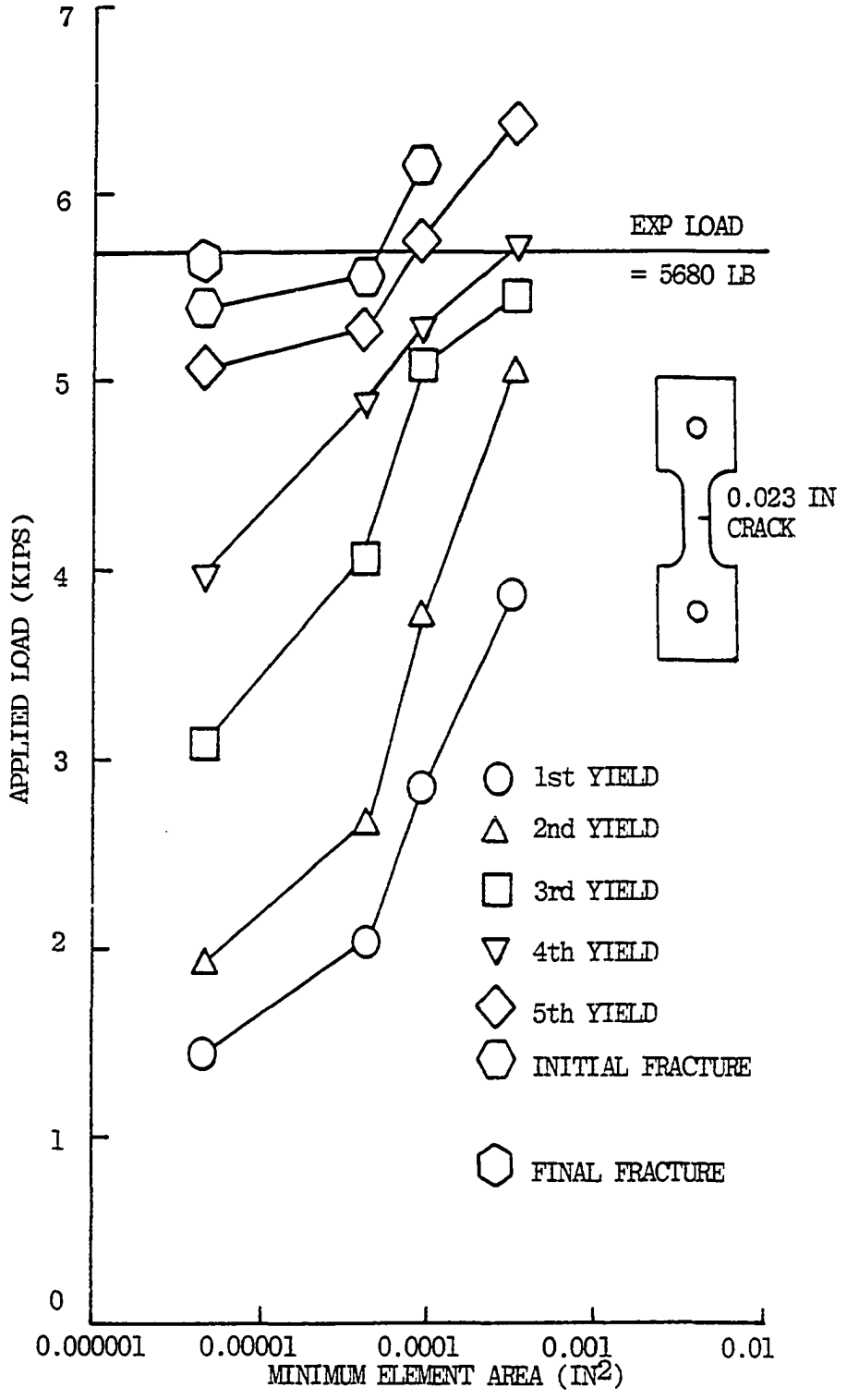

Figure 6.2. Numerical Convergence, Cracked Specimen Analysis.

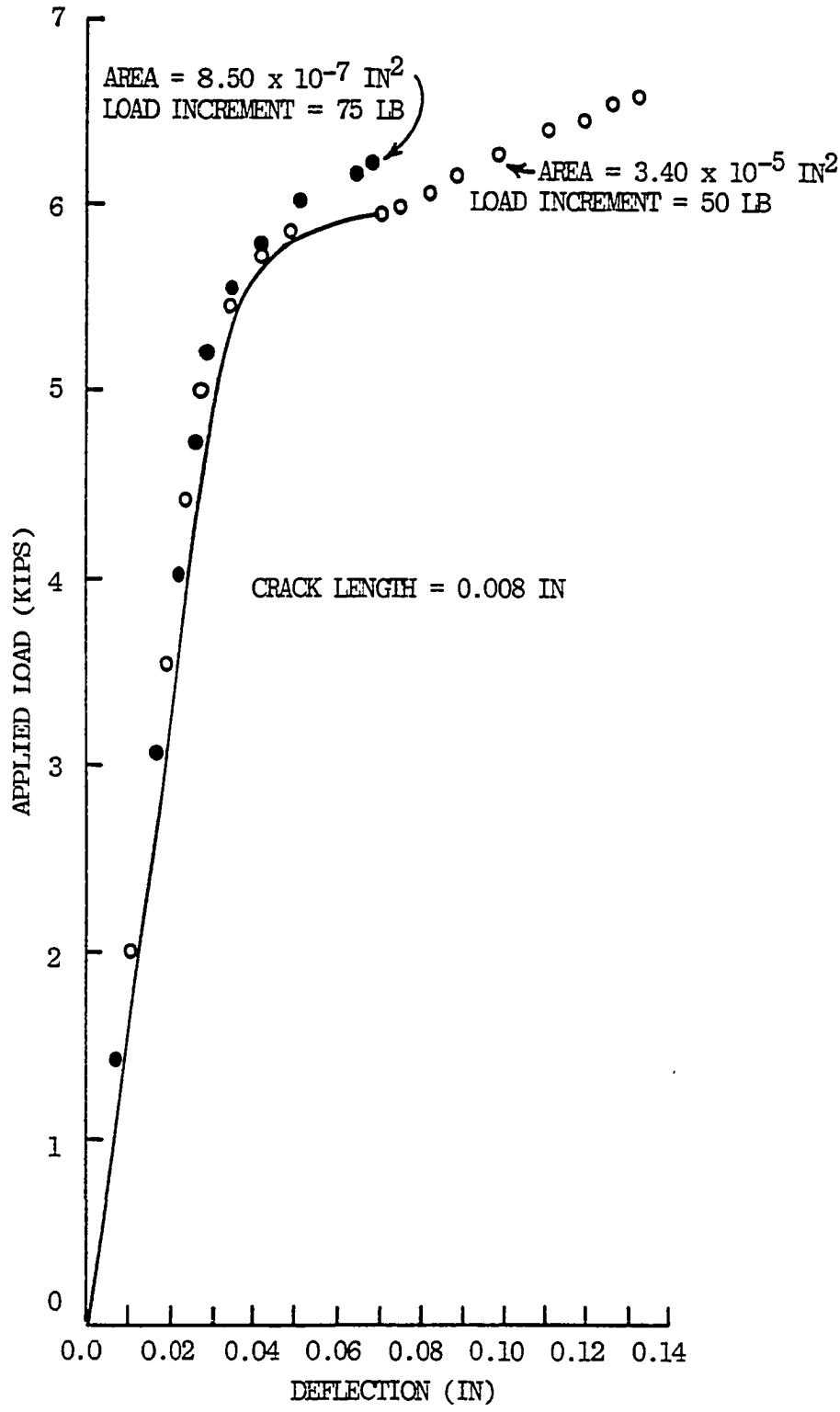

Figure 6.3. Effects of Load Increment and Element Size for the Cracked Specimen Analysis.

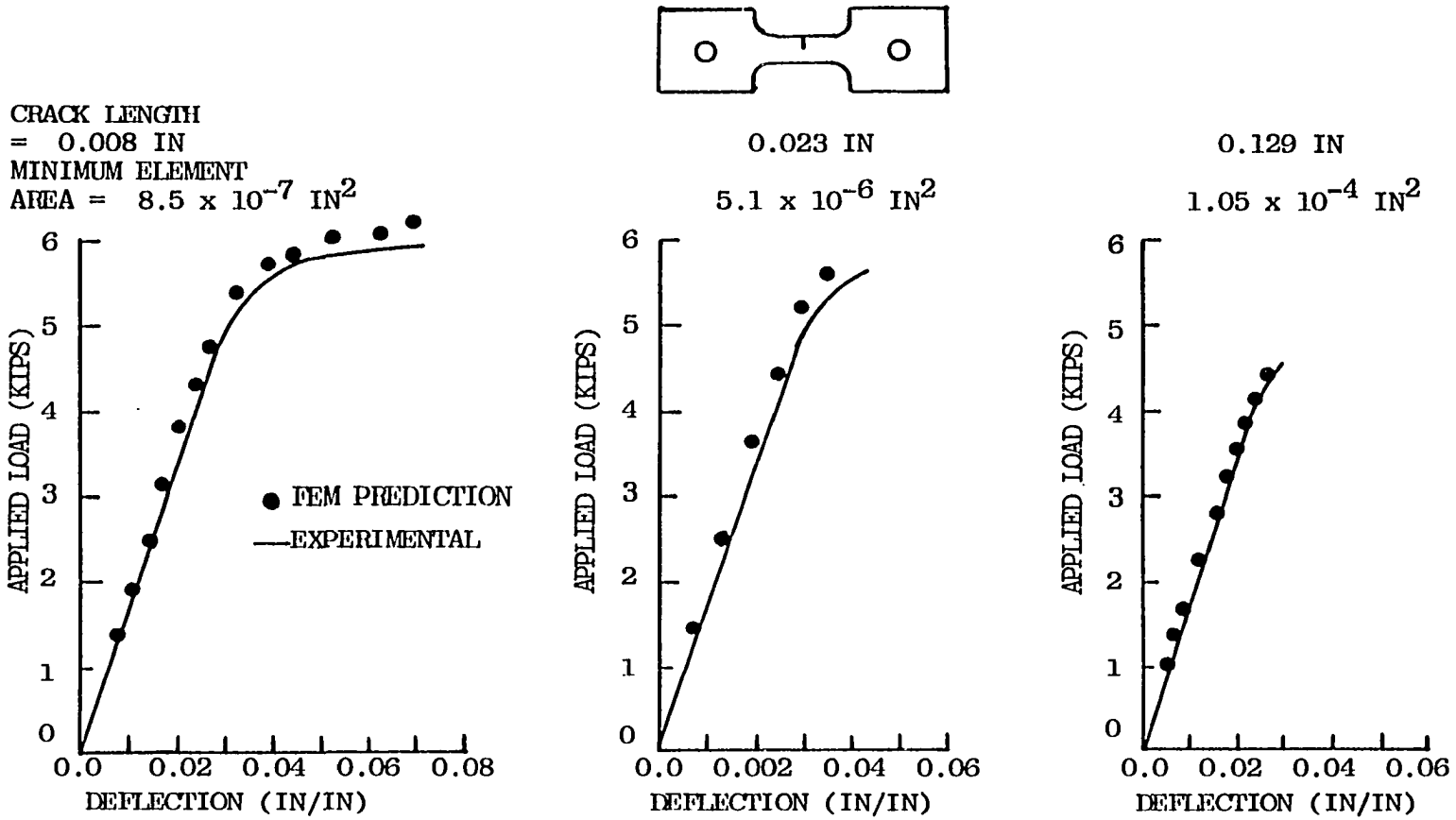

Figure 6.4. Load Deflection Curves for Cracked Specimen Analysis.

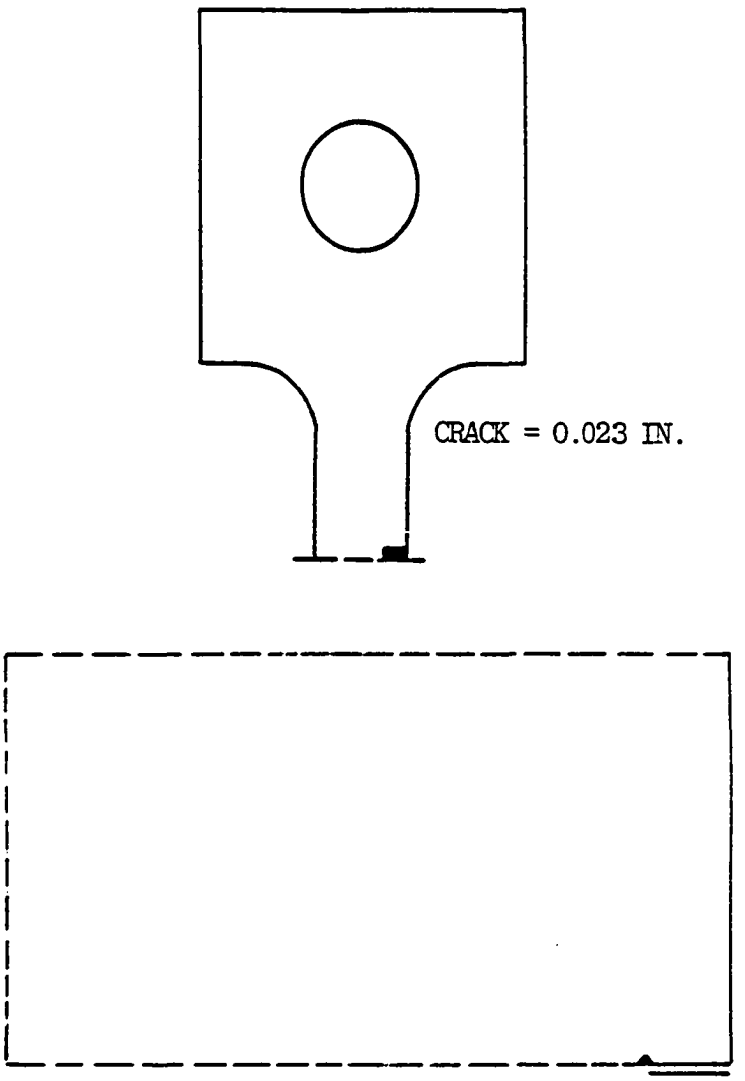

Figure 6.5a. Yield Regions, Load = 1806 LB.

Figure 6.5b. Yield Regions, Load = 3020 LB.

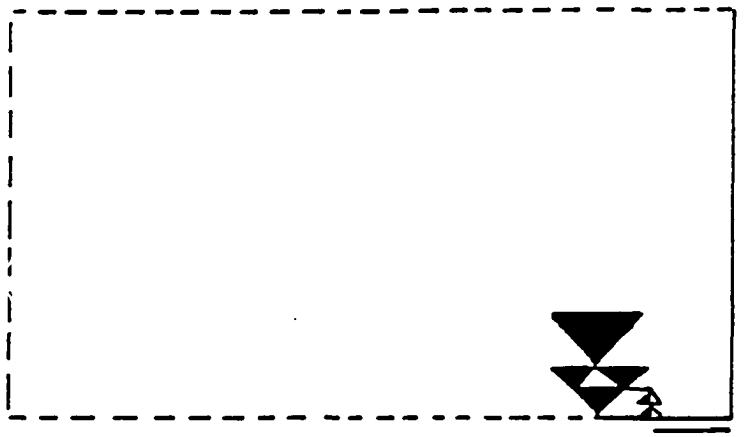

Figure 6.5c. Yield Regions, Load = 4000 LB.

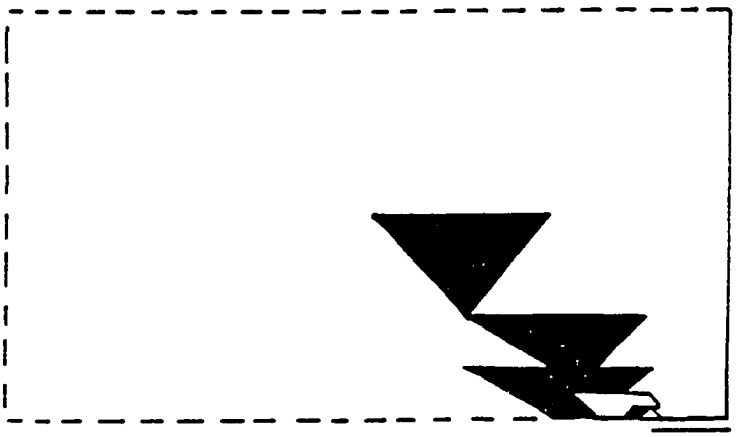

Figure 6.5d. Yield Regions, Load = 4500 LB.

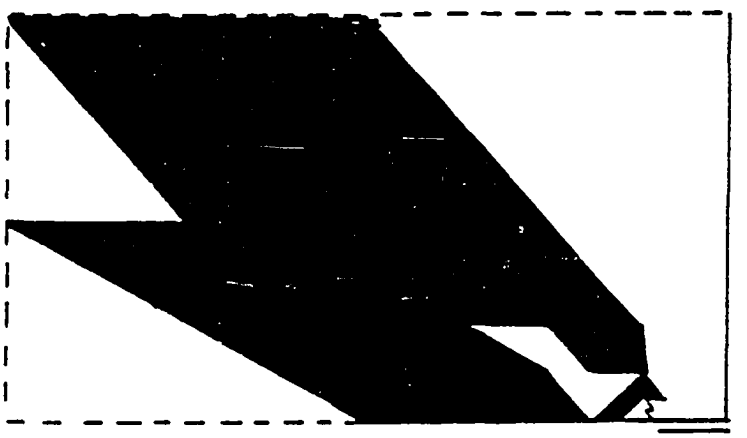

Figure 6.5e. Yield Regions, Load = 5000 LB.

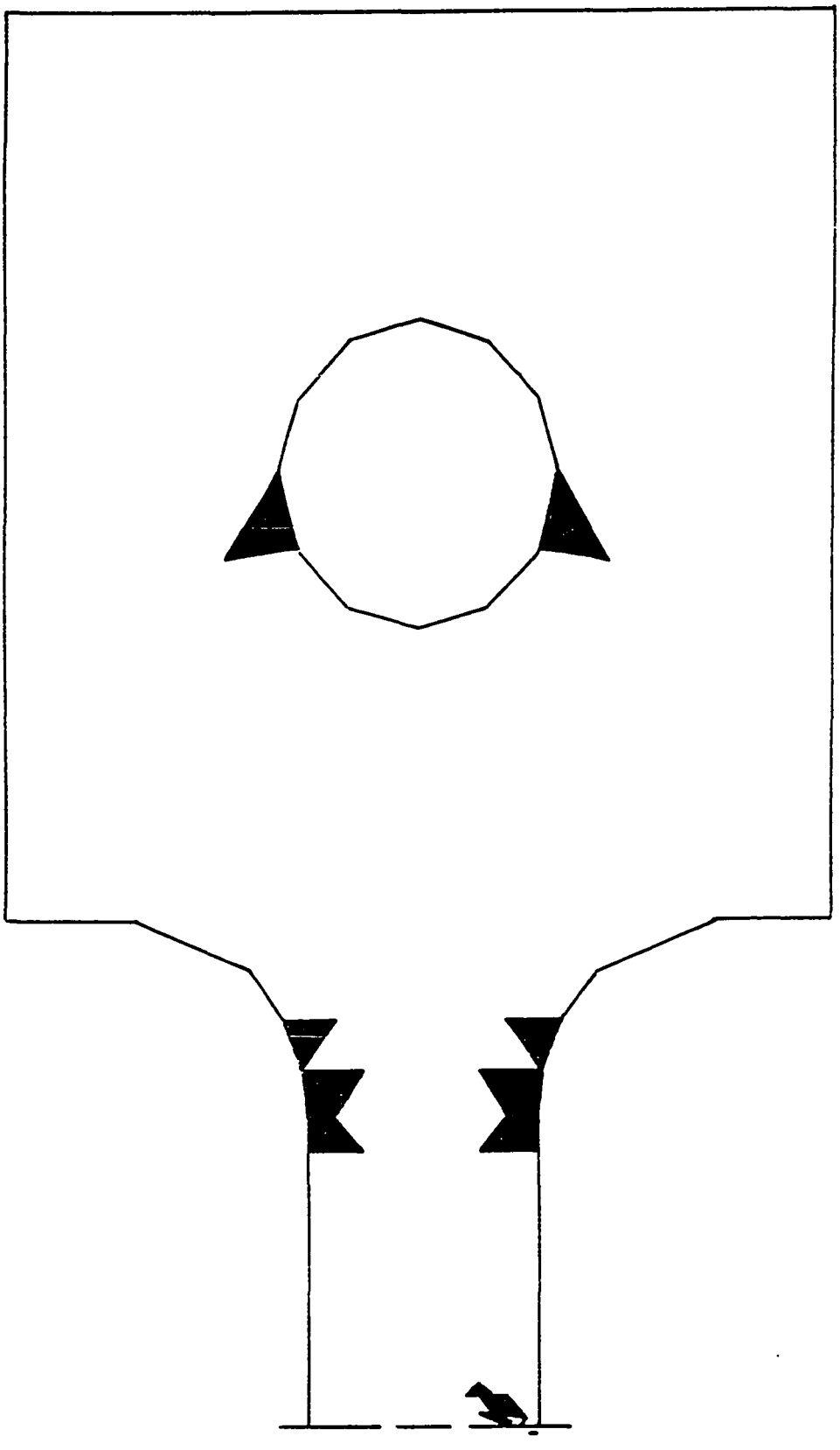

Figure 6.5f. Yield Regions, Load = 5000 LB, Overall Results.

Figure 6.5g. Yield Regions, Load = 5200 LB.

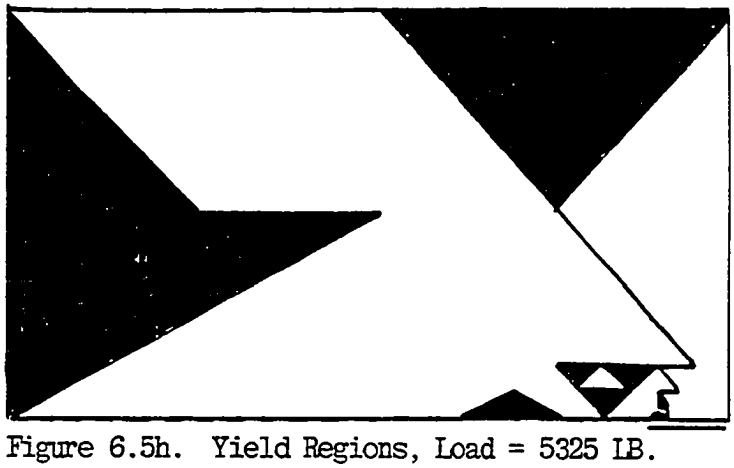

Figure 6.5h. Yield Regions, Load = 5325 LB.

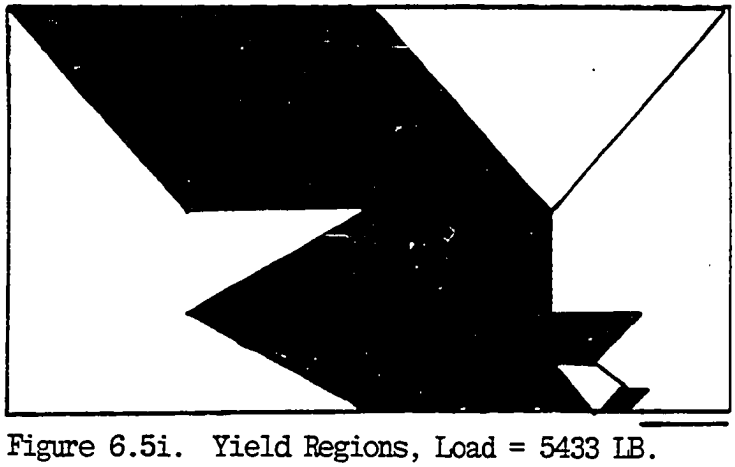

Figure 6.5i. Yield Regions, Load = 5433 LB.

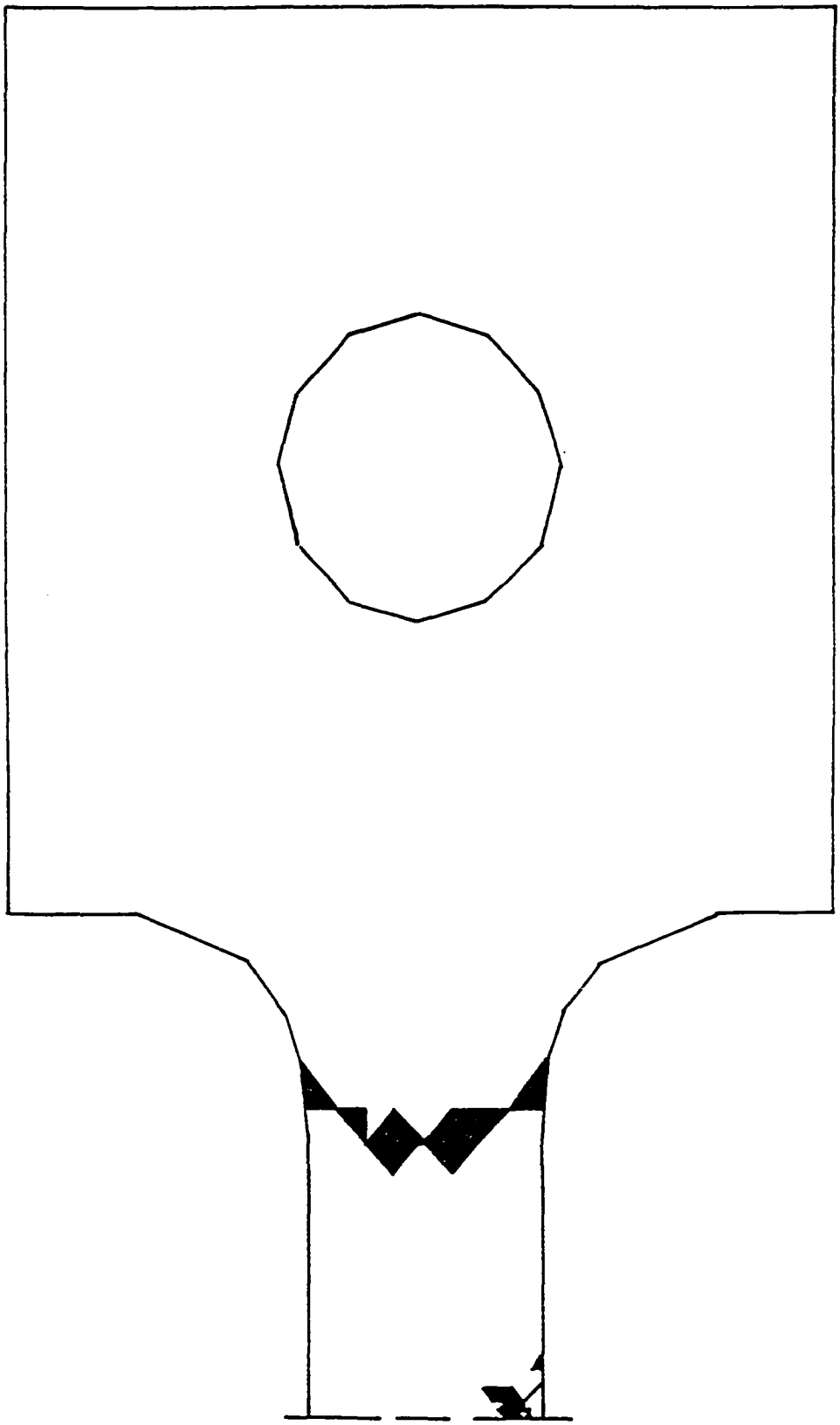

Figure 6.5j. Yield Regions, Load = 5433 LB, Overall Results.

load that corresponds to Fig. 6.5c, yielding also begins at the hole. The first yield zone extends past the enlarged area of the figure (as shown in Figure 6.5e) with the entire specimen shown in Figure 6.5f for the same load. Figures 6.5g, h and i show the further advance of the yield zones as load increases. At load level corresponding to Figure 6.5g, all five zones are present. In Figure 6.5h, the specimen has reached the load at which initial fracture occurs and Figure 6.5i shows the zones just prior to unstable fracture. Notice that the entire neck, except at the tip, is in the second yield region.

VI.4 Cracked Specimen Analysis Summary

The FEM analysis of the sharply notched specimens described in this chapter further verifies the abilities demonstrated in the previous two chapters, and confirms the ability to predict specimen deflections for sharply notched specimens.

CHAPTER VII

CONCLUSIONS AND RECOMMENDATIONS

The finite element program developed during this study has been shown to predict load deflection curves, load and deflection at fracture, fracture paths, initiation sites, crack growth, and stable or unstable crack propagation. The accuracy of the method is highly dependent on the element size along the crack path. The use of properly refined meshes yields accurate results.

The method is completely general in that it can analyze any two-dimensional isotropic structure subjected to plane stress and uniaxial loading. The loading restriction can be removed by substituting a failure criterion which is more suitable than the maximum strain criterion. While this method represents a valuable design tool for a limited class of problems, it more importantly demonstrates the potential of the finite element method for the direct prediction of fracture. The current program required only minor alterations to a standard plane stress finite element program to

give accurate analysis of elasto-plastic fracture problems. Since finite element programs have already been written to analyze plane strain, three dimensional and thermal loading problems, if similar modifications could be made to these programs, then it would be possible to directly predict fracture for these cases under monotonically increasing load. The only restriction on this approach appears to be the computer storage and computational time. These become less significant as the program effectiveness improves, refinements such as substructuring are incorporated, better solution techniques are found, and as computer capabilities continue to expand.

The direct prediction of cyclic fracture would be an even more valuable application of the approach contained in this work. Again the basic procedures developed in this study should apply with appropriate modifications.

Each of these capabilities needs to be verified, but the excellent results obtained in the present study suggest that the concept is valid and worthy of further development. The rewards for such a work could be enormous.

BIBLIOGRAPHY

1. Wood, H. A., and Trapp, W. J. "Research and Application Problems in Fracture of Materials and Structures in the United States Air Force." Engineering Fracture Mechanics, Vol. 5, 1973, pp. 119-145.

2. Hoeppner, D. W., and Krupp, W. E. "Prediction of Component Life by Application of Fatigue Crack Growth Knowledge." Engineering Fracture Mechanics, Vol. 6, 1974, pp. 47-70.

3. Boyd, G. M. "From Griffith to COD and Beyond." Engineering Fracture Mechanics, Vol. 4, 1972, pp. 459-482.

4. Anderson, H. "A Finite-Element Representation of Stable Crack Growth." J. Mech. Phys. Solids, Vol. 21, 1973, pp. 337-356.

5. Light, M. F., Luxmore, A., and Evans, W. T. "Prediction of Slow Crack Growth by a Finite Element Method." International Journal of Fracture, Vol. 11, 1975, p. 1045.

6. Newman, J. C. Jr., and Arman, H. Jr. "Elastic-Plastic Analysis of Propagating Crack under Cyclic Loading." AIAA Journal, Vol. 13, No. 8, 1975, pp. 1017-1023.

7. Ogura, K., and Ohji, K. "FEM Analysis of Crack Closure and Delay Effect in Fatigue Crack Growth under Variable Amplitude Loading." Engineering Fracture Mechanics, Vol. 9, 1977, pp. 471-480.

8. Ohji, K., Ogura, K., and Ohkubo, Y. "Cyclic Analysis of a Propagating Crack and its Correlation with Fatigue Crack Growth." Engineering Fracture Mechanics, Vol. 7, 1975, pp. 457-464.

9. Socie, D. F. "Prediction of Fatigue Crack Growth in Notched Members under Variable Amplitude Loading Histories." Engineering Fracture Mechanics, Vol. 9, 1977, pp. 849-865.

10. Newman, J. C. Jr. "Finite-Element Analysis of Crack Growth under Monotonic and Cyclic Loading." ASTM STP 637, American Society for Testing and Materials, 1977, pp. 56-80.

11. Miller, R. E. Jr., Backman, B. F., Hansteen, H. B., Lewis, C. M., Samuel, R. A., and Varanasi, S. R. "Recent Advances in Computerized Aerospace Structural Analysis and Design." Computers and Structures, Vol. 7, 1977, pp. 315-326.

12. Zienkiewicz, O. C. The Finite Element Method in Engineering Science. London: McGraw-Hill, 1971.

13. Bert, C. W., Mills, E. J., and Hyler, W. S. "Effect of Variation in Poisson's Ratio on Plastic Tensile Instability." Journal of Basic Engineering, Trans. ASME, Vol. 89D, 1967, pp. 35-39.

14. Nadai, A. Theory of Flow and Fracture of Solids. Vol. 1, 2nd ed. New York: McGraw-Hill, 1950, pp. 379-387.

15. Aerospace Structural Metals Handbook, Vol. II. Syracuse: Syracuse University Press, 1963.

16. MIL-HDBK-5. Department of Defense, 1962.

17. Drucker, D. C. "A Continuum Approach to the Fracture of Metals." Fracture of Solids, Proceedings, Institute of Metals Division, American Institute of Mining, Metallurgical, and Petroleum Engineers, 1962, pp. 3-50.

APPENDIX I

THE FINITE ELEMENT PROGRAM, FRACTURE

This appendix contains the finite element FRACTURE. A sample of the program output is also included at the end of the program.

```
C     ************************************************************************
C     *                                                                      *
C     *                            FRACTURE                                  *
C     *                                                                      *
C     *                     BY R.G. BELIE, 11 APRIL 1978                     *
C     *                                                                      *
C     *       A FINITE ELEMENT PROGRAM WITH ELASTOPLASTIC                    *
C     *       CRITERIA TO PREDICT CRACK GROWTH IN MONOTONICALLY              *
C     *       LOADED PLANAR STRUCTURES                                       *
C     *                                                                      *
C     *  **          MODIFICATIONS OF SUBROUTINES WRITTEN          **      *
C     *  **               BY J.N. REDDY ARE ANNOTATED              **      *
C     *                                                                      *
C     ************************************************************************
C
C
0001        IMPLICIT REAL*8(A-H,O-Z)
0002        DIMENSION X(500),Y(500),NOD(800,3),VBDY(100),U( 900)
           1,GSTIF( 900,62),          IBDY(100),ET(10,2),XNUT(10,2),STRAIN(10,2
           2),IEP(800),EXT(800),EYT(800),EZT(800),GXYT(800),IEF(300),EXEL(800)
           3 ,EYEL(800),EZEL(800),GXYEL(800),B(800,3),C(800,3),ECH(800)
0003        NRMAX=900
0004        NCMAX=62
0005        NRMAXH=NRMAX/2
0006        NEMMAX=800
0007        NDF=2
0008        NPE=3
0009        ITFAIL=0
0010        FLOAD=0.0
0011        XLOAD=0.0
0012        ITIME=1
C
0013        CALL IREAD(NNM,NEM,NRMAX,NCMAX,NDF,NPE,NBDY,NHBW,NEQ,NRMAXH,
           1NEMMAX,X,Y,NOD,VBDY,IBDY,ISTYPE)
C
0014        CALL PROP(ET,XNUT,STRAIN,IEP,NEMMAX,ECH)
C
0015      2 CALL ASSEM(NNM,NEM,NRMAX,NCMAX,NDF,NPE,NBDY,NHBW,NEQ,NRMAXH,
           1NEMMAX,X,Y,NOD,GSTIF,B,C, VBDY,IBDY,ET,XNUT,IEP,ITFAIL,ECH,ITIME,
           2STRAIN)
C
0016        CALL SOLVE1(NRMAX,NCMAX,NEQ,NHBW,GSTIF,U)
C
0017        CALL FAIL(ITIME,U,NRMAX,XLOAD,B,C,NEM,XNUT,STRAIN,IEF,NEMMAX,
           1EXT,EYT,EZT,GXYT,NEF,NOD,IEP,FLOAD,XLOADI,EXEL,EYEL,EZEL,GXYEL,
           2IFTYPE,ISTYPE,ECH,UTI,UII)
C
0018        CALL CHANG(IEF,IEP,NEF,NEMMAX,ECH,STRAIN)
C
0019        ITIME=2
0020        IF(ITIME.EQ.2)GO TO 2
0021        STOP
0022        END
```

```
0001            SUBROUTINE IREAD(NNM,NEM,NRMAX,NCMAX,NDF,NPE,NBDY,NHBW,NEQ,NRMAXH,
               1NEMMAX,X,Y,NOD,VBDY,IBDY,ISTYPE)
      C
      C     THIS SUBROUTINE READS AND PRINTS OUT GEOMETRIC AND CONSTRAINT
      C     DATA, AND CALCULATES THE HALF BAND WIDTH, NHBW
      C
0002            IMPLICIT REAL*8(A-H,O-Z)
0003            DIMENSION X(NRMAXH),Y(NRMAXH),NOD(NEMMAX,NPE),VBDY(100),IBDY(100)
      C     ....READ IN DATA FROM THE MESH GENERATOR....
0004            READ(5,900)ISTYPE,IDIV,DCRACK,WHBAR,DHBAR,WHTOP,DTOP,DHOLE,RHOLE,R
               1FIL
0005          900 FORMAT(I1,I2,8F8.4)
0006            GO TO (1,2,3,4),ISTYPE
0007            1 WRITE(6,981)
0008              GO TO 5
0009            2 WRITE(6,982)
0010              GO TO 5
0011            3 WRITE(6,983)
0012              GO TO 5
0013            4 WRITE(6,984)
0014            5 IIDIV=IDIV*8
0015              WRITE(6,985)IIDIV ,WHBAR,DHBAR,WHTOP,DTOP,RHOLE,DHOLE,RFIL
0016          981 FORMAT(1H1,48X,'MESH FOR FRACTURE STUDY',//,48X,'SINGLE EDGE NOTC'
               1,'H SPECIMEN'//)
0017          982 FORMAT(1H1,48X,'MESH FOR FRACTURE STUDY',//,48X,'DOUBLE EDGE NOTC'
               1,'H SPECIMEN'//)
0018          983 FORMAT(1H1,48X,'MESH FOR FRACTURE STUDY',//,48X,'90 DEG EDGE NOTC'
               1,'H SPECIMEN'//)
0019          984 FORMAT(1H1,48X,'MESH FOR FRACTURE STUDY',//,48X,'ASSYMM EDGE NOTC'
               1,'H SPECIMEN'//)
0020          985 FORMAT(1H ,15X,'DIVISIONS AT CENTER SECTION = ',I3,
               1', BAR HALF WIDTH = ',F8.4,', BAR HALF LENGTH = ',F8.4,//,16X,
               2'TOP HALF WIDTH = ',F8.4,', TOP LENGTH = ',F8.4,' , HOLE RADIUS ='
               3,' ',F8.4,', LOCATION FROM THE TOP = ',F8.4, //,16X,'FILLET RADIU'
               4,'S = ',F8.4,///)
0021              READ(5,932)NNM
0022              WRITE(6,902)NNM
0023          902 FORMAT(1H ,'THE NUMBER OF NODES = ',I4,//,1H ,3('NODE',9X,'X',15X,
               1'Y',12X)/)
0024              NM=NNM-2
0025              DO 15 I=1,NM,3
0026              READ(5,930) N,X(N),Y(N),NI,X(NI),Y(NI),NNN,X(NNN),Y(NNN)
0027              WRITE(6,931)N,X(N),Y(N),NI,X(NI),Y(NI),NNN,X(NNN),Y(NNN)
0028           15 CONTINUE
0029          930 FORMAT(3(I4,2F10.4))
0030          931 FORMAT(1H ,3(I4,2(3X,E12.5),8X))
0031              NNN=NNM/3
0032              NNN=NNN*3
0033              IF(NNN.EQ.NNM-1) READ(5,930)N,X(N),Y(N)
0034              IF(NNN.EQ.NNM-1)WRITE(6,931)N,X(N),Y(N)
0035              IF(NNN.EQ.NNM-2) READ(5,930)N,X(N),Y(N),NI,X(NI),Y(NI)
0036              IF(NNN.EQ.NNM-2)WRITE(6,931)N,X(N),Y(N),NI,X(NI),Y(NI)
```

```
0037              READ(5,932)NEM
0038            932 FORMAT(I4)
0039              NE=NEM-2
0040              WRITE(6,951)NEM
0041            951 FORMAT(//,1H ,'THE NUMBER OF ELEMENTS IS ',I4,//)
0042              WRITE(6,950)
0043            950 FORMAT(2X,////,    ' ELEMENT CONNECTIVITY',//,
                   11X,3(7X,'ELEM  NODE1 NODE2 NODE3')//)
0044              DO 20 I=1,NE,3
0045              READ(5,933)NE1,NOD(NE1,1),NOD(NE1,2),NOD(NE1,3),
                  1             NE2,NOD(NE2,1),NOD(NE2,2),NOD(NE2,3),
                  2             NE3,NOD(NE3,1),NOD(NE3,2),NOD(NE3,3)
0046             20 WRITE(6,93)NE1,NOD(NE1,1),NOD(NE1,2),NOD(NE1,3),
                  1             NE2,NOD(NE2,1),NOD(NE2,2),NOD(NE2,3),
                  2             NE3,NOD(NE3,1),NOD(NE3,2),NOD(NE3,3)
0047            933 FORMAT(12I4)
0048             93 FORMAT(2X,3(4X,4(2X,I4),2X))
0049              NE=NEM/3
0050              NE=NE *3
0051              IF(NE.EQ.NEM-1) READ(5,933)NE1,NOD(NE1,1),NOD(NE1,2),NOD(NE1,3)
0052              IF(NE.EQ.NEM-1 )WRITE(6,93) NE1,NOD(NE1,1),NOD(NE1,2),NOD(NE1,3)
0053              IF(NE.EQ.NEM-2) READ(5,933)NE1,NOD(NE1,1),NOD(NE1,2),NOD(NE1,3),
                 1NE2,NOD(NE2,1),NOD(NE2,2),NOD(NE2,3)
0054              IF(NE.EQ.NEM-2)WRITE(6,93) NE1,NOD(NE1,1),NOD(NE1,2),NOD(NE1,3),
                 1NE2,NOD(NE2,1),NOD(NE2,2),NOD(NE2,3)
                C      ....... COMPUTE THE HALF BAND WIDTH..............
0055              NHBW=0
0056              DO 30 N=1,NEM
0057              DO 30 I=1,NPE
0058              DO 30 J=1,NPE
0059              NW=(IABS(NOD(N,I)-NOD(N,J))+1)*NDF
0060             30 IF (NHBW.LT.NW) NHBW=NW
0061              PRINT 903, NHBW
                C      ....READ IN CONSTRAINT DATA.....
0062              READ(5,901)NBDY
0063              WRITE(6,908)NBDY
0064              DO 56 I=1,NBDY
0065              READ(5,901)II,ID,GFI
0066              WRITE(6,909)II,ID,GFI
0067              IBDY(I)=(II-1)*NDF+ID
0068              VBDY(I)=GFI
0069             56 CONTINUE
0070              NEQ=NNM*NDF
0071            903 FORMAT(//, ' THE HALF BAND WIDTH IS ',I5,///)
0072            901 FORMAT(2I5,F10.3)
0073            908 FORMAT(//,2X,'THE NUMBER OF CONSTRAINTS IS ',I5,//,3X,
                   1'NODE  DIRECTION    VALUE',/)
0074            909 FORMAT(2X,I4,6X,I2,3X,F10.3)
0075              RETURN
0076              END
```

```
0001            SUBROUTINE PROP(ET,XNUT,STRAIN,IEP,NEMMAX,ECH)
                C
                C     THIS SUBROUTINE TABULATES THE MATERIAL PROPERTIES
                C
0002            IMPLICIT REAL*8(A-H,O-Z)
0003            DIMENSION ET(10,2),XNUT(10,2),STRAIN(10,2),IEP(NEMMAX),ECH(NEMMAX)
0004            DO 1 I=1,NEMMAX
0005          1 IEP(I)=1
                C     **** STEEL PROPERTIES ****
0006            ET(1,1)=29000000.
0007            XNUT(1,1)=0.318
0008            STRAIN(1,1)=0.002
                C     **** ALUMINUM PROPERTIES ****
0009            ET(1,2)=10500000.
0010            ET(2,2)=1183000.
0011            ET(3,2)=462000.
0012            ET(4,2)=271000.
0013            ET(5,2)=152000.
0014            ET(6,2)=50300.
0015            ET(6,2)=65000.
0016            ET(7,2)=0.0
0017            XNUT(1,2)=0.313
0018            XNUT(2,2)=0.375
0019              UT(3,2)=0.443
0020            ...UT(4,2)=0.467
0021            XNUT(5,2)=0.484
0022            XNUT(6,2)=0.491
0023            XNUT(7,2)=0.5
0024            STRAIN(1,2)=0.00472
0025            STRAIN(2,2)=0.00753
0026            STRAIN(3,2)=0.01814
0027            STRAIN(4,2)=0.03286
0028            STRAIN(5,2)=0.07817
0029            STRAIN(6,2)=0.17383
0030            STRAIN(6,2)=0.14291
0031            STRAIN(7,2)=999.
0032            DO 3 I=1,6
0033          3 ECH(I)=STRAIN(1,1)
0034            DO 2 I=7,NEMMAX
0035          2 ECH(I)=STRAIN(1,2)
0036            RETURN
0037            END
```

```
0001            SUBROUTINE ASSEM(NNM,NEM,NRMAX,NCMAX,NDF,NPE,NODY,NHBW,NEQ,NRMAXH,
               1NEMMAX,X,Y,NOD,GSTIF,B,C, VBDY,IBDY,ET,XNUT,IEP,ITFAIL,ECH,ITIME,
               2STRAIN)
      C      ** MODIFICATION OF A PROGRAM BY J.N. REDDY **
      C
      C      THIS SUBROUTINE ASSEMBLES THE GLOBAL STIFFNESS MATRIX
      C
0002            IMPLICIT REAL*8(A-H,O-Z)
0003            DIMENSION X(NRMAXH),Y(NRMAXH),NOD(NEMMAX,NPE),VBDY(100),
               1GSTIF(NRMAX,NCMAX),          ELXY(3,2),ELSTIF(6,6),ET(10,2),
               2XNUT(10,2),IBDY(100),IEP(NEMMAX),ECH(NEMMAX),STRAIN(10,2)
               3,B(NEMMAX,3),C(NEMMAX,3),BETA(3),GAMA(3)
      C      ..... INITIALIZE THE GLOBAL STIFFNESS MATRIX ........
0004            DO 50 I=1,NEQ
0005            DO 50 J=1,NHBW
0006         50 GSTIF(I,J)=0.0
0007            NN=NDF*NPE
0008            DO 150 N=1,NEM
0009            IMTYPE=1
0010            IF(N.GT.6)IMTYPE=2
0011            IF(STRAIN(IEP(N),IMTYPE).EQ.999.)GO TO 52
0012            IF(STRAIN(IEP(N),IMTYPE).EQ.ECH(N))GO TO 57
0013            E=ET(1,IMTYPE)
0014            XNU=XNUT(1,IMTYPE)
0015            GO TO 55
0016         57 E=ET(IEP(N),IMTYPE)
0017            XNU=XNUT(IEP(N),IMTYPE)
0018            GO TO 55
0019         52 E=0.0
0020            XNU=0.5
0021         55 CONTINUE
0022            DO 60 I=1,NPE
0023            NI=NOD(N,I)
0024            ELXY(I,1)=X(NI)
0025         60 ELXY(I,2)=Y(NI)
0026            CALL STIFF (NPE,NN ,ELXY,ELSTIF,E,XNU,BETA,GAMA,DET)
0027            DO 65 I=1,3
0028            B(N,I)=BETA(I)/DET
0029         65 C(N,I)=GAMA(I)/DET
      C      ..... ASSEMBLE ELEMENT STIFFNESS MATRICES TO GET GLOBAL STIFFNESS
0030            DO 140 I=1,NPE
0031            NR=(NOD(N,I)-1)*NDF
0032            DO 140 II=1,NDF
0033            NR=NR+1
0034            L=(I-1)*NDF+II
0035            DO 130 J=1,NPE
0036            NCL=(NOD(N,J)-1)*NDF
0037            DO 120 JJ=1,NDF
0038            M=(J-1)*NDF+JJ
0039            NC=NCL+JJ+1-NR
0040            IF (NC) 120,120,110
0041        110 GSTIF(NR,NC)=GSTIF(NR,NC)+ELSTIF(L,M)
```

```
0042          120 CONTINUE
0043          130 CONTINUE
0044          140 CONTINUE
0045          150 CONTINUE
          C       ..... IMPOSE BOUNDARY CONDITIONS ........
0046              DO 170 I=1,NBDY
0047              IE=IBDY(I)
0048              VE=VBDY(I)
0049          170 CALL BNDRY (NRMAX,NCMAX,NEQ,NHBW,GSTIF,GF,IE,VE)
0050              DO 180 I=1,NEQ
0051              IF(GSTIF(I,1).NE.0.0)GO TO 180
0052              CALL BNDRY(NRMAX,NCMAX,NEQ,NHBW,GSTIF,GF,I,0.0)
0053              WRITE(6,900)I
0054          900 FORMAT(1H ,'ROW ',I5,' HAS BEEN CONSTRAINED')
0055          180 CONTINUE
0056              RETURN
0057              END
```

```
0001            SUBROUTINE STIFF(NPE,NN,    ELXY,ELSTIF,E,ANU,BETA,GAMA,DET)
                C       **  MODIFICATION BASED ON SUBROUTINE STIFF  BY J.N. REDDY  **
                C
                C     THIS SUBROUTINE CALCULATES THE ELEMENT STIFFNESS MATRIX
                C
0002            IMPLICIT REAL*8(A-H,O-Z)
0003            DIMENSION ELXY(3,2),ELSTIF(NN,NN),X(3),Y(3)
0004            DIMENSION B(3,6),BT(6,3),STR(3,6),D(3,3)
0005            DIMENSION           GAMA(3),BETA(3)
0006            T=0.127
0007            DO 10 I=1,3
0008            DO 10 J=1,3
0009          10 D(I,J)=0.0
                C     ..... PLANE STRESS CASE(ISOTROPIC).....
0010            C1=E/(1.0-ANU*ANU)
0011            D(1,1)=C1
0012            D(1,2)=ANU*C1
0013            D(3,3)=0.5*(1.0-ANU)*C1
0014            D(2,1)=D(1,2)
0015            D(2,2)=D(1,1)
                C     ..... STIFFNESS MATRIX FOR CONSTANT STRAIN TRIANGLE CASE.........
0016           50 DO 70 I=1,NPE
0017              X(I)=ELXY(I,1)
0018              Y(I)=ELXY(I,2)
0019              DO 60 K=1,NN
0020           60 B(I,K)=0.0
0021           70 CONTINUE
0022              DO 80 I=1,NPE
0023              J=I+1
0024              IF (J.GT.NPE) J=J-NPE
0025              K=J+1
0026              IF (K.GT.NPE) K=K-NPE
0027              BETA(I)=Y(J)-Y(K)
0028              GAMA(I)=X(K)-X(J)
0029           80 CONTINUE
0030              DET=X(1)*(Y(2)-Y(3))+X(2)*(Y(3)-Y(1))+X(3)*(Y(1)-Y(2))
0031              DO 100 I=1,NPE
0032              J=2*(I-1)+1
0033              L=2*I
0034              B(1,J)=BETA(I)/DET
0035              B(3,J)=GAMA(I)/DET
0036              B(2,L)=GAMA(I)/DET
0037              B(3,L)=BETA(I)/DET
0038          100 CONTINUE
                C     FOR CONSTANT STRAIN TRIANGLE CASE THE STIFFNESS MATRIX IS EQUAL TO
                C                   K = A*T*(BT)*(D)*(B)
0039              DO 110 I=1,3
0040              DO 110 J=1,NN
0041          110 BT(J,I)=0.5*DET*T*B(I,J)
0042              CALL MATMLT (D,3,3,B,NN,STR)
0043              CALL MATMLT (BT,NN,3,STR,NN,ELSTIF)
0044              RETURN
0045              END
```

```
0001            SUBROUTINE MATMLT (A,M,N,B,L,C)
                C       **  MODIFICATION BASED ON SUBROUTINE MATMLT BY J.N. REDDY  **
                C       SUBROUTINE FOR MATRIX MULTIPLICATION
                C       THIS PROGRAM MULTIPLIES A (M,N) BY B(N,L) TO GIVE C(M,L)
0002            IMPLICIT REAL*8(A-H,O-Z)
0003            DIMENSION A(M,N),B(N,L),C(M,L)
0004            DO 10 I=1,M
0005            DO 10 J=1,L
0006            C(I,J)=0.
0007            DO 10 K=1,N
0008         10 C(I,J)=C(I,J)+A(I,K)*B(K,J)
0009            RETURN
0010            END
```

```
0001            SUBROUTINE BNDRY (NRMAX,NCMAX,NEQ,NHBW,S,SL,IE,SVAL)
                C       **  MODIFICATION BASED ON SUBROUTINE BNDRY  BY J.N. REDDY  **
                C       THIS PROGRAM IMPOSES THE PRESCRIBED BOUNDARY CONDITIONS ON THE
                C       THE SYSTEM MATRIX(BANDED SYNMETRIC MATRIX)
                C       S IS THE SYSTEM MATRIX (STIFFNESS MATRIX)
                C       SL IS THE LOAD VECTOR
                C       IE IS THE LABEL OF THE VARIABLE THAT IS PRESCRIBED
                C       SVAL IS THE VALUE OF THE PRESCRIBED VARIABLE
0002            IMPLICIT REAL*8(A-H,O-Z)
0003            DIMENSION S(NRMAX,NCMAX)
0004            IT=NHBW-1
0005            I=IE-NHBW
0006            DO 10 II=1,IT
0007            I=I+1
0008            IF (I.LT.1) GO TO 10
0009            J=IE-I+1
0010            S(I,J)=0.0
0011         10 CONTINUE
0012            S(IE,1)=1.0
0013            I=IE
0014            DO 20 II=2,NHBW
0015            I=I+1
0016            IF (I.GT.NEQ) GO TO 20
0017            S(IE,II)=0.0
0018         20 CONTINUE
0019            RETURN
0020            END
```

```
0001            SUBROUTINE SOLVE1(NRW,NCW,NEQNS,NBW,BAND,RHS)
                C       **  MODIFICATION BASED ON SUBROUTINE SOLVE  BY J.N. REDDY  **
                C      THIS PROGRAM SOLVES A BANDED SYMMETRIC SYSTEM OF EQUATIONS
                C      THE BANDED MATRIX IS INPUT THROUGH BAND(NEQNS,NBW)
                C      RHS IS THE RIGHT HAND SIDE (FORCE VECTOR) OF THE SYSTEM
                C      NEQNS IS THE NO. OF EQUATIONS(EQUAL TO ACTUAL NO. OF ROWS)
                C      NBW IS THE HALF BANDWIDTH OF THE SYSTEM
0002            IMPLICIT REAL*8(A-H,O-Z)
0003            DIMENSION BAND(NRW,NCW),RHS(NRW)
0004            DO 5 I=1,NEQNS
0005          5 RHS(I)=0.0
0006            RHS(2)=1.0
0007            NEQNS=NEQNS-1
0008            DO 30 NPIV=1,NEQNS
0009            NPIVOT=NPIV+1
0010            LSTSUB=NPIV+NBW-1
0011            IF (LSTSUB.GT.NEQNS) LSTSUB=NEQNS
0012            DO 20 NROW=NPIVOT,LSTSUB
                C       INVERT ROWS AND COLUMNS FOR ROW FACTOR
0013            NCOL=NROW-NPIV+1
0014            FACTOR=BAND(NPIV,NCOL)/BAND(NPIV,1)
0015            DO 10 NCOL=NROW,LSTSUB
0016            ICOL=NCOL-NROW+1
0017            JCOL=NCOL-NPIV+1
0018         10 BAND(NROW,ICOL)=BAND(NROW,ICOL)-FACTOR*BAND(NPIV,JCOL)
0019         20 RHS(NROW)=RHS(NROW)-FACTOR*RHS(NPIV)
0020         30 CONTINUE
0021            DO 90 IJK=2,NEQNS
0022            NPIV=NEQNS-IJK+2
0023            RHS(NPIV)=RHS(NPIV)/BAND(NPIV,1)
                C       ALTHOUGH ZEROING ELEMENTS IN MATRIX, DONT BOTHER TO OPERATE ON TH
0024            LSTSUB=NPIV-NBW+1
0025            IF (LSTSUB.LT.1) LSTSUB=1
0026            NPIVOT=NPIV-1
0027            DO 80 JKI=LSTSUB,NPIVOT
0028            NROW=NPIVOT-JKI+LSTSUB
0029            NCOL=NPIV-NROW+1
0030            FACTOR=BAND(NROW,NCOL)
0031         80 RHS(NROW)=RHS(NROW)-FACTOR*RHS(NPIV)
0032         90 CONTINUE
0033            RHS(1)=RHS(1)/BAND(1,1)
0034            RETURN
0035            END
```

```
0001            SUBROUTINE FAIL(ITIME,U,NRMAX,XLOAD,B,C,NEM,XNU,STRAIN,IEF,NEMMAX,
               1EXT,EYT,EZT,GXYT,NEF,NOD,IFT,FLOAD,XLOADI,EXEL,EYEL,EZEL,GXYEL,
               2IFTYPE,ISTYPE,ECH,UTI,UII)
          C      **** THIS SUBROUTINE DETERMINES 1) THE NEXT ELEMENT(S) TO YIELD,
          C           CHANGE MODULUS, OR FRACTURE 2) THE LOAD FOR THIS FAILURE,
          C           AND 3) THE DEFLECTION AT THE PIN CENTER NOD ****
0002            IMPLICIT REAL*8(A-H,O-Z)
0003            DIMENSION U(NRMAX),B(NEMMAX,3),C(NEMMAX,3),EX(800   ),EY(800),
               1 GXY(800   ),XNU(10,2),STRAIN(10,2),IEF(300),EZ(800),
               2            EZT(NEMMAX),GXYT(NEMMAX),EXT(NEMMAX),NOD(NEMMAX,3),
               3            EXEL(NEMMAX),EYEL(NEMMAX),EZEL(NEMMAX),GXYEL(NEMMAX)
               4,EYT(NEMMAX),IFT(NEMMAX),EPRIN(3),ECH(NEMMAX)
          C      **** CALCULATE INCREMENTAL STRAIN IN X AND Y DIRECTION AND
          C           SHEAR STRAIN ****
0004            IMTYPE=2
0005            DO 10 I=7,NEM
0006            CCNU=XNU(IFT(I),IMTYPE)/(1.0-(XNU(IFT(I),IMTYPE))**2)
0007            EX(I)=0.0
0008            EY(I)=0.0
0009            EZ(I)=0.0
0010            GXY(I)=0.0
0011            DO 11 J=1,3
0012            NODE2=NOD(I,J)*2
0013            NODE1=NODE2-1
0014            EX(I)=EX(I)+B(I,J)*U(NODE1)
0015            EY(I)=EY(I)+C(I,J)*U(NODE2)
0016            GXY(I)=GXY(I)+B(I,J)*U(NODE2)+C(I,J)*U(NODE1)
0017         11 CONTINUE
0018            EZ(I)=-CCNU*(EX(I)+EY(I)+XNU(IFT(I),IMTYPE)*(EX(I)+EY(I)))
0019         10 CONTINUE
0020            IF(ITIME.EQ.1.OR.IFTYPE.EQ.1)UII=U(2)
0021            EMAX=0.0
0022            IF(ITIME.NE.1)GO TO 20
0023            ITIME=2
          C      **** CALCULATE FIRST ELEMENT TO YIELD ****
          C      **** MAX NORMAL STRAIN CRITERIA ****
0024            IFTYPE=0
0025            DO 30 I=7,NEM
0026            EPLUS=EX(I)+EY(I)
0027            EMINUS=EX(I)-EY(I)
0028            ESQRT=((EMINUS)**2+(GXY(I))**2)**0.5
0029            EPRIN(1)=0.5*(EPLUS+ESQRT)
0030            EPRIN(2)=0.5*(EPLUS-ESQRT)
0031            EPRIN(3)=EZ(I)
0032            DO 30 II=1,3
0033            IF(EPRIN(II)-EMAX)30,40,50
0034         40 NEF=NEF+1
0035            IF(NEF.EQ.301)GO TO 60
0036            IEF(NEF)=I
0037            GO TO 30
0038         60 WRITE(6,902)
0039        902 FORMAT(1H ,'*** MORE THAN 300 ELEMENTS FAILED ***')
```

```
0040            CALL EXIT
0041         50 NEF=1
0042            IEF(NEF)=I
0043            EMAX=EPRIN(II)
0044         30 CONTINUE
0045            XLOAD=STRAIN(1,2)/EMAX
0046            UT1=U(2)*XLOAD
0047            DO 70 I=7,NEM
0048            EXT(I)=EX(I)*XLOAD
0049            EYT(I)=EY(I)*XLOAD
0050            EZT(I)=EZ(I)*XLOAD
0051            GXYT(I)=GXY(I)*XLOAD
0052            EXEL(I)=EX (I)
0053            EYEL(I)=EY (I)
0054            EZEL(I)=EZ (I)
0055            GXYEL(I)=GXY (I)
0056         70 CONTINUE
0057            IF(ISTYPE.EQ.2.OR.ISTYPE.EQ.3)XLOAD=XLOAD*2.0
0058            XLOADI=XLOAD
0059            WRITE(6,960)XLOAD,UT1
0060       960 FORMAT(1H1,48X,'LOAD DEFLECTION HISTORY'///,1H ,'FAILURE ',
               1'(  INITIAL YIELD  ) OCCURRED AT A LOAD OF ',F12.2,' WITH A ',
               2'DEFLECTION AT THE PIN OF ',E12.5)
0061            DO 150 I=1,NEF
0062       150 WRITE(6,930)IEF(I),IFT(I)
0063            WRITE(6,980)
0064            RETURN
0065         20 INCRE=0
           C       ....CALCULATE NEXT ELEMENTS TO YIELD, CHANGE MODULUS, OR FRACTURE
0066            X1=1.0
0067            NEF=0
0068            XFMIN=9999999.
           C       ....APPROXIMATE NEXT FAILURE LOAD....
0069            DO 22 I=7,NEM
0070            IF(ECH(I).EQ.999.)GO TO 22
0071            DEPR=.5*(EX (I)+EY (I)+((EX (I)-EY (I))**2+(GXY (I))**2)**0.5)
0072            EPRI=.5*(EXT(I)+EYT(I)+((EXT(I)-EYT(I))**2+(GXYT(I))**2)**0.5)
0073            XF=(ECH(I)          -EPRI)/DEPR
0074            IF(XF.LE.0.0)GO TO 23
0075            IF(XF.LT.XFMIN)XFMIN=XF
0076         23 IF(IFTYPE.NE.1)GO TO 22
0077            EXEL(I)=EX(I)
0078            EYEL(I)=EY(I)
0079            EZEL(I)=EZ(I)
0080            GXYEL(I)=GXY(I)
0081         22 CONTINUE
0082            XLINCR=XFMIN*5.0
           C       IF(XLINCR.LT.50.)XLINCR=50.
0083            WRITE(6,970)XLINCR
0084       970 FORMAT(1H ,'LOAD INCREMENT = ',E12.5)
0085       100 IOUT=0
0086            IF(INCRE.NE.0)X1=0.2
```

```
0087              IF(XLINCR.LT.200.0)XI=1.0
0088              DO 80 I=7,NEM
0089              EMAX=ECH(I)
0090              IF(STRAIN(IFT(I),2).EQ.999.0)GO TO 80
0091              EXT(I)=EXT(I)+EX(I)*XLINCR*XI
0092              EYT(I)=EYT(I)+EY(I)*XLINCR*XI
0093              EZT(I)=EZT(I)+EZ(I)*XLINCR*XI
0094              GXYT(I)=GXYT(I)+GXY(I)*XLINCR*XI
0095              EPLUS=EXT(I)+EYT(I)
0096              EMINUS=EXT(I)-EYT(I)
0097              ESQRT=((EMINUS)**2+(GXYT(I))**2)**0.5
0098              EPRIN(1)=0.5*(EPLUS+ESQRT)
0099              EPRIN(2)=0.5*(EPLUS-ESQRT)
0100              EPRIN(3)=EZ(I)
0101              DO 81 II=1,3
0102              IF(EPRIN(II).LT.EMAX)GO TO 81
0103              NEF=NEF+1
0104              IOUT=1
0105              IF(NEF.NE.301)GO TO 82
0106              WRITE(6,902)
0107              DO 83 J=1,99
0108           83 WRITE(6,951)IEF(J)
0109          951 FORMAT(1H ,'ELEMENT ',I5,' FAILED')
0110              CALL EXIT
0111           82 IEF(NEF)=I
0112           81 CONTINUE
0113           80 CONTINUE
0114              INCRE=INCRE+1
0115              IF(IOUT.EQ.0)GO TO 100
0116              XINCR=INCRE-1
0117              XINCR=XINCR*XLINCR*XI+XLINCR
0118              UT1=UT1+U(2)*XINCR
0119              IFTYPE=0
0120              IF(ISTYPE.EQ.2.OR.ISTYPE.EQ.3)XINCR=XINCR*2.0
0121              XLOAD=XLOAD+XINCR
0122              WRITE(6,915)NEF
0123          915 FORMAT(1H ,I3,' ELEMENTS FAILED DURING THIS LOAD STEP')
0124              WRITE(6,910)XLOAD,UT1
0125          910 FORMAT(    1H ,'FAILURE (YIELD OR FRACTURE) OCCURRED AT A LOAD OF '
                 1,F12.2,' WITH A DEFLECTION AT THE PIN OF ',E12.5)
0126              DO 120 I=1,NEF
0127              IF(STRAIN(IFT(IEF(I))+1,2).EQ.999.)GO TO 130
0128              WRITE(6,930)IEF(I),IFT(IEF(I))
0129          930 FORMAT(1H ,'ELEMENT ',I5,' YIELDED FOR THE ',I5,' TIME')
0130              GO TO 120
0131          130 WRITE(6,940)IEF(I)
0132          940 FORMAT(1H ,'ELEMENT ',I5,' FRACTURED')
0133              IFTYPE=1
0134          120 CONTINUE
0135              WRITE(6,980)
0136          980 FORMAT(//,1H ,53X,'***********',///)
0137              IF(IFTYPE.EQ.0)RETURN
```

```
0138            IF(XLOAD.LT.FLOAD)WRITE(6,950)FLOAD
0139          950 FORMAT(///,1H ,'****** CRACK INSTABILITY OCCURRED AT A LOAD OF ',
                 1F12.2,' *******',//)
0140            FLOAD=XLOAD
0141            UT1=UT1-UT1*FLOAD
0142            XLOAD=0.0
              C     .... UNLOAD SPECIMEN ALONG ELASTIC SLOPE ....
0143            XSTYPE=1.0
0144            IF(ISTYPE.EQ.2.OR.ISTYPE.EQ.3)XSTYPE=.5
0145            DO 140 I=7,NEM
0146            IF(STRAIN(IFT(I),2).EQ.999.)GO TO 145
0147            DO 147 II=1,NEF
0148            IF(IEF(II).EQ.I)GO TO 145
0149          147 CONTINUE
0150            IF(STRAIN(IFT(I),2).NE.ECH(I))GO TO 145
0151            IF(IFT(I).EQ.1)GO TO 145
0152            EPLUS=EXT(I)+EYT(I)
0153            EMINUS=EXT(I)-EYT(I)
0154            ESQRT=((EMINUS)**2+(GXYT(I))**2)**0.5
0155            EPRIN(1)=0.5*(EPLUS+ESQRT)
0156            ECH(I)=EPRIN(1)
0157          145 EXT(I)=EXT(I)-EXEL(I)*FLOAD*XSTYPE
0158            EYT(I)=EYT(I)-EYEL(I)*FLOAD*XSTYPE
0159            EZT(I)=EZT(I)-EZEL(I)*FLOAD*XSTYPE
0160            GXYT(I)=GXY(I)-GXYEL(I)*FLOAD*XSTYPE
0161          140 CONTINUE
0162            RETURN
0163            END
```

```
0001              SUBROUTINE CHANG(IEF,IFT,NEF,NEMMAX,ECH,STRAIN)
0002              IMPLICIT REAL*8(A-H,O-Z)
0003              DIMENSION          IFT(NEMMAX),ECH(NEMMAX),STRAIN(10,2),IEF(300)
0004              IMTYPE=2
                C     .... UPDATES  THE TANGENT MATERIAL LOCATION INDEX ....
0005              DO 80 N=1,NEF
0006              IF(STRAIN(IFT(IEF(N))+1 ,2).EQ.999.)IFT(IEF(N))=IFT(IEF(N))+1
0007              IF(STRAIN(IFT(IEF(N)),IMTYPE).NE.ECH(IEF(N)))GO TO 85
0008              IFT(IEF(N))=IFT(IEF(N))+1
0009             85 ECH(IEF(N))=STRAIN(IFT(IEF(N)),IMTYPE)
0010             80 CONTINUE
0011              RETURN
0012              END
```

MESH FOR FRACTURE STUDY

DOUBLE EDGE NOTCH SPECIMEN

DIVISIONS AT CENTER SECTION = 8. BAR HALF WIDTH = 0.4120. BAR HALF LENGTH = 4.5550

TOP HALF WIDTH = 1.4970. TOP LENGTH = 2.9310. HOLE RADIUS = 0.5000. LOCATION FROM THE TOP = 1.4850

FILLET RADIUS = 0.6250

THE NUMBER OF NODES = 226

NODE	X	Y	NODE	X	Y	NODE	X	Y
1	0.0	0.30700D 01	2	0.0	0.35700D 01	3	0.25000D 00	0.35030D 01
4	0.43300D 00	0.33200D 01	5	0.50000D 00	0.30700D 01	6	0.43300D 00	0.28200D 01
7	0.25000D 00	0.26370D 01	8	0.0	0.25700D 01	9	0.43300D 00	0.28200D 01
10	0.25000D 00	0.26370D 01	11	0.0	0.25700D 01	12	0.0	0.38200D 01
13	0.28700D 00	0.37629D 01	14	0.53030D 00	0.36003D 01	15	0.69290D 00	0.33570D 01
16	0.75000D 00	0.30700D 01	17	0.69290D 00	0.27830D 01	18	0.53030D 00	0.25397D 01
19	0.28700D 00	0.23771D 01	20	0.0	0.23200D 01	21	0.48300D 00	0.29406D 01
22	0.59650D 00	0.29265D 01	23	0.21380D 00	0.21788D 01	24	0.47900D 00	0.22886D 01
25	0.21380D 00	0.19950D 01	26	0.89120D 00	0.28562D 01	27	0.74150D 00	0.25314D 01
28	0.0	0.41875D 01	29	0.42760D 00	0.41024D 01	30	0.79020D 00	0.38602D 01
31	0.10324D 01	0.34976D 01	32	0.11175D 01	0.30700D 01	33	0.10324D 01	0.26423D 01
34	0.79020D 00	0.22798D 01	35	0.42760D 00	0.20376D 01	36	0.0	0.19525D 01
37	0.0	0.45550D 01	38	0.74850D 00	0.45550D 01	39	0.11227D 01	0.41837D 01
40	0.14970D 01	0.38125D 01	41	0.14970D 01	0.30700D 01	42	0.14970D 01	0.23275D 01
43	0.11227D 01	0.19563D 01	44	0.77520D 00	0.19969D 01	45	0.59750D 00	0.19138D 01
46	0.41960D 00	0.18308D 01	47	0.20990D 00	0.17882D 01	48	0.0	0.17882D 01
49	0.14970D 01	0.45550D 01	50	0.14970D 01	0.16240D 01	51	0.12647D 01	0.32838D 01
52	0.12647D 01	0.28562D 01	53	0.11227D 01	0.23275D 01	54	0.30900D 00	0.16240D 01
55	0.20600D 00	0.16240D 01	56	0.10300D 00	0.16240D 01	57	0.0	0.16240D 01
58	0.10370D 01	0.16240D 01	59	0.14970D 01	0.32838D 01	60	0.66200D 00	0.16240D 01
61	0.14970D 01	0.28562D 01	62	0.41200D 00	0.16240D 01	63	0.90610D 00	0.18105D 01
64	0.84950D 00	0.16240D 01	65	0.53700D 00	0.16240D 01	66	0.62360D 00	0.14677D 01
67	0.49570D 00	0.13115D 01	68	0.75570D 00	0.15571D 01	69	0.51780D 00	0.15459D 01
70	0.51780D 00	0.14677D 01	71	0.55970D 00	0.14025D 01	72	0.48580D 00	0.13896D 01
73	0.45390D 00	0.13115D 01	74	0.46380D 00	0.12481D 01	75	0.41200D 00	0.14677D 01
76	0.33900D 00	0.14677D 01	77	0.20600D 00	0.14677D 01	78	0.10300D 00	0.14677D 01
79	0.0	0.14677D 01	80	0.41200D 00	0.13115D 01	81	0.30900D 00	0.13115D 01
82	0.20600D 00	0.13115D 01	83	0.10300D 00	0.13115D 01	84	0.0	0.13115D 01
85	0.41200D 00	0.13896D 01	86	0.36050D 00	0.13896D 01	87	0.43290D 00	0.12481D 01
88	0.36050D 00	0.12481D 01	89	0.43160D 00	0.11552D 01	90	0.30900D 00	0.12334D 01
91	0.25750D 00	0.12334D 01	92	0.30900D 00	0.10771D 01	93	0.25750D 00	0.10771D 01
94	0.37040D 00	0.99900D 00	95	0.37040D 00	0.94750D 00	96	0.30900D 00	0.11552D 01
97	0.20600D 00	0.11552D 01	98	0.10300D 00	0.11552D 01	99	0.0	0.11552D 01

100	0.37040D 00	0.11552D 01	101	0.41690D 00	0.10771D 01	102	0.37040D 00	0.10771D 01
103	0.41200D 00	0.99900D 00	104	0.30900D 00	0.99900D 00	105	0.20600D 00	0.99900D 00
106	0.10300D 00	0.99900D 00	107	0.0	0.99900D 00	108	0.41200D 00	0.89600D 00
109	0.30900D 00	0.89600D 00	110	0.20600D 00	0.89600D 00	111	0.10300D 00	0.89600D 00
112	0.0	0.89600D 00	113	0.41200D 00	0.79300D 00	114	0.30900D 00	0.79300D 00
115	0.20600D 00	0.79300D 00	116	0.10300D 00	0.79300D 00	117	0.0	0.79300D 00
118	0.41200D 00	0.69000D 00	119	0.30900D 00	0.69000D 00	120	0.20600D 00	0.69000D 00
121	0.10300D 00	0.69000D 00	122	0.0	0.69000D 00	123	0.41200D 00	0.58700D 00
124	0.30900D 00	0.58700D 00	125	0.20600D 00	0.58700D 00	126	0.10300D 00	0.58700D 00
127	0.0	0.58700D 00	128	0.41200D 00	0.53550D 00	129	0.36050D 00	0.53550D 00
130	0.30900D 00	0.53550D 00	131	0.25750D 00	0.53550D 00	132	0.20600D 00	0.53550D 00
133	0.15450D 00	0.53550D 00	134	0.10300D 00	0.53550D 00	135	0.51500D-01	0.53550D 00
136	0.0	0.53550D 00	137	0.41200D 00	0.48190D 00	138	0.36050D 00	0.48190D 00
139	0.30900D 00	0.48190D 00	140	0.25750D 00	0.48190D 00	141	0.20600D 00	0.48190D 00
142	0.15450D 00	0.48190D 00	143	0.10300D 00	0.48190D 00	144	0.51500D-01	0.48190D 00
145	0.0	0.48190D 00	146	0.41200D 00	0.42840D 00	147	0.36050D 00	0.42840D 00
148	0.30900D 00	0.42840D 00	149	0.25750D 00	0.42840D 00	150	0.20600D 00	0.42840D 00
151	0.15450D 00	0.42840D 00	152	0.10300D 00	0.42840D 00	153	0.51500D-01	0.42840D 00
154	0.0	0.42840D 00	155	0.41200D 00	0.37480D 00	156	0.36050D 00	0.37480D 00
157	0.30900D 00	0.37480D 00	158	0.25750D 00	0.37480D 00	159	0.20600D 00	0.37480D 00
160	0.15450D 00	0.37480D 00	161	0.10300D 00	0.37480D 00	162	0.51500D-01	0.37480D 00
163	0.0	0.37480D 00	164	0.41200D 00	0.32130D 00	165	0.36050D 00	0.32130D 00
166	0.30900D 00	0.32130D 00	167	0.25750D 00	0.32130D 00	168	0.20600D 00	0.32130D 00
169	0.15450D 00	0.32130D 00	170	0.10300D 00	0.32130D 00	171	0.51500D-01	0.32130D 00
172	0.0	0.32130D 00	173	0.41200D 00	0.26770D 00	174	0.36050D 00	0.26770D 00
175	0.30900D 00	0.26770D 00	176	0.25750D 00	0.26770D 00	177	0.20600D 00	0.26770D 00
178	0.15450D 00	0.26770D 00	179	0.10300D 00	0.26770D 00	180	0.51500D-01	0.26770D 00
181	0.0	0.26770D 00	182	0.41200D 00	0.21420D 00	183	0.36050D 00	0.21420D 00
184	0.30900D 00	0.21420D 00	185	0.25750D 00	0.21420D 00	186	0.20600D 00	0.21420D 00
187	0.15450D 00	0.21420D 00	188	0.10300D 00	0.21420D 00	189	0.51500D-01	0.21420D 00
190	0.0	0.21420D 00	191	0.41200D 00	0.16060D 00	192	0.36050D 00	0.16060D 00
193	0.30900D 00	0.16060D 00	194	0.25750D 00	0.16060D 00	195	0.20600D 00	0.16060D 00
196	0.15450D 00	0.16060D 00	197	0.10300D 00	0.16060D 00	198	0.51500D-01	0.16060D 00
199	0.0	0.16060D 00	200	0.41200D 00	0.10710D 00	201	0.36050D 00	0.10710D 00
202	0.30900D 00	0.10710D 00	203	0.25750D 00	0.10710D 00	204	0.20600D 00	0.10710D 00
205	0.15450D 00	0.10710D 00	206	0.10300D 00	0.10710D 00	207	0.51500D-01	0.10710D 00
208	0.0	0.10710D 00	209	0.41200D 00	0.53500D-01	210	0.36050D 00	0.53500D-01
211	0.30900D 00	0.53500D-01	212	0.25750D 00	0.53500D-01	213	0.20600D 00	0.53500D-01
214	0.15450D 00	0.53500D-01	215	0.10300D 00	0.53500D-01	216	0.51500D-01	0.53500D-01
217	0.0	0.53500D-01	218	0.41200D 00	0.0	219	0.36050D 00	0.0
220	0.30900D 00	0.0	221	0.25750D 00	0.0	222	0.20600D 00	0.0
223	0.15450D 00	0.0	224	0.10300D 00	0.0	225	0.51500D-01	0.0
226	0.0	0.0						

THE NUMBER OF ELEMENTS IS 375

ELEMENT CONNECTIVITY

ELEM	NODE1	NODE2	NODE3	ELEM	NODE1	NODE2	NODE3	ELEM	NODE1	NODE2	NODE3
1	1	3	2	2	1	4	3	3	1	5	4
4	1	6	5	5	1	7	6	6	1	8	7
7	2	3	13	8	3	4	14	9	4	5	15
10	5	21	22	11	9	10	18	12	10	11	19
13	2	13	12	14	3	14	13	15	4	15	14
16	5	16	15	17	5	22	16	18	9	18	17
19	10	19	18	20	11	20	19	21	12	29	28
22	12	13	29	23	13	14	29	24	14	30	29
25	14	31	30	26	14	15	31	27	15	16	31
28	16	32	31	29	16	26	32	30	16	17	26
31	17	18	27	32	18	34	27	33	18	24	34
34	18	19	24	35	19	20	23	36	20	36	23
37	28	38	37	38	28	29	38	39	29	30	38
40	30	39	38	41	30	40	39	42	30	31	40
43	31	51	40	44	32	41	51	45	52	42	61
46	52	33	42	47	33	53	42	48	53	43	42
49	38	39	49	50	39	40	49	51	42	43	50
52	43	58	50	53	34	44	43	54	34	35	44
55	35	45	44	56	35	46	45	57	35	47	46
58	25	36	47	59	36	48	47	60	64	58	63
61	60	63	44	62	60	44	45	63	60	45	46
64	60	46	65	65	54	62	46	66	54	46	47
67	54	47	55	68	56	55	47	69	56	47	48
70.	56	48	57	71	66	68	60	72	65	69	60
73	69	66	60	74	71	66	70	75	85	72	75
76	74	67	73	77	75	62	54	78	76	75	54
79	77	76	54	80	77	54	55	81	81	80	86
82	81	86	76	83	81	76	77	84	82	81	77
85	77	55	56	86	78	77	56	87	79	78	56
88	79	56	57	89	83	82	77	90	83	77	78
91	83	78	79	92	84	83	79	93	88	80	81
94	96	100	88	95	97	96	91	96	97	91	82
97	104	94	102	98	92	102	96	99	93	96	97
100	105	93	97	101	97	82	83	102	98	97	83
103	99	98	83	104	99	83	84	105	106	105	97
106	106	97	98	107	106	98	99	108	107	106	99
109	108	103	95	110	109	108	95	111	110	109	104
112	110	104	105	113	114	113	108	114	114	108	109
115	114	109	110	116	115	114	110	117	110	105	106
118	111	110	106	119	112	111	106	120	112	106	107
121	116	115	110	122	116	110	111	123	116	111	112
124	117	116	112	125	118	113	114	126	119	118	114
127	120	119	114	128	120	114	115	129	124	123	118
130	124	118	119	131	124	119	120	132	125	124	120

133	120	115	116
136	122	116	117
139	126	121	122
142	129	123	124
145	131	124	125
148	133	125	126
151	135	126	127
154	138	128	129
157	140	139	130
160	141	140	132
163	142	133	134
166	144	134	135
169	147	146	137
172	148	147	139
175	149	140	141
178	151	141	142
181	153	152	143
184	154	153	145
187	156	147	148
190	158	148	149
193	160	159	150
196	161	160	152
199	162	153	154
202	165	155	156
205	167	166	157
208	168	167	159
211	169	160	161
214	171	161	162
217	174	173	164
220	175	174	166
223	176	167	168
226	178	168	169
229	180	179	170
232	181	180	172
235	183	174	175
238	185	175	176
241	187	186	177
244	188	187	179
247	189	180	181
250	192	182	183
253	194	193	184
256	195	194	186
259	196	187	188
262	198	188	189
265	201	200	191
268	202	201	193
271	203	194	195
274	205	195	196
277	207	206	197
280	208	207	199

134	121	120	116
137	126	125	120
140	127	126	122
143	130	129	124
146	132	131	125
149	134	133	126
152	136	135	127
155	138	129	130
158	140	130	131
161	142	141	132
164	143	142	134
167	144	135	136
170	147	137	138
173	149	148	139
176	150	149	141
179	151	142	143
182	153	143	144
185	156	155	146
188	157	156	148
191	158	149	150
194	160	150	151
197	162	161	152
200	163	162	154
203	165	156	157
206	167	157	158
209	169	168	159
212	170	169	161
215	171	162	163
218	174	164	165
221	176	175	166
224	177	176	168
227	178	169	170
230	180	170	171
233	183	182	173
236	184	183	175
239	185	176	177
242	187	177	178
245	189	188	179
248	190	189	181
251	192	183	184
254	194	184	185
257	196	195	186
260	197	196	188
263	198	189	190
266	201	191	192
269	203	202	193
272	204	203	195
275	205	196	197
278	207	197	198
281	210	209	200

135	122	121	116
138	126	120	121
141	129	128	123
144	131	130	124
147	133	132	125
150	135	134	126
153	138	137	128
156	139	138	130
159	140	131	132
162	142	132	133
165	144	143	134
168	145	144	136
171	147	138	139
174	149	139	140
177	151	150	141
180	152	151	143
183	153	144	145
186	156	146	147
189	158	157	148
192	159	158	150
195	160	151	152
198	162	152	153
201	165	164	155
204	166	165	157
207	167	158	159
210	169	159	160
213	171	170	161
216	172	171	163
219	174	165	166
222	176	166	167
225	178	177	168
228	179	178	170
231	180	171	172
234	183	173	174
237	185	184	175
240	186	185	177
243	187	178	179
246	189	179	180
249	192	191	182
252	193	192	184
255	194	185	186
258	196	186	187
261	198	197	188
264	199	198	190
267	201	192	193
270	203	193	194
273	205	204	195
276	206	205	197
279	207	198	199
282	210	200	201

283	210	201	202	284	211	210	202	285	212	211	202
286	212	202	203	287	212	203	204	288	213	212	204
289	214	213	204	290	214	204	205	291	214	205	206
292	215	214	206	293	216	215	206	294	216	206	207
295	216	207	208	296	217	216	208	297	219	218	209
298	219	209	210	299	219	210	211	300	220	219	211
301	221	220	211	302	221	211	212	303	221	212	213
304	222	221	213	305	223	222	213	306	223	213	214
307	223	214	215	308	224	223	215	309	225	224	215
310	225	215	216	311	225	216	217	312	226	225	217
313	6	22	21	314	6	17	22	315	17	16	22
316	35	34	24	317	35	24	19	318	23	35	19
319	25	35	23	320	36	25	23	321	47	35	25
322	32	51	31	323	51	41	59	324	51	59	40
325	52	41	32	326	52	61	41	327	33	52	32
328	100	89	88	329	33	34	53	330	34	43	53
331	63	43	44	332	63	58	43	333	60	64	63
334	62	65	46	335	68	58	64	336	68	64	60
337	70	66	69	338	75	70	69	339	75	69	62
340	69	65	62	341	72	71	70	342	72	70	75
343	86	85	75	344	86	75	76	345	67	71	72
346	73	67	72	347	80	73	72	348	80	72	85
349	80	85	86	350	87	74	73	351	87	73	80
352	88	87	80	353	89	74	87	354	89	87	88
355	103	101	102	356	102	101	89	357	102	89	100
358	102	100	96	359	96	88	90	360	90	88	81
361	91	90	81	362	91	81	82	363	96	90	91
364	93	92	96	365	94	103	102	366	104	102	92
367	104	92	93	368	105	104	93	369	95	103	94
370	95	94	104	371	109	95	104	372	17	33	26
373	33	32	26	374	27	33	17	375	34	33	27

THE HALF BAND WIDTH IS 48

THE NUMBER OF CONSTRAINTS IS 39

NODE	DIRECTION	VALUE
1	1	0.0
2	1	0.0
8	1	0.0
11	1	0.0
12	1	0.0
20	1	0.0
28	1	0.0

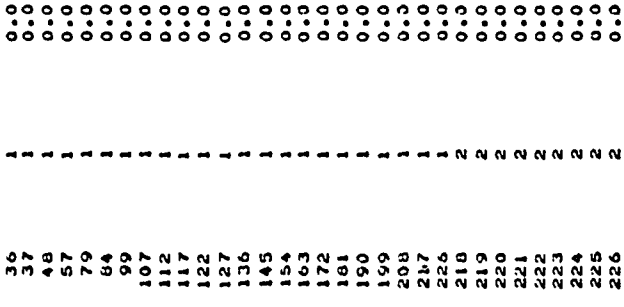
36 1 0.0
37 1 0.0
48 1 0.0
57 1 0.0
79 1 0.0
84 1 0.0
99 1 0.0
107 1 0.0
112 1 0.0
117 1 0.0
122 1 0.0
127 1 0.0
136 1 0.0
145 1 0.0
154 1 0.0
163 1 0.0
172 1 0.0
181 1 0.0
190 1 0.0
199 1 0.0
208 1 0.0
217 1 0.0
226 1 0.0
216 2 0.0
219 2 0.0
220 2 0.0
221 2 0.0
222 2 0.0
223 2 0.0
224 2 0.0
225 2 0.0
226 2 0.0

LOAD DEFLECTION HISTORY

```
FAILURE (  INITIAL YIELD  ) OCCURRED AT A LOAD OF      3774.23 WITH A DEFLECTION AT THE PIN OF  0.11349D-01
ELEMENT    76 YIELDED FOR THE      1 TIME

                                                  **********

LOAD INCREMENT =  0.17341D 02
  1 ELEMENTS FAILED DURING THIS LOAD STEP
FAILURE (YIELD OR FRACTURE) OCCURRED AT A LOAD OF      3800.91 WITH A DEFLECTION AT THE PIN OF  0.11454D-01
ELEMENT   356 YIELDED FOR THE      1 TIME

                                                  **********

LOAD INCREMENT =  0.99004D 02
  1 ELEMENTS FAILED DURING THIS LOAD STEP
FAILURE (YIELD OR FRACTURE) OCCURRED AT A LOAD OF      4006.92 WITH A DEFLECTION AT THE PIN OF  0.12054D-01
ELEMENT   353 YIELDED FOR THE      1 TIME

                                                  **********

LOAD INCREMENT =  0.83544D 02
  5 ELEMENTS FAILED DURING THIS LOAD STEP
FAILURE (YIELD OR FRACTURE) OCCURRED AT A LOAD OF      4341.10 WITH A DEFLECTION AT THE PIN OF  0.13066D-01
ELEMENT   350 YIELDED FOR THE      1 TIME
ELEMENT   351 YIELDED FOR THE      1 TIME
ELEMENT   354 YIELDED FOR THE      1 TIME
ELEMENT   355 YIELDED FOR THE      1 TIME
ELEMENT   357 YIELDED FOR THE      1 TIME

                                                  **********

LOAD INCREMENT =  0.47180D 02
  1 ELEMENTS FAILED DURING THIS LOAD STEP
FAILURE (YIELD OR FRACTURE) OCCURRED AT A LOAD OF      4435.46 WITH A DEFLECTION AT THE PIN OF  0.13357D-01
ELEMENT   358 YIELDED FOR THE      1 TIME

                                                  **********
```

```
LOAD INCREMENT =  0.52311D 02
  2 ELEMENTS FAILED DURING THIS LOAD STEP
FAILURE (YIELD OR FRACTURE) OCCURRED AT A LOAD OF      4540.08 WITH A DEFLECTION AT THE PIN OF  0.13683D-01
ELEMENT    97 YIELDED FOR THE      1 TIME
ELEMENT   315 YIELDED FOR THE      1 TIME

                                                   ***********

LOAD INCREMENT =  0.93306D 01
  1 ELEMENTS FAILED DURING THIS LOAD STEP
FAILURE (YIELD OR FRACTURE) OCCURRED AT A LOAD OF      4558.74 WITH A DEFLECTION AT THE PIN OF  0.13742D-01
ELEMENT   345 YIELDED FOR THE      1 TIME

                                                   ***********

LOAD INCREMENT =  0.10124D 02
  1 ELEMENTS FAILED DURING THIS LOAD STEP
FAILURE (YIELD OR FRACTURE) OCCURRED AT A LOAD OF      4578.99 WITH A DEFLECTION AT THE PIN OF  0.13807D-01
ELEMENT   365 YIELDED FOR THE      1 TIME

                                                   ***********

LOAD INCREMENT =  0.46873D 02
  1 ELEMENTS FAILED DURING THIS LOAD STEP
FAILURE (YIELD OR FRACTURE) OCCURRED AT A LOAD OF      4672.73 WITH A DEFLECTION AT THE PIN OF  0.14108D-01
ELEMENT   328 YIELDED FOR THE      1 TIME

                                                   ***********

LOAD INCREMENT =  0.51882D 02
  1 ELEMENTS FAILED DURING THIS LOAD STEP
FAILURE (YIELD OR FRACTURE) OCCURRED AT A LOAD OF      4776.50 WITH A DEFLECTION AT THE PIN OF  0.14441D-01
ELEMENT    94 YIELDED FOR THE      1 TIME

                                                   ***********

LOAD INCREMENT =  0.10289D 02
  1 ELEMENTS FAILED DURING THIS LOAD STEP
FAILURE (YIELD OR FRACTURE) OCCURRED AT A LOAD OF      4797.07 WITH A DEFLECTION AT THE PIN OF  0.14508D-01
ELEMENT   346 YIELDED FOR THE      1 TIME
```

23 LOAD INCREMENTS OMITTED FOR BREVITY

```
LOAD INCREMENT =  0.66430D 01
  2 ELEMENTS FAILED DURING THIS LOAD STEP
FAILURE (YIELD OR FRACTURE) OCCURRED AT A LOAD OF      5290.54 WITH A DEFLECTION AT THE PIN OF  0.16796D-01
ELEMENT    117 YIELDED FOR THE      1 TIME
ELEMENT    355 YIELDED FOR THE      2 TIME

                                                    ************

LOAD INCREMENT =  0.83518D 01
  1 ELEMENTS FAILED DURING THIS LOAD STEP
FAILURE (YIELD OR FRACTURE) OCCURRED AT A LOAD OF      5307.25 WITH A DEFLECTION AT THE PIN OF  0.16960D-01
ELEMENT    112 YIELDED FOR THE      1 TIME

                                                    ************

LOAD INCREMENT =  0.72432D 01
  4 ELEMENTS FAILED DURING THIS LOAD STEP
FAILURE (YIELD OR FRACTURE) OCCURRED AT A LOAD OF      5321.73 WITH A DEFLECTION AT THE PIN OF  0.17104D-01
ELEMENT    113 YIELDED FOR THE      1 TIME
ELEMENT    122 YIELDED FOR THE      1 TIME
ELEMENT    123 YIELDED FOR THE      1 TIME
ELEMENT    125 YIELDED FOR THE      1 TIME

                                                    ************

LOAD INCREMENT =  0.12074D 02
  3 ELEMENTS FAILED DURING THIS LOAD STEP
FAILURE (YIELD OR FRACTURE) OCCURRED AT A LOAD OF      5345.88 WITH A DEFLECTION AT THE PIN OF  0.17356D-01
ELEMENT    100 YIELDED FOR THE      1 TIME
ELEMENT    118 YIELDED FOR THE      1 TIME
ELEMENT    119 YIELDED FOR THE      1 TIME

                                                    ************

LOAD INCREMENT =  0.50215D 01
  1 ELEMENTS FAILED DURING THIS LOAD STEP
FAILURE (YIELD OR FRACTURE) OCCURRED AT A LOAD OF      5355.92 WITH A DEFLECTION AT THE PIN OF  0.17464D-01
ELEMENT    357 YIELDED FOR THE      2 TIME
```

****

LOAD INCREMENT = 0.16860D 02
2 ELEMENTS FAILED DURING THIS LOAD STEP
FAILURE (YIELD OR FRACTURE) OCCURRED AT A LOAD OF 5389.64 WITH A DEFLECTION AT THE PIN OF 0.17828D-01
ELEMENT 105 YIELDED FOR THE 1 TIME
ELEMENT 358 YIELDED FOR THE 2 TIME

****

LOAD INCREMENT = 0.13008D 02
1 ELEMENTS FAILED DURING THIS LOAD STEP
FAILURE (YIELD OR FRACTURE) OCCURRED AT A LOAD OF 5415.66 WITH A DEFLECTION AT THE PIN OF 0.18115D-01
ELEMENT 353 YIELDED FOR THE 2 TIME

****

LOAD INCREMENT = 0.53889D 01
2 ELEMENTS FAILED DURING THIS LOAD STEP
FAILURE (YIELD OR FRACTURE) OCCURRED AT A LOAD OF 5426.44 WITH A DEFLECTION AT THE PIN OF 0.18234D-01
ELEMENT 97 YIELDED FOR THE 2 TIME
ELEMENT 365 YIELDED FOR THE 2 TIME

****

LOAD INCREMENT = 0.11995D 02
1 ELEMENTS FAILED DURING THIS LOAD STEP
FAILURE (YIELD OR FRACTURE) OCCURRED AT A LOAD OF 5450.43 WITH A DEFLECTION AT THE PIN OF 0.18500D-01
ELEMENT 341 YIELDED FOR THE 1 TIME

****

LOAD INCREMENT = 0.69775D 01
3 ELEMENTS FAILED DURING THIS LOAD STEP
FAILURE (YIELD OR FRACTURE) OCCURRED AT A LOAD OF 5464.38 WITH A DEFLECTION AT THE PIN OF 0.18654D-01
ELEMENT 95 YIELDED FOR THE 1 TIME
ELEMENT 140 YIELDED FOR THE 2 TIME
ELEMENT 349 YIELDED FOR THE 1 TIME

****

124 LOAD INCREMENTS OMITTED FOR BREVITY

```
ELEMENT    141 YIELDED FOR THE      5 TIME

                                                    ***********

LOAD INCREMENT =  0.93744D 01
  4 ELEMENTS FAILED DURING THIS LOAD STEP
FAILURE (YIELD OR FRACTURE) OCCURRED AT A LOAD OF      7316.34 WITH A DEFLECTION AT THE PIN OF  0.12144D 00
ELEMENT     93 YIELDED FOR THE      4 TIME
ELEMENT     97 YIELDED FOR THE      5 TIME
ELEMENT    129 YIELDED FOR THE      5 TIME
ELEMENT    365 YIELDED FOR THE      5 TIME

                                                    ***********

LOAD INCREMENT =  0.99726D 01
  5 ELEMENTS FAILED DURING THIS LOAD STEP
FAILURE (YIELD OR FRACTURE) OCCURRED AT A LOAD OF      7336.29 WITH A DEFLECTION AT THE PIN OF  0.12455D 00
ELEMENT     80 YIELDED FOR THE      1 TIME
ELEMENT    111 YIELDED FOR THE      5 TIME
ELEMENT    115 YIELDED FOR THE      5 TIME
ELEMENT    337 YIELDED FOR THE      2 TIME
ELEMENT    371 YIELDED FOR THE      5 TIME

                                                    ***********

LOAD INCREMENT =  0.51797D 01
  4 ELEMENTS FAILED DURING THIS LOAD STEP
FAILURE (YIELD OR FRACTURE) OCCURRED AT A LOAD OF      7346.65 WITH A DEFLECTION AT THE PIN OF  0.12618D 00
ELEMENT    109 YIELDED FOR THE      5 TIME
ELEMENT    110 YIELDED FOR THE      5 TIME
ELEMENT    114 YIELDED FOR THE      5 TIME
ELEMENT    360 YIELDED FOR THE      4 TIME

                                                    ***********

LOAD INCREMENT =  0.52621D 01
  3 ELEMENTS FAILED DURING THIS LOAD STEP
FAILURE (YIELD OR FRACTURE) OCCURRED AT A LOAD OF      7357.17 WITH A DEFLECTION AT THE PIN OF  0.12787D 00
ELEMENT     79 YIELDED FOR THE      1 TIME
ELEMENT    369 YIELDED FOR THE      5 TIME
ELEMENT    370 YIELDED FOR THE      5 TIME
```

****

LOAD INCREMENT = 0.14630D 02
2 ELEMENTS FAILED DURING THIS LOAD STEP
FAILURE (YIELD OR FRACTURE) OCCURRED AT A LOAD OF 7386.43 WITH A DEFLECTION AT THE PIN OF 0.13259D 00
ELEMENT 104 YIELDED FOR THE 3 TIME
ELEMENT 361 YIELDED FOR THE 4 TIME

****

LOAD INCREMENT = 0.13829D 02
2 ELEMENTS FAILED DURING THIS LOAD STEP
FAILURE (YIELD OR FRACTURE) OCCURRED AT A LOAD OF 7414.09 WITH A DEFLECTION AT THE PIN OF 0.13706D 00
ELEMENT 64 YIELDED FOR THE 1 TIME
ELEMENT 81 YIELDED FOR THE 3 TIME

****

LOAD INCREMENT = 0.10238D 02
4 ELEMENTS FAILED DURING THIS LOAD STEP
FAILURE (YIELD OR FRACTURE) OCCURRED AT A LOAD OF 7434.57 WITH A DEFLECTION AT THE PIN OF 0.14036D 00
ELEMENT 112 YIELDED FOR THE 5 TIME
ELEMENT 117 YIELDED FOR THE 5 TIME
ELEMENT 125 YIELDED FOR THE 5 TIME
ELEMENT 357 YIELDED FOR THE 5 TIME

****

LOAD INCREMENT = 0.15507D 02
2 ELEMENTS FAILED DURING THIS LOAD STEP
FAILURE (YIELD OR FRACTURE) OCCURRED AT A LOAD OF 7465.58 WITH A DEFLECTION AT THE PIN OF 0.14549D 00
ELEMENT 90 YIELDED FOR THE 2 TIME
ELEMENT 113 YIELDED FOR THE 5 TIME

****

LOAD INCREMENT = 0.53713D 01
3 ELEMENTS FAILED DURING THIS LOAD STEP
FAILURE (YIELD OR FRACTURE) OCCURRED AT A LOAD OF 7476.32 WITH A DEFLECTION AT THE PIN OF 0.14727D 00
ELEMENT 92 YIELDED FOR THE 2 TIME

```
ELEMENT    350 YIELDED FOR THE      5 TIME
ELEMENT    366 YIELDED FOR THE      5 TIME

                                                          ***********


LOAD INCREMENT =  0.67150D 01
  3 ELEMENTS FAILED DURING THIS LOAD STEP
FAILURE (YIELD OR FRACTURE) OCCURRED AT A LOAD OF      7489.75 WITH A DEFLECTION AT THE PIN OF  0.14952D 00
ELEMENT     91 YIELDED FOR THE      2 TIME
ELEMENT    367 YIELDED FOR THE      5 TIME
ELEMENT    368 YIELDED FOR THE      6 TIME

                                                          ***********


LOAD INCREMENT =  0.24885D 02
  4 ELEMENTS FAILED DURING THIS LOAD STEP
FAILURE (YIELD OR FRACTURE) OCCURRED AT A LOAD OF      7539.52 WITH A DEFLECTION AT THE PIN OF  0.15791D 00
ELEMENT     75 YIELDED FOR THE      3 TIME
ELEMENT    120 YIELDED FOR THE      6 TIME
ELEMENT    140 FRACTURED
ELEMENT    362 YIELDED FOR THE      4 TIME

                                                          ***********


LOAD INCREMENT =  0.13521D 04
  2 ELEMENTS FAILED DURING THIS LOAD STEP
FAILURE (YIELD OR FRACTURE) OCCURRED AT A LOAD OF      5408.24 WITH A DEFLECTION AT THE PIN OF  0.12932D 00
ELEMENT    149 FRACTURED
ELEMENT    150 FRACTURED

                                                          ***********


****** CRACK INSTABILITY OCCURRED AT A LOAD OF      7539.52 ******


LOAD INCREMENT =  0.16620D 04
  1 ELEMENTS FAILED DURING THIS LOAD STEP
FAILURE (YIELD OR FRACTURE) OCCURRED AT A LOAD OF      4653.60 WITH A DEFLECTION AT THE PIN OF  0.11021D 00
ELEMENT    148 FRACTURED
```

```
                                                  ***********

****** CRACK INSTABILITY OCCURRED AT A LOAD OF      5408.24 ******

LOAD INCREMENT =  0.13860D 04
  3 ELEMENTS FAILED DURING THIS LOAD STEP
FAILURE (YIELD OR FRACTURE) OCCURRED AT A LOAD OF      3880.91 WITH A DEFLECTION AT THE PIN OF  0.93687D-01
ELEMENT    146 FRACTURED
ELEMENT    147 FRACTURED
ELEMENT    151 FRACTURED

                                                  ***********

****** CRACK INSTABILITY OCCURRED AT A LOAD OF      4653.60 ******

LOAD INCREMENT =  0.93025D 03
  1 ELEMENTS FAILED DURING THIS LOAD STEP
FAILURE (YIELD OR FRACTURE) OCCURRED AT A LOAD OF      2232.61 WITH A DEFLECTION AT THE PIN OF  0.77012D-01
ELEMENT    145 FRACTURED

                                                  ***********

****** CRACK INSTABILITY OCCURRED AT A LOAD OF      3880.91 ******

LOAD INCREMENT =  0.72705D 03
  2 ELEMENTS FAILED DURING THIS LOAD STEP
FAILURE (YIELD OR FRACTURE) OCCURRED AT A LOAD OF      1744.92 WITH A DEFLECTION AT THE PIN OF  0.68134D-01
ELEMENT    143 FRACTURED
ELEMENT    144 FRACTURED
```

```
                                                  ***********

****** CRACK INSTABILITY OCCURRED AT A LOAD OF      2232.61 ******

LOAD INCREMENT =  0.52672D 03
  1 ELEMENTS FAILED DURING THIS LOAD STEP
FAILURE (YIELD OR FRACTURE) OCCURRED AT A LOAD OF      1264.14 WITH A DEFLECTION AT THE PIN OF  0.60211D-01
ELEMENT   142 FRACTURED

                                                  ***********

*****  CRACK INSTABILITY OCCURRED AT A LOAD OF      1744.92 ******

LOAD INCREMENT =  0.24367D 03
  1 ELEMENTS FAILED DURING THIS LOAD STEP
FAILURE (YIELD OR FRACTURE) OCCURRED AT A LOAD OF       584.80 WITH A DEFLECTION AT THE PIN OF  0.52490D-01
ELEMENT   141 FRACTURED

                                                  ***********

*****  CRACK INSTABILITY OCCURRED AT A LOAD OF      1264.14 ******

IHC2091I IBCOM - PROGRAM INTERRUPT (P) - DIVIDE CHECK OLD PSW IS  071D000FA2437BDE . REGISTER CONTAINED   3F1C133326D1E810

TRACEBACK  ROUTINE  CALLED FROM ISN   REG. 14   REG. 15   REG.  0   REG.  1

           FAIL                0017   4242D04E  004307D0  000001C5  003A0EEC

           MAIN                       00008C72  013A0D18  00BEFB70  0043EFF8

ENTRY POINT=  013A0D18
```

```
STANDARD FIXUP TAKEN . EXECUTION CONTINUING
IHC2091 IBCOM - PROGRAM INTERRUPT (P) - DIVIDE CHECK OLD PSW IS  071D000FA2437BDE . REGISTER CONTAINED   3F1BA9C69C8FDF30
TRACEBACK  ROUTINE  CALLED FROM ISN   REG. 14   REG. 15   REG.  0   REG.  1
           FAIL                0017   4242D04E  00430700  000001C5  003A0EEC
           MAIN                       0000BC72  013A0D18  00BEFB70  0043EFF8
ENTRY POINT=  013A0D18
STANDARD FIXUP TAKEN . EXECUTION CONTINUING
IHC2091 IBCOM - PROGRAM INTERRUPT (P) - DIVIDE CHECK OLD PSW IS  071D000FA2437BDE . REGISTER CONTAINED   3F1BCAB96100DAE0
TRACEBACK  ROUTINE  CALLED FROM ISN   REG. 14   REG. 15   REG.  0   REG.  1
           FAIL                0017   4242D04E  00430700  000001C5  003A0EEC
           MAIN                       0000BC72  013A0D18  00BEFB70  0043EFF8
ENTRY POINT=  013A0D18
STANDARD FIXUP TAKEN . EXECUTION CONTINUING
IHC2091 IBCOM - PROGRAM INTERRUPT (P) - DIVIDE CHECK OLD PSW IS  071D000FA2437BDE . REGISTER CONTAINED   3F1BDAE50BDFF160
TRACEBACK  ROUTINE  CALLED FROM ISN   REG. 14   REG. 15   REG.  0   REG.  1
           FAIL                0017   4242D04E  00430700  000001C5  003A0EEC
           MAIN                       0000BC72  013A0D18  00BEFB70  0043EFF8
ENTRY POINT=  013A0D18
STANDARD FIXUP TAKEN . EXECUTION CONTINUING
IHC2091 IBCOM - PROGRAM INTERRUPT (P) - DIVIDE CHECK OLD PSW IS  071D000FA2437BDE . REGISTER CONTAINED   3F1C0A2BE7D90470
TRACEBACK  ROUTINE  CALLED FROM ISN   REG. 14   REG. 15   REG.  0   REG.  1
           FAIL                0017   4242D04E  00430700  000001C5  003A0EEC
           MAIN                       0000BC72  013A0D18  00BEFB70  0043EFF8
ENTRY POINT=  013A0D18
STANDARD FIXUP TAKEN . EXECUTION CONTINUING
```

```
IHC900I EXECUTION TERMINATING DUE TO ERROR COUNT FOR ERROR NUMBER  209
IHC209I IBCOM - PROGRAM INTERRUPT (P) - DIVIDE CHECK OLD PSW IS  071D000FA2437DDE . REGISTER CONTAINED  3F1C285E701C23F0
TRACEBACK  ROUTINE  CALLED FROM ISN   REG. 14   REG. 15   REG.  0   REG.  1
           FAIL                0017   4242D04E   00430700   000001C5   003A0EEC
           MAIN                       0300BC72   013A0D18   00BEF870   0043EFF8
ENTRY POINT=  013A0D18
```